



KATHOLIEKE UNIVERSITEIT
LEUVEN

Arenberg Doctoral School of Science, Engineering & Technology
Faculty of Science
Department of Physics and Astronomy

Supersymmetric D-particles and black holes in type II string theory

Walter VAN HERCK

Dissertation presented in partial
fulfillment of the requirements for
the degree of Doctor of Science

January 2011

Supersymmetric D-particles and black holes in type II string theory

Walter Van Herck

Supervisor:

Prof. Dr. W. Troost¹

Members of the Examination Board:

Prof. Dr. D. Bollé¹,

Prof. Dr. F. Denef^{1,2},

Prof. Dr. A. Klemm³,

Prof. Dr. J. Rogiers¹,

Prof. Dr. A. Van Proeyen¹,

Dissertation presented in
partial fulfillment of the
requirements for the degree
of Doctor of Science

¹ Instituut voor Theoretische Fysica, Katholieke Universiteit Leuven,
Celestijnenlaan 200D, 3001 Leuven, Belgium

² Department of Physics, Harvard University, Jefferson 570, 17 Oxford
Street, Cambridge MA 02138, United States

³ Physikalisches Institut der Universität Bonn, Nußallee 12, D-53115
Bonn, Germany

January 2011

©2011 Katholieke Universiteit Leuven – Faculty of Science
Geel Huis, Kasteelpark Arenberg 11 bus 2100
B-3001 Heverlee, Belgium

Cover Illustration: ESO/L. Calçada/M. Kornmesser

Alle rechten voorbehouden. Niets uit deze uitgave mag worden vermenigvuldigd en/of openbaar gemaakt worden door middel van druk, fotocopie, microfilm, elektronisch of op welke andere wijze ook zonder voorafgaande schriftelijke toestemming van de uitgever.

All rights reserved. No part of the publication may be reproduced in any form by print, photoprint, microfilm or any other means without written permission from the publisher.

D/2011/10.705/5
ISBN 978-90-8649-388-3

Voor papa

Dankwoord

Deze verhandeling markeert voor mij een belangrijk punt in een meerdere jaren omvattende onderneming. Gedurende die jaren heb ik het geluk gekend om mensen rond mij te hebben die me, op soms zeer verschillende terreinen, hebben bijgestaan en op die manier hebben bijgedragen aan deze verwezenlijking. Ik wens dan ook hier even plaats te maken om mijn dankbaarheid jegens hen uit te drukken.

Mijn promotor, Walter, wens ik te bedanken voor zijn flexibiliteit tijdens mijn licentiaatsstudies, de kansen die hij me bood, zijn beschikbaarheid en deskundige raad in zowel technische als minder technische zaken en voor de ruimte die hij me gaf om mijn eigen weg te vinden in het onderzoekslandschap. Hij speelde een prominente rol bij mijn ontwikkeling als wetenschapper.

De overige leden van de examenjury dank ik voor het aandachtig lezen van dit manuscript en hun interesse tijdens de private verdediging. In het bijzonder wil ik Albrecht Klemm bedanken voor de levendige discussies tijdens het tweede gedeelte hiervan en voor de moeite die hij zich getroost heeft om naar het besneeuwde Leuven af te reizen.

De collega's op 'het zesde' ben ik dankbaar voor de talrijke contacten en discussies, al dan niet gerelateerd aan de natuurkunde. Als men een weg kan beoordelen aan de hand van de vriendschappen die men onderweg sluit, voel ik me een bevoorrecht man. Aldo, Andres, Bert, Bram, Darya, Dieter, Frederik, Gabi, Iwein, Jan D.R., Jan R., Joke, Joris, Laura, Marco, Paul K., Paul S., Thomas V.R., Thomas W. en Ulf, bedankt voor alles. Aan Anita, Anneleen, Bavo, Christine en Filip ben ik dank verschuldigd voor hun hulp bij allerhande administratieve en IT-gerelateerde kwesties.

Ook de talrijke contacten extra muros bedank ik voor het delen van kennis en vriendschap. In het bijzonder wil ik hier François en Wieland vermelden voor onvergetelijke en warme herinneringen tijdens conferenties en cursussen.

Dr. Janssens, bedankt voor de hulp op lichamelijk gebied en voor de interesse die u toonde in mijn onderzoek.

Mijn vrienden en kennissen ben ik dankbaar voor hun steun en om mijn leven te verrijken. An, jou wil ik hier apart vermelden omwille van je bereidheid om steeds weer de kinderen op te vangen wanneer dit nodig was.

Mijn familie wens ik te bedanken voor hun onvoorwaardelijke steun en het geloof dat ze steeds in mij hebben. Wanneer ik hindernissen overwin en mijn ambities nastreef, is dit door en voor hen. Mama, Koen, Annelies, Iseo, Paul, Miet, Rudi, Elke en Jens: bedankt! Zoals een ontdekkingsreiziger een haven behoeft om naar terug te keren, zo bood mijn gezin me een plaats waar ik gewoon mezelf kan zijn. Daarbovenop hebben zij ook heel wat geduld met mij uitgeoefend en talrijke offers gebracht, waarvoor mijn oprechte dank, Joke, Aelin en Arwen.

Tot slot wens ik deze verhandeling op te dragen aan mijn papa. Hij is de movens causa voor het durven nastreven van mijn dromen en zoveel meer. . .

Contents

Contents	iii
List of Figures	vii
List of Tables	ix
1 Introduction	1
1.1 Why do we need a new theory?	1
1.2 Black holes and their microstates	6
1.3 Personal research work	8
1.4 Overview of this thesis	9
2 Classical black holes	11
2.1 The Schwarzschild solution	12
2.1.1 A first encounter	12
2.1.2 Penrose diagrams and causal properties	13
2.1.3 The Rindler approximation and Unruh effect	15
2.2 Black hole thermodynamics	17
2.3 The information paradox and quantum gravity	20
2.4 Summary	22

3	BPS states in string theory	23
3.1	String theory	24
3.1.1	Polyakov action and the string coupling	25
3.1.2	D–branes and open strings	28
3.1.3	Low energy effective actions	31
3.2	$\mathcal{N} = 2$ in various dimensions	32
3.2.1	The $\mathcal{N} = 2$ algebra	32
3.2.2	Representations and BPS states	33
3.3	Attractor mechanism	36
3.3.1	Type IIB on $M_4 \times X$	37
3.3.2	BPS states	38
3.3.3	Supersymmetric black holes	40
3.4	Split flow trees	43
3.5	Elliptic genera	45
3.6	D–particle microstates from split flow trees	50
3.7	Summary	50
4	A refined calculation of the index for BPS D–particles	53
4.1	Supergravity/B brane correspondence	54
4.2	Branes and the topological B model	57
4.2.1	A supersymmetric non–linear sigma model	57
4.2.2	The topological B model	58
4.2.3	B branes and examples	60
4.3	Refined index calculation for three models	63
4.3.1	General strategy	64
4.3.2	Example 1: the sextic	69
4.3.3	Example 2: the octic	77
4.3.4	Example 3: the decantic	86

4.3.5 Discussion of the results	94
4.4 Summary	96
5 Conclusion	99
A Calabi Yau geometry	103
A.1 Complex geometry and Kähler manifolds	103
A.2 Calabi Yau manifolds	106
B Categories and sheaves	115
B.1 Categories, morphisms and functors	115
B.2 Abelian and derived categories	117
B.3 Sheaves	121
B.4 Schemes	124
C D–brane charges	127
C.1 K–theory charge	127
C.2 Some useful examples	129
D Nederlandse Samenvatting	131
Bibliography	134

List of Figures

1.1	The physics cube	4
2.1	Penrose diagram of Minkowski space	14
2.2	Penrose diagram of Schwarzschild solution	15
2.3	Penrose diagram of a collapsing shell	16
2.4	Rindler coordinate system	18
3.1	Closed string interaction	27
3.2	Open/closed string duality	30
3.3	Split flow tree	45
4.1	Supergravity–Topological B model correspondence	55
4.2	Moduli profile at decreasing string coupling	56
4.3	Existence of split flows	65
4.4	A fibered moduli space	66
4.5	The marginal limit in the B model	68
A.1	Hodge diamond of a Calabi Yau with $SU(3)$ holonomy	107
C.1	Unstable D–brane on non–trivial homotopy class	128

List of Tables

3.1	Multiplets in type II	37
A.1	Gopakumar–Vafa invariants for the sextic	111
A.2	Gopakumar–Vafa invariants for the octic	111
A.3	Gopakumar–Vafa invariants for the decantic	112

Chapter 1

Introduction

The title of this thesis may raise many questions for the reader, like: What does it mean? Why should one study this subject? Why did the author direct its research towards this field and how did this happen?

The aim of this introductory chapter is to provide the context in which these questions can be answered and is structured as follows. The first section elaborates on the motivational aspects of this thesis by asking why a physicist should be concerned with new theories and in which situations this new theory should be applicable. This leads us to the study of black holes and their microstates, which is covered in the next section. Having clarified the physical context in which my research, presented in this thesis, is situated, a section about the main research activities of the author is presented. Finally, the reader can find an overview of this thesis, indicating the general structure and brief outlines of each chapter.

1.1 Why do we need a new theory?

The past century, physicists have been extremely successful in formulating physical theories, capable of describing, explaining and predicting physical phenomena from the subatomic scale to the huge scale of galaxies and our universe. This prosperous period for theoretical physics is mainly due to two, very different, fundamental physical theories: Quantum Field Theory and General Relativity¹.

¹When theories have met with such a battery of convincing experimental data as these have, and consequently have been widely accepted by the physics community, they deserve to be capitalized.

Einstein's theory of General Relativity describes the physics of gravitation and corrects the previously accepted theory of gravitation by Newton. In this theory, mass and energy, which are related by the famous equation $E = mc^2$, give rise to a curvature of spacetime. This curvature influences the motion of particles, moving in spacetime, thereby exhibiting gravitational attraction to other masses or forms of energy. It is formulated as a classical field theory, where the curvature is determined by the metric field. The field equations can be stated as:

$$R_{\mu\nu} - \frac{1}{2}g_{\mu\nu} R = \frac{8\pi G_N}{c^4} T_{\mu\nu}, \quad (1.1)$$

where the Ricci tensor $R_{\mu\nu}$ and the Ricci scalar R are constructed from the metric tensor field $g_{\mu\nu}$, G_N is Newton's constant, c is the speed of light in vacuum and $T_{\mu\nu}$ is the energy-momentum tensor, describing the energy content in spacetime. This energy-momentum tensor is usually seen as arising from a different theory, and many textbooks give various examples of such tensors in specific cases, like non-interacting matter distributions, perfect liquids, etc.

The Standard Model of particle physics on the other hand is formulated as a Quantum Field Theory and describes the three other known forces in our universe: the weak and strong interactions and electromagnetism. Physical observables in a quantum theory are represented by operators, acting on the Hilbert space of states. This is very different from a classical field theory, where these observables are functions on the phase space of the system. These operators give rise to physical amplitudes and probabilities of measuring a certain value for a given measurement, whereas a classical theory would give a definite answer in this case. Nevertheless, the Standard Model enables physicists to describe and predict many properties of elementary particle interactions. Moreover, the calculations involved often lead to extremely accurate results, confirmed by particle experiments. As an example, some calculations in Quantum Electrodynamics, the electromagnetic part of the Standard Model, have been confirmed to within ten parts in a billion, rendering it one of the most precise physical theories ever. To give an impression of the way the Standard Model is formulated, the Lagrangian density of the theory, which contains the particle content and their interactions, can be succinctly written as:

$$\begin{aligned} \mathcal{L}_{\text{SM}} = & -\frac{1}{4}F_{\mu\nu}F^{\mu\nu} + i\bar{\psi}\not{D}\psi + \text{h.c.} \\ & + \psi_i y_{ij} \psi_j \phi + \text{h.c.} + |D_\mu \phi|^2 - V(\phi), \end{aligned} \quad (1.2)$$

where +h.c. denotes adding the Hermitian conjugate of the preceding term. In this expression, the first term describes the propagation and self-interaction of the gauge bosons (whose field strength is given by the tensor field $F_{\mu\nu}$ and who are the carriers of the forces in the theory). The next term, and its Hermitian conjugate, describes the fermionic matter content ψ of the Standard Model and its interactions with the gauge bosons. Then there is a term which denotes the

Yukawa interactions between the matter particles and the Higgs boson ϕ , which at low energy is responsible for giving the various particles a mass. The y_{ij} in this term are the coupling constants, which should be determined by experiment. The last terms are the kinetic and potential energy terms for the Higgs boson and provide a mass for the gauge bosons. The mass of the particles arises mainly because the potential energy term $V(\phi)$ gives rise to a vacuum expectation value for the Higgs boson, which couples to the other particles through the Yukawa terms and the kinetic energy terms of the Higgs boson. For completeness, it should also be mentioned that in the notation of equation (1.2), a lot of the details of the theory are obscured. For example, the fermion fields, denoted by ψ , actually describe three generations of leptons and quarks, where the quarks are triplets under the strong $SU(3)$ gauge group. For ease of notation, all their corresponding indices have been left out of the Lagrangian density.

The Standard Model is not without its challenges however. The famous Higgs particle for example, in the preceding formulation responsible for giving the various particles a mass, has not been detected yet in particle experiments. As another example, it is not known if and how the different gauge interactions unify at a certain energy scale. This last issue is related to the possible existence of a larger symmetry group in physics, called supersymmetry, which relates bosonic fields and particles with fermionic ones and vice versa. These two questions, and lots of others, are meant to be addressed by the experiments planned for the Large Hadron Collider at CERN.

This said, one may wonder why we need a new theory. After all, General Relativity and the Standard Model are very successful theories, describing all of the known four forces and, with the exception of dark matter and energy, also all the matter content in the universe. The problem with these two theories however, is that they are incompatible with each other. To see this, one can look back at Einstein's field equations (1.1). On the right hand side, we have the energy momentum tensor, which for Standard Model particles is a quantum operator. On the left hand side there should thus also appear a quantum operator and the equations should be understood as operator equations. This implies a quantization of General Relativity, which, at least at the perturbative level, is an open problem because the theory is unrenormalizable. So the conventional methods in Quantum Field Theory, which are extremely successful for the Standard Model, simply do not work for Einstein's theory. But why then are these theories so extremely successful in describing physics at such a broad spectrum of length and energy scales?

Figure 1.1 illustrates what is going on by looking at the domains of validity of different physical theories. The three axes denote the dimensionless ratios \hbar/S , r_S/L and v/c . Let us comment first on what these mean. The parameter v/c is the ratio of a typical speed of a particle or system to the speed of light. When it is small, the system is non-relativistic, while at $v/c \sim 1$ relativistic effects become important. This explains the transition from classical mechanics to special

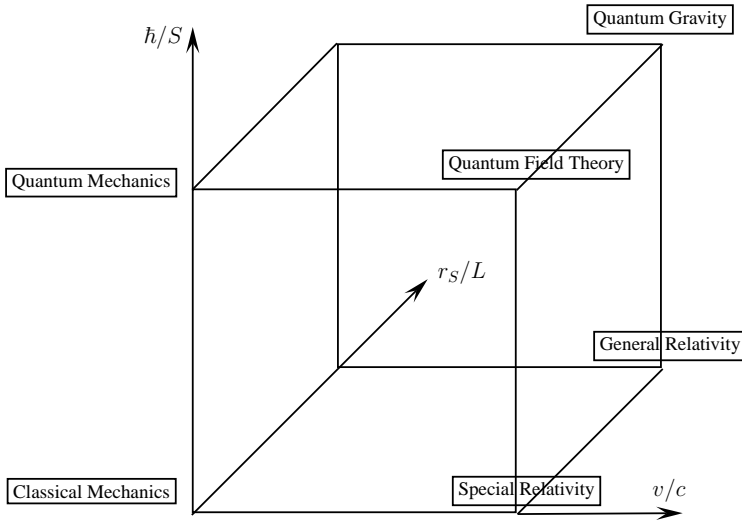


Figure 1.1: The physics cube.

relativity at the bottom front of the cube.

\hbar/S is the ratio of Planck's reduced constant \hbar to the action of the system under consideration (more accurately, it should denote the ratio to the change of the action under measurable fluctuations of position or other physical observables). This action becomes small for small particles and descriptions at short time scales. In this case, the quantum mechanical nature of the system must be incorporated to have an accurate description of its dynamics. This is illustrated by the presence of quantum mechanics and Quantum Field Theory at the top front of the cube: Quantum Field Theory combines special relativity and quantum mechanics.

At last, r_S/L is the ratio of the Schwarzschild radius to a typical length scale in the physical system. It can be also be written as $\frac{2G_N M}{Lc^2}$, where M denotes a mass scale. General relativistic corrections to classical physics thus become important at high energies, or mass, and short length scales. Note also that the empty vertices of the cube should correspond to the non-relativistic versions of quantum gravity and General Relativity.

While $0 \leq v/c \leq 1$, it may be useful to provide the reader with some quantitative intuition about these other ratios. To start with \hbar/S , we will turn to a more simple approach using the Heisenberg uncertainty relations:

$$\Delta p \Delta x \geq \hbar/2, \quad (1.3)$$

where Δp and Δx denote the uncertainty in momentum and position respectively.

Suppose a billiard ball with weight² 0.22 kg is localized to within 0.1 mm. Applying the Heisenberg uncertainty relations, its wavefunction would spread out 1 mm over a period of about $1.3 \cdot 10^{19}$ year, which is considerably longer than the age of our universe. Doing the same calculation for an electron, confined within atomic distance ($\sim 10^{-10}$ m), we find that its wavefunction spreads out over 600 km in one second³. This demonstrates why atomic physics should be treated quantum mechanically, while billiard players can content themselves using classical mechanics.

An example of the corrections to the classical theory, induced by General Relativity, is the anomalous precession of Mercury around the sun. At its closest point, the perihelion, Mercury is about $1.5 \cdot 10^7 r_S$ away from the sun, where $r_S \sim 3$ km is the Schwarzschild radius of the sun. The anomalous precession of its orbit per orbital period $\delta\phi$, due to General Relativistic effects, obeys

$$\frac{2\pi}{\delta\phi} \sim 1.2 \cdot 10^7, \quad (1.4)$$

which is of the same order as L/r_S .

Returning to figure 1.1, one sees that both Quantum Field Theory and General Relativity are relativistic theories, incorporating effects that occur at speeds close to the speed of light. But a fundamental theory of physics should be able to combine both the quantum mechanical nature of reality and gravity. Such a theory is then called a quantum theory of gravitation or quantum gravity for short. To understand in which conditions this theory would considerably deviate from Quantum Field Theory or General Relativity, it is instructive to combine the three fundamental constants G_N , \hbar and c into a fundamental length scale, called the Planck length:

$$l_P \equiv \sqrt{\frac{G_N \hbar}{c^3}} \approx 1.616252 \cdot 10^{-35} \text{ m}. \quad (1.5)$$

At length scales of the order l_P , quantum gravity effects are expected to become important. One can equally well define a mass or energy scale with these fundamental constants, leading to the Planck mass

$$m_P \equiv \sqrt{\frac{\hbar c}{G_N}} \approx 1.2209 \cdot 10^{19} \text{ GeV}/c^2, \quad (1.6)$$

whose energy scale (of order 10^{19} GeV) is many orders of magnitude larger than the one currently envisaged at the Large Hadron Collider, which is $14 \cdot 10^3$ GeV.

²The author used the standard weights for billiard balls used in carambole, reflecting his own preference for this game.

³This last example was used in [1] to demonstrate the fact that a second is a very long time on the atomic scale and electrons will delocalize over much shorter time scales in electrical conductors for example.

String theory is a prime candidate for such a theory of quantum gravity. It replaces the point particles of Quantum Field Theory with dynamical one-dimensional objects, called strings, and inevitably contains gravity. Because of the one-dimensional nature of these fundamental constituents, the theory contains a parameter with length dimension, the string length l_s .

At low energies, compared to the inverse string length⁴, the strings will behave very much like the familiar point particles of Quantum Field Theory. At high energies however, this behaviour drastically changes, due to this length scale, which tends to delocalize string interactions (in section 3.1, we will show how this comes about). This means that if we set the string length of the order of the Planck length, new physical phenomena will appear at this energy scale, which could cure the issues encountered by a straightforward attempt to quantize General Relativity. That it really does, is not trivial and much of the work in this thesis is devoted to studying this subject in some particular cases.

1.2 Black holes and their microstates

In this thesis, we will venture into the world of a special class of black holes in string theory, thereby showing how string theory resolves a fundamental issue appearing in the classical description of black holes. In this introductory section, the nature of this challenge for a new physical theory will be described. This will allow us to state how one expects a theory of quantum gravity to overcome this obstacle.

The Schwarzschild solution was the first non-trivial solution to Einstein's field equations in empty space and describes a spherically symmetric spacetime around a massive object. Since the solution is valid for empty space, where the energy-momentum tensor vanishes, one can only use it to describe the gravitational effects outside this same object. This solution has been confirmed by many experiments. For example, the motion of planets around the sun can be described by the planets following geodesic curves in the Schwarzschild solution caused by the mass of the sun. It should therefore be taken as a serious solution in General Relativity, describing real physical situations.

When the radius of the massive object drops below a certain value, determined by the mass of the object, the solution will describe a black hole, which is a gravitational solution that exhibits an event horizon. Such a horizon shields the outside environment of the black hole from its inside. More explicitly, events occurring inside the horizon can never influence the outside region. This is often colloquially stated by saying that even light cannot escape the black hole. Note however that the inverse statement is not true: objects outside the horizon can fall

⁴We use units in which both Planck's constant \hbar and the speed of light c are set to one. In this way, energy will have the dimension of inverse length.

into the black hole, thereby influencing its interior. Such a Schwarzschild black hole, like many of its generalizations that include charges and angular momenta, exhibits a number of properties that require attention.

Firstly, it contains a spacetime singularity, which is a locus in spacetime where a number of physical observables diverge, most notably the mass density. It is hard to make sense of this kind of singularities and this particular problem is often partly avoided by the cosmic censorship hypothesis, which states that singularities are always hidden behind an event horizon, preventing an outside observer to ‘see’ the singularity. That this does not solve the problem is clear: one could ask what would happen to an observer falling into a black hole and what he will observe. This type of singularity is not unique to gravitational theories however. In classical electrodynamics, the charge density of a pointlike charge, like the electron, also becomes infinite at the locus of the particle. But in this case, Quantum Field Theory comes to the rescue through the renormalization procedure. As was already mentioned in the previous section, we cannot apply these same methods to General Relativity, forcing physicists to look for different ways of explaining, describing and possibly resolving the gravitational singularity.

A second issue with classical black holes is their uniqueness. Regardless of whether a Schwarzschild black hole is formed through the collapse of a star or by the collapse of a gigantic ball of water, the end result will look exactly the same if their mass was equal: a spacetime singularity, surrounded by an event horizon. The same is true for generalizations of black holes: the solutions are completely determined by their mass, charges and angular momentum. It thus seems that one is unable to trace back the black hole to its origins. While this may seem like a more philosophical problem, its appearance in a physical theory is rather awkward, since both in classical as in quantum theories, there is a clear notion of preservation of information that seems to be violated here. In chapter 2, we will go a little bit deeper into this subject.

So how should a theory of quantum gravity resolve this issue? An obvious answer to this question would be that the theory does not give one unique solution for a given mass, but a multitude of states. As an extra requirement, the number of states for a given mass should be large enough to account for the possible origins of the black hole.

A remarkable result by Bekenstein and Hawking [2, 3] was that there is an entropy associated to a black hole that can be interpreted as a measure for this number of microstates. This entropy is proportional to the horizon area, suggesting that the physical degrees of freedom of a black hole live on the horizon. Since then, various attempts have been undertaken to account for this number in different physical situations and in certain limits of the theory.

This also marks the point where string theory comes in. In [4], the entropy of black holes is considered as arising from string configurations with ends frozen

at the horizon. This produces the right magnitude as the Bekenstein–Hawking entropy. In [5] and [6], the degeneracy of supersymmetric black holes is calculated by reducing the D–brane worldvolume theory to a two–dimensional conformal field theory.

At last, I would like to mention the fuzzball proposal for black holes (see [7, 8, 9, 10] and references therein). In this proposal, black hole geometries are fuzzy objects that are completely regular (i.e. without spacetime singularities) and where the horizon only appears as an effective artifact for observers on short time scales, as compared to the evaporation time of the black hole.

1.3 Personal research work

While thinking about the general structure of this thesis, the author had to answer an important question: should he give short accounts of every research activity he was involved with and try to glue these together into a patchwork or would it be better to concentrate on one important aspect of his research, thereby providing a more coherent text? The latter was chosen, because in this way, the text could also serve as a specialized treatment of the subject involved, without delving into less related concepts and issues. However, because the text also needs to serve as an important milestone for the completion of a doctoral study period, the present section gives a very brief overview of the publications in which the author was involved as a (co–)author.

The research during my doctoral studies began with the study of matrix coordinates of multiple D–branes and the way these transform under general coordinate transformations of spacetime [11]. D–branes, which are higher–dimensional objects in string theory, would turn out to play an important role in the remainder of my research. When multiple D–branes are put together to form a stack, the Born–Infeld gauge group is extended from N copies of $U(1)$ to $U(N)$. At the same time, the embedding coordinates of the D–brane, specifying how it is embedded into the full spacetime, become matrix valued coordinates. Since these do not generically commute, it is an open question how they should transform under general coordinate transformations of the bulk spacetime. The article studied this problem from an algebraic viewpoint, defining matrix coordinate transformations and representations of these.

In [12], the study of black holes first appeared in my research. In this work, a map was analyzed between five–dimensional fuzzball solutions and four–dimensional multicentered solutions, which also form a central object of study in this thesis. More explicitly, a map was found between five–dimensional supertube solutions, appearing in the fuzzball picture, and multicentered solutions in four dimensions. The dipole charge of the supertube solutions, characteristic in the fuzzball proposal,

gets mapped to the $D6\text{-}\overline{D6}$ dipole charge of the multicentered solution. This provides for an intuitive connection between fuzzball geometries and multicentered black hole solutions.

Another collaboration [13] took a first step in analyzing black hole microstates in five dimensions beyond the so-called probe approximation. One often studies the degeneracy of black hole microstates by looking at D-brane probe configurations near the horizon (see [14, 15, 16, 17] for examples). In [13], we studied the backreaction of such wrapped brane states. This resulted in a supersymmetric embedding of Gödel space in M-Theory.

The next two articles [18, 19] form the main subject of this thesis. They deal with a method to calculate exact degeneracies for small charge BPS solutions in type II string theory. The main idea underlying this research is a correspondence between the low energy supergravity description of string theory, in which the BPS solutions appear as, possibly multicentered, black holes or D-particles, and a topological field theory, where these same states are objects in the derived category of coherent sheaves. While this category may at first sight seem like a rather technical mathematical construction, it proves to be a very useful tool to obtain exact results on the degeneracies of the states under consideration. To avoid running ahead of things or to spoil the surprises waiting to be uncovered by the reader, the details of this subject will be left for the remaining chapters.

1.4 Overview of this thesis

Each chapter in this thesis will start with a short overview of its content and the context in which the relevant research is situated. After the content itself, which constitutes the main part of each chapter, a summary is provided, containing the main results and some general conclusions. The reader who is less familiar with some technical aspects of string theory or black hole physics, should be able to grasp the general idea of each chapter from its introduction and summary.

We will start in chapter 2 with a treatment of black holes in General Relativity. First, the Schwarzschild solution is presented, together with some approximate geometries and Penrose diagrams to show the causal nature of these geometries. Then, the important subject of black hole thermodynamics is embarked upon, where the large number of microstates will make its first appearance. Finally, the information paradox is stated, together with its possible resolution in a theory of quantum gravity.

Chapter 3 lays the foundations for the study of BPS states in string theory. It introduces the main aspects of string theory we will be concerned with and provides a short overview of the $\mathcal{N} = 2$ supersymmetry algebra and its representations. It

then proceeds by looking at the attractor mechanism, which plays a crucial role in the description of supersymmetric black holes in supergravity. The chapter concludes by describing split flow trees and elliptic genera, tools we will often refer to, sometimes implicitly, in later sections.

The main results of part of my research will then be presented in chapter 4. It starts with stating a correspondence between black holes in supergravity and D-brane states in string theory. The next section then provides a framework to study these supersymmetric D-brane states using a topological field theory, which goes by the name ‘the topological B model’. The actual results of my research and the calculations involved, are treated in section 4.3. A summary concludes the chapter, revisiting the results and implications of this work.

A general conclusion and summary of the thesis is given in chapter 5. A Dutch summary, containing the essence of chapter 5 plus some material from this introduction is given in appendix D. The other three appendices are meant to give a brief introduction to some of the mathematical tools that are widely used in the research, presented in this thesis: appendix A introduces Calabi Yau manifolds and their most relevant properties; appendix B provides a brief description of some mathematical structures in category theory and algebraic geometry, while appendix C gives the main formulas regarding conserved D-brane charges.

Depending on the motivation and background of the reader, two different reading paths are proposed: if the reader only wants a general overview of the research covered in this thesis and is not concerned with the technical details, he can restrict his attention to the short opening paragraphs and summaries of each chapter, while also going through the last chapter, which stresses the main points and presents some conclusions. The more technically oriented reader, wishing to learn the nuts and bolts of the calculations involved, can pay a closer attention to the body of chapter 4 and those topics in the background information he is not already familiar with. Of course, as always in life, there exist many paths in between these extremes that may appeal more to some individuals.

Chapter 2

Classical black holes

To be able to appreciate how string theory resolves many of the paradoxes encountered when trying to describe quantum fields in a black hole background, this chapter will introduce some of the basic techniques and statements about black holes in General Relativity. We refer the reader to [20, 21, 22, 23], which, in increasing order of complexity and length, introduce Einstein's theory of General Relativity and contain much of the basic material about black hole solutions of this theory. The behaviour of quantum fields in a curved background, such as black holes, is treated in [24], while [25] focuses more on the information paradox and the way string theory can provide for solutions.

In the following sections, we will follow a similar journey as in the first chapters of [25], concentrating on stating the questions raised by doing Quantum Field Theory in a black hole background, thereby revealing the information paradox. The possible resolution of these difficulties and apparent inconsistencies, through the use of string theory, constitutes one of the main motivations of the work presented in this thesis.

After giving a brief overview of the Schwarzschild solution in the first section, where concepts as black holes, horizons and singularities are introduced, we will move on to describe the laws of black hole thermodynamics in section 2.2. At last, in section 2.3, we turn our attention to the information paradox and how a theory of quantum gravity can provide for a solution.

2.1 The Schwarzschild solution

The first non-trivial solution to Einstein's field equations was discovered by Karl Schwarzschild shortly after the publication of the theory of General Relativity. It describes a static, spherically symmetric black hole in empty space. More precisely, it is a solution to the sourceless Einstein field equations:

$$R_{\mu\nu} = 0 \tag{2.1}$$

where $R_{\mu\nu}$ is the Ricci tensor.

This section will describe the Schwarzschild solution from different perspectives and in various coordinate systems. The aim is to provide the reader with an overview of the intrinsic properties of black holes by studying this prototypical example.

2.1.1 A first encounter

General Relativity without sources can be formulated using the following Einstein–Hilbert action:

$$S = \int d^4x \sqrt{-g} R, \tag{2.2}$$

where R is the Ricci scalar. The equations of motion, derived by varying the action with respect to the metric $g^{\mu\nu}$, give $R_{\mu\nu} = 0$. The Schwarzschild metric is a spherically symmetric solution of this equation. It is most often written as follows¹:

$$ds^2 = - \left(1 - \frac{2M}{r}\right) dt^2 + \left(1 - \frac{2M}{r}\right)^{-1} dr^2 + r^2 d\Omega_2^2 \tag{2.3}$$

with $d\Omega_2^2 = d\theta^2 + \sin^2\theta d\phi^2$ the line element of a unit radius two-sphere. The coordinates (t, r, θ, ϕ) are called Schwarzschild coordinates and describe an inertial frame of a distant observer. One can easily verify that at large r , the metric and Christoffel symbols become those of flat Minkowski space. Moreover, the acceleration of a test particle at rest and outside the horizon, is

$$\frac{d^2r}{dt^2} = \frac{M(2M - r)}{r^3} = -\frac{M}{r^2} + \mathcal{O}(1/r^3), \tag{2.4}$$

which allows the identification of M as the mass of the Schwarzschild geometry.

¹In this chapter, we use units for which Newton's constant $G_N = 1$, as is common in the literature on General Relativity

Probably the first thing one notices about this metric, is that the metric component g_{rr} diverges for $r \rightarrow 2M$. Yet, as we will show, this locus does not constitute a singularity of spacetime. Note that the metric component is a coordinate dependent quantity, so its divergence could be caused by the specific choice of coordinates. If we construct scalars from the Riemann tensor, they will never diverge at the horizon. For example, we have

$$R^{\mu\nu\rho\sigma} R_{\mu\nu\rho\sigma} = \frac{48M^2}{r^6}, \quad (2.5)$$

indicating a singularity at $r \rightarrow 0$, but not at $r = 2M$. This also implies that for large black holes, $M \gg 1$, this scalar quantity becomes very small at the horizon, where $r = 2M$. This behaviour for scalars, constructed from the Riemann tensor, is generic and the horizon does not in any way constitute a singular locus of the Schwarzschild geometry.

As a consequence, the locus $r = 2M$ is locally not distinct from its surroundings and as such, a local observer passing this locus, will not notice anything special about it. Nevertheless, this locus, which we will refer to as the horizon, has some special global features. It marks the boundary between the region where light rays, and consequently also timelike trajectories, will always hit the singularity at $r \rightarrow 0$, and the region where light can escape to spatial infinity.

To explore the causal properties of the Schwarzschild solution and its horizon, we will now construct its Penrose diagram.

2.1.2 Penrose diagrams and causal properties

A very convenient way of studying the causal properties of spherically symmetric spacetimes is by constructing a *Penrose diagram*. Because of the spherical symmetry, one concentrates on the radial and time coordinates of a specific solution, keeping in mind that each point of fixed time and radial distance has a two-sphere associated with it, representing the angular coordinates. The Penrose diagram will then encode the radial and time dependent part of the spacetime geometry in such a way that lightcones are always represented by cones with boundaries at 45 degrees.

As an example, let us first discuss the Penrose diagram for Minkowski spacetime. We start with coordinates for which the Minkowski line element takes the form $ds^2 = -dt^2 + dr^2 + r^2 d\Omega_2^2$, where $d\Omega_2^2$ again represents the line element of a unit radius two-sphere. Next, we perform the following coordinate transformation:

$$\begin{aligned} Y^+ &= \tanh(t + r) \\ Y^- &= \tanh(t - r). \end{aligned} \quad (2.6)$$

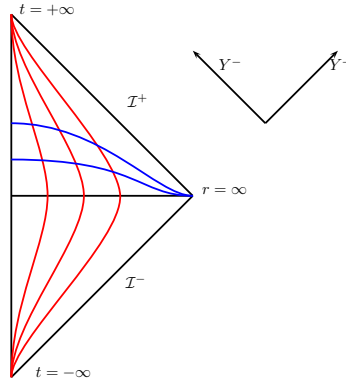


Figure 2.1: Penrose diagram of Minkowski space. \mathcal{I}^+ and \mathcal{I}^- represent future and past lightlike infinity. The red lines are lines of constant radial distance r , while the blue lines mark hypersurfaces of constant time t .

Since $dY^\pm = (dt \pm dr)/\cosh^2(t \pm r)$, these directions represent out- and ingoing radial lightlike directions. Furthermore, since $0 \leq r < \infty$ and $-\infty < t < \infty$, we have $Y^+ \geq Y^-$, $Y^+ < 1$ and $Y^- > -1$. The associated Penrose diagram is then drawn in figure 2.1, where \mathcal{I}^+ and \mathcal{I}^- do not strictly belong to Minkowski space as they represent the points at infinity ($Y^+ = 1$ and $Y^- = -1$ respectively). In this diagram, every spacelike surface ends in the point $r = \infty$, while timelike trajectories end in the point $t = +\infty$. The lightlike infinities \mathcal{I}^- and \mathcal{I}^+ denote the start- and endpoints of light rays. Note the idiosyncratic way in which lightrays are represented in this diagram: the lightcone at each point in this diagram is formed by two intersecting lines in the directions Y^+ and Y^- respectively.

Similarly, one can construct a Penrose diagram for the Schwarzschild solution, as in figure 2.2. Here, the geometry has been maximally continued, resulting in the addition of regions *III* and *IV*. Region *I* corresponds to the part of spacetime outside the horizon, while region *II* represents the part of spacetime inside the horizon. The diagram clearly demonstrates that a light ray or a timelike trajectory can cross the horizon from region *I* to *II*, while the reverse is not possible. Every timelike trajectory starting in region *II* will end at the future spacelike singularity.

To understand why the horizon is a global feature of the geometry, we will now look at the formation of a Schwarzschild black hole through the collapse of a massless spherical shell. The region in the interior of the shell will be just Minkowski space, while the exterior region is described by the Schwarzschild geometry. By gluing together parts of the respective Penrose diagrams, we obtain the diagram from figure 2.3. While the notion of a black hole only makes sense after the shell crosses its Schwarzschild radius, the horizon already begins to form at an earlier stage.

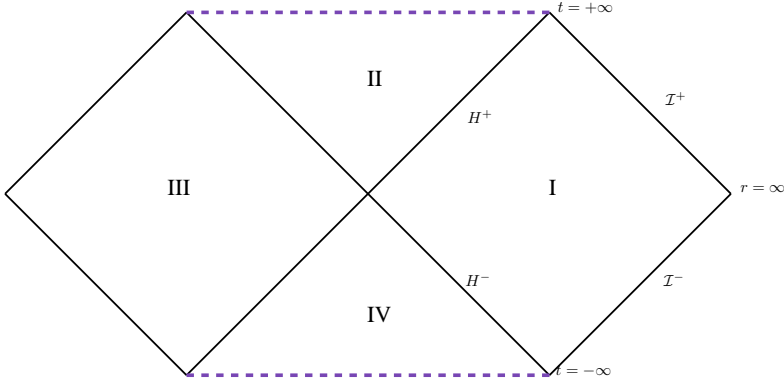


Figure 2.2: Penrose diagram of Schwarzschild solution. \mathcal{I}^+ and \mathcal{I}^- again represent future and past lightlike infinity. H^+ and H^- denote the extended future and past horizons. Only the regions *I* and *II* are covered by the usual Schwarzschild coordinates of equation (2.3). The dotted purple lines mark the locations of the past and future spacelike singularity.

The presence of this horizon inside the collapsing shell, which grows gradually to the Schwarzschild radius, depends on the future collapse of the shell. This fact demonstrates that a horizon is not a local but a global feature, which may depend on past and future events. In Schwarzschild coordinates, the horizon looks like a cone, which is just a specific lightcone in the Minkowski geometry at the interior of the shell, glued to a cylinder of fixed radius $r = 2M$. Inspection of the Penrose diagram then indeed shows that it forms the boundary of light rays that are confined to this region and will end at the singularity and an exterior region from which light rays can escape to infinity (\mathcal{I}^+ in figure 2.3).

2.1.3 The Rindler approximation and Unruh effect

A very useful coordinate system to describe the near horizon region of a large black hole, are the Rindler coordinates. Starting from the Schwarzschild metric, one replaces the radial coordinate r with the proper radial distance from the horizon:

$$\rho \equiv \int_{2M}^r dr' \sqrt{g_{rr}(r')}, \quad (2.7)$$

which can be approximated close to the horizon by $\rho \approx 2\sqrt{2M(r-2M)}$. In this approximation, the line element reduces to

$$ds^2 = -\rho^2 \left(\frac{dt}{4M} \right)^2 + d\rho^2 + r^2 d\Omega_2^2. \quad (2.8)$$

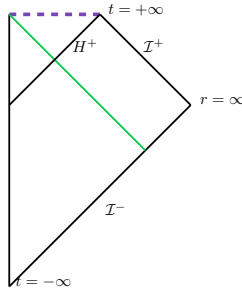


Figure 2.3: Penrose diagram of a collapsing shell. The green lightlike line represents the collapsing massless shell. The dotted purple line marks the spacelike singularity. A black hole is formed at the intersection of the worldvolume of the shell (green line) and the horizon H^+ .

This line element can be further simplified by defining $\omega \equiv t/4M$ and using Cartesian coordinates x, y in a small angular region of the horizon. We then get

$$ds^2 = -\rho^2 d\omega^2 + d\rho^2 + dx^2 + dy^2, \quad (2.9)$$

which is just Minkowski spacetime, described by so-called Rindler coordinates. This can be seen by introducing the coordinates $T \equiv \rho \sinh \omega$ and $Z \equiv \rho \cosh \omega$, which puts the line element into the more familiar form:

$$ds^2 = -dT^2 + dZ^2 + dx^2 + dy^2. \quad (2.10)$$

This indicates that this approximation neglects the tidal effects at the horizon, which can be made arbitrarily small by increasing the size of the black hole, and that a straight (timelike) line in Minkowski coordinates describes an infalling particle or observer.

This description of the near horizon region, where a static observer with fixed Schwarzschild radial coordinate, subject to the gravitational attraction of the black hole, corresponds to an accelerating observer in flat space is a nice example of Einstein's equivalence principle. This principle states that, with the exception of tidal effects, gravitational effects are indistinguishable from effects due to acceleration.

Figure 2.4 shows the relation between the Minkowski coordinates T, Z and the Rindler coordinates ω, ρ . It also clarifies that an observer at fixed radial distance $\rho = \text{constant}$ from the horizon can be described by an accelerating observer in flat space. Calculation of the Christoffel symbols of the Rindler metric reveals that such an observer has proper acceleration $1/\rho$. Although the accelerated observer

moves in flat space, he or she will also experience a horizon: as the figure shows, no event in region II can ever influence an observer with fixed ρ moving in region I .

An important result by Unruh [26] states that a uniformly accelerated observer in empty flat space will see a vacuum structure that looks like a thermal bath with temperature:

$$T_U = \frac{a}{2\pi}, \quad (2.11)$$

with a the proper acceleration of the observer. In our case, this gives $T_U = 1/2\pi\rho$.

To understand the appearance of a thermal vacuum structure for accelerated observers, note that in Quantum Field Theory the vacuum receives quantum corrections due to particles going in loops. For an observer with an event horizon, such as the accelerating one in figure 2.4, loops that wind around the origin, which is the location of the horizon from the point of view of the accelerated observer, will appear as particles emitted from the horizon at past infinity and falling back into it at future infinity [27, 28]. This is the origin of the Unruh effect, causing the horizon to look as a thermal region for an accelerated observer.

Formulated in relation to the dimensionless time ω , the Unruh temperature has the universal value of $1/2\pi$. Since this dimensionless time is related to Schwarzschild time by $\omega = t/4M$, a Schwarzschild observer will see the region close to the horizon as having a temperature $T_S = 1/8\pi M$. This remarkable result leads to the thermodynamic description of black holes, which will form the subject of the next section.

2.2 Black hole thermodynamics

As found in the previous section, an observer at a large distance from a Schwarzschild black hole of mass M , will see the region close to the horizon as a thermal ensemble of temperature $T_S = 1/8\pi M$. This indicates that we can write the first law of thermodynamics as follows:

$$dM = TdS = \frac{1}{8\pi M}dS, \quad (2.12)$$

with S the entropy of the black hole. One easily deduces the famous Bekenstein–Hawking entropy [2, 3] of the Schwarzschild black hole:

$$S = 4\pi M^2 = \frac{A_h}{4}, \quad (2.13)$$

where $A_h = 4\pi(2M)^2$ is the horizon area of the black hole.

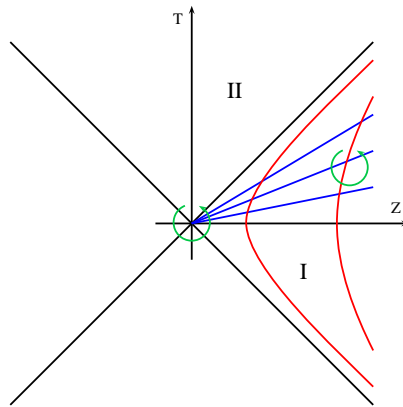


Figure 2.4: The Rindler coordinate system of the near horizon region of a Schwarzschild black hole. The red curves are lines of fixed radial distance ρ , while the blue lines are surfaces of constant time ω . The diagonal lines are the locations of the horizon. In green, two particle loops are indicated, contributing to the vacuum structure according to Quantum Field Theory. The particle loop around the origin is seen by the accelerated observer as a particle emitted from the horizon at past infinity and falling back into it at future infinity.

It is remarkable that this entropy does not scale with volume, as would be expected for an extensive quantity, but with area. Since the entropy gives a measure of the effective physical degrees of freedom in a system, one is led to the idea that the black hole horizon is the place where these degrees of freedom reside. Strikingly, this is in agreement with what an outside observer would see when witnessing matter falling into a black hole: the particles never seem to reach the horizon and form extremely thin layers around it.

An infalling observer however would not notice anything special about crossing the horizon, since, as mentioned before, the horizon is a global feature of a black hole, depending on both future and past events. The discrepancy between these observations is one of the most puzzling aspects of black holes, and is believed by some to point at crucial aspects of a theory of quantum gravity. Such a theory should, at the very least, reconcile or explain these conflicting observations.

Another striking feature related to this Bekenstein–Hawking entropy, is that by studying quantum fields in the vicinity of a black hole horizon, one recovers an entropy which is proportional to the horizon area, but diverges. By introducing a cutoff distance, such that the fields are not allowed within this distance from the horizon, one can show that by taking this cutoff of the order of the Planck length, one recovers the usual Bekenstein–Hawking entropy of a black hole (see

for example [25]). This led to the notion of a stretched horizon, situated outside the event horizon at distance of the order the Planck length. The physical degrees of liberty then seem to live on this stretched horizon. Again, this agrees well with what an outside observer would see.

One can generalize this law for black holes with charges and angular momentum, which would result in:

$$dM = TdS + \Omega_H dJ + Qd\phi, \quad (2.14)$$

with Ω_H the angular velocity at the horizon, J the angular momentum and Q and ϕ the electric charge and potential at the horizon. This law is very similar in nature to the first law of thermodynamics, which is $dE = TdS + PdV$.

The other fundamental laws of thermodynamics also have a corresponding formulation in black hole physics [29], as follows:

Zeroth law This law corresponds to the fact that the surface gravity at the horizon, which is proportional to the temperature $\kappa = 2\pi T$ is constant over the horizon.

First law This law was already discussed previously: $dM = TdS + \Omega_H dJ + Qd\phi$.

Second law Classically, this states that the entropy of the black hole, which is proportional to its horizon area, is a non-decreasing function of time. This corresponds to the classical notion of a black hole that can only grow by infalling matter. When considering multiple black holes that coalesce, this law implies that the total horizon area is non-decreasing. When including quantum effects, thereby allowing the black hole to evaporate by Hawking radiation, one should generalize this by saying that the total entropy of the black hole and Hawking radiation is non-decreasing [3]: $\Delta S_{total} = \Delta S_{BH} + \Delta S_{Hawking} \geq 0$.

Third law To see how this law is stated in the context of black holes, one must consider extremal black holes, which are solutions that saturate a certain mass bound $M \geq |Q|$, where Q is a combination of the charges and angular momenta of the black hole. One can show that these extremal black holes develop an infinitely long throat at the horizon, which implies that no finite process can ever create such extremal states. The Hawking temperature of these states is zero, which nicely corresponds to the original statement of the third law of thermodynamics and also agrees with the expectation that these states should be stable and not evaporate.

2.3 The information paradox and quantum gravity

As stated in section 2.1.3, an outside observer at fixed radial distance to the horizon will see its environment as a thermal region with temperature $T_S = 1/8\pi M$. This temperature is of the same order as the maximal effective potential for particles with zero angular momentum, so that some of these particles could escape to infinity. This radiation was first described by Hawking [3] and is referred to as Hawking radiation. The result of this radiative leaking is that the black hole slowly evaporates. Since the radiation originates at the horizon and the matter forming the black hole falls into the singularity in finite time, this radiation can carry no information about the original matter and therefore should be completely thermal. This implies that information gets lost: it does not matter if the black hole was formed by a collapsing star or by the collapse of a giant ball of water, what comes out is just thermal radiation.

The loss of information constitutes a serious challenge for our laws of nature, as both in classical physics and in quantum theory, there is a very precise statement that ensures the conservation of information.

In classical physics, this is Liouville's theorem, stating that the probability distribution function is constant along any trajectory in phase space. To make this more precise, take the phase space of a physical system to consist of the canonical coordinates q_i and their conjugate momenta p_i . The system at a fixed time can be described by the phase space distribution function $\rho(q_i, p_i)$, which determines the probability of finding the system in an infinitesimal volume $d^n q d^n p$ of phase space:

$$dP(q_i, p_i) = \rho(q_i, p_i) d^n q d^n p, \quad (2.15)$$

where the probability of finding the system in a fixed volume V of phase space is found by integrating dP over this volume:

$$P(V) = \int_V dP = \int_V \rho(q_i, p_i) d^n q d^n p. \quad (2.16)$$

This probability should of course be invariant under canonical transformations of the coordinates q_i and p_i . Since the volume element $d^n q d^n p$ itself is invariant under these canonical transformations and thus also under Hamiltonian flow, we have

$$\frac{d\rho}{dt} = \frac{\partial \rho}{\partial t} + \frac{\partial \rho}{\partial q_i} \dot{q}_i + \frac{\partial \rho}{\partial p_i} \dot{p}_i = 0, \quad (2.17)$$

where a dot denotes a derivative with respect to time t . This implies that the Shannon entropy, which is a measure of the amount of information that is needed to completely specify the system or equivalently the uncertainty inherent in describing

a system by a probability density function ρ , is also invariant under Hamiltonian flow:

$$\frac{dI(\rho)}{dt} \equiv \frac{d}{dt} \int_{\Gamma} \rho(q_i, p_i) \ln(\rho(q_i, p_i)) d^n q d^n p = 0, \quad (2.18)$$

where $I(\rho)$ is the Shannon entropy and an irrelevant factor of $1/\ln(2)$ was left out². The information contained in the system, described by the probability density function $\rho(q_i, p_i)$, is thus seen to be a conserved quantity. It is in this way that in classical physics we say that information is never lost.

In quantum theory, the relevant statement is unitarity of the evolution operator. Uncertainty in quantum mechanical systems is described by defining a density operator

$$\hat{\rho} \equiv \sum_i p_i |\psi_i\rangle \langle \psi_i|, \quad (2.19)$$

with p_i the probability that the system is in the state $|\psi_i\rangle$ and where a discrete number of states was assumed for simplicity. Under unitary evolution of the states $|\psi_i\rangle$, determined by a Hamiltonian operator \hat{H} , the density operator obeys the von Neumann equation:

$$\frac{\partial \hat{\rho}}{\partial t} = \frac{1}{i\hbar} [\hat{H}, \hat{\rho}], \quad (2.20)$$

which also implies that the von Neumann entropy

$$S(\hat{\rho}) \equiv \text{Tr} \hat{\rho} \ln(\hat{\rho}) \quad (2.21)$$

is conserved. This can be easily seen from equation (2.19) if we evolve the states $|\psi_i\rangle$ by a unitary time evolution operator.

In order not to abandon this quite fundamental notion of information preservation, a consistent quantum theory of gravity is expected to resolve the information paradox by providing a description of black holes in terms of a large amount of microstates. The Hawking radiation could then contain information about the exact microstate distribution of the black hole, thereby leaking information back to its environment. It is important to note that this suggests that the information, contained in the microstate description, is available at the horizon, where the radiation originates. The fuzzball proposal, already briefly mentioned in the introduction, makes this rather explicit by providing microstate geometries that differ on the scale of the horizon radius.

²By definition, the Shannon entropy uses the binary logarithm $\text{blog}(\rho)$ to give the uncertainty the dimension of number of bits. The ratio is given by $\ln(\rho) = \ln(2) \text{blog}(\rho)$, which just gives an extra factor of $\ln(2)$.

2.4 Summary

In this chapter, we have described the causal properties of black holes by looking at a specific example, the Schwarzschild solution. This causal structure can best be seen by a coordinate transformation that results in a Penrose diagram, representing the radial and time part of spacetime and where the lightlike directions are at 45 degree angles. These diagrams can also be used to picture the formation of a Schwarzschild black hole by a collapsing shell. In this case, the global nature of the event horizon became apparent.

A different coordinate transformation, followed by an approximation that neglects the tidal effects of gravitation, which is argued to be allowed at the horizon for large black holes, leads to the Rindler approximation. In this approximation, which is flat, a static Schwarzschild observer appears as an accelerating observer in Minkowski space. Again, there seems to be a region in spacetime that can never exert influence on this accelerating observer. The notion of an event horizon is thus seen to be similar to systems with an accelerating observer.

The Unruh effect is then shown to arise for accelerating observers, implying that a static Schwarzschild observer will see the horizon as a thermal region with a temperature $1/8\pi M$, where M is the mass of the black hole. This observation leads in a natural way to a law that is very reminiscent of the first law of thermodynamics, suggesting that the black hole has an associated entropy, which equals one quarter of its horizon area. As the entropy of a system gives a measure for the number of physical degrees of freedom, this scaling behaviour seems to indicate that the degrees of freedom of a black hole live on the horizon, a statement that is confirmed by the viewpoint of an outside observer: all infalling matter forms thin shells around the horizon, without ever falling through it, as far as the distant observer can see.

At last, the information paradox was discussed. The apparent violation of information conservation by the evaporation of a black hole by Hawking radiation was shown to conflict with the fundamental properties of both classical and quantum theories. The resolution of this paradox in some specific cases will form a central theme in this thesis.

The topics we discussed in this chapter set the stage for the remainder of this thesis. More specifically, we will see how string theory provides for a microstate description of specific classes of black holes, thereby giving a microscopic foundation for the macroscopic Bekenstein–Hawking entropy.

Chapter 3

BPS states in string theory

In this chapter, we will lay the foundations for the description of BPS states in type IIA string theory, compactified on a Calabi–Yau threefold. The main motivation for studying this subsector of states in string theory comes from a correspondence between these states and supersymmetric black hole states in supergravity. Because BPS states are protected by supersymmetry, they can be studied in different regimes of the theory. One of the common techniques to get a grasp on the elusive nature of black hole microstates, expected to provide for a microscopic interpretation of their macroscopic entropy, is by tuning the string coupling to zero. If this process can be done adiabatically and in a reversible way, the entropy of the system should remain fixed. At a certain point, the system would cease to represent a black hole and what remains is just a complex state in string theory, consisting of excited strings and, possibly, D–branes. The degeneracy of these states can then be counted and its logarithm compared to the Bekenstein–Hawking entropy of the original black hole.

The reason for studying this correspondence in a model that has $\mathcal{N} = 2$ supersymmetry and restricting to the states that preserve half of this supersymmetries, is mainly a trade–off between calculational feasibility and phenomenological complexity. The more supersymmetry is broken, the more difficult it becomes to analyze the resulting theory quantitatively. On the other hand, having a lot of supersymmetries results in a theory whose properties can become too trivial. Just as in the case of Seiberg–Witten theory, $\mathcal{N} = 2$ seems to be a middle way, having enough supersymmetries to do exact calculations, but not too much to spoil the possibility of interesting and complex physical phenomena.

In the first section, a brief overview of string theory will be given, highlighting some of the peculiar properties that distinguish it from ordinary quantum field theory. These exact same properties, that are forced upon us by the theory in the sense

that no one has put in these features by hand, have inspired many physicists to believe that string theory is a right step in the direction of a genuine unified theory of nature. The next section will introduce the main elements, common to theories with $\mathcal{N} = 2$ supersymmetry. After these very basic and introductory sections, the real adventure begins by exploring in subsequent sections the attractor mechanism, split flow trees and elliptic genera, which are among the main tools we will use throughout this thesis to describe and analyze BPS states. In the final section, a short account is given as to how these tools could be used to calculate degeneracies of D-particles. The method, described in this section will form the basis of a more refined method, developed by the author and collaborators, and constitutes the main part of this thesis (chapter 4).

3.1 String theory

Originally developed as a model to account for the large number of resonances in the strong interaction and in particular their organization along linearly rising Regge trajectories, string theory has become the favorite unification tool for a large part of the high energy physics community. The need for such a theory developed out of the difficulties in trying to reconcile Einstein's theory of General Relativity and Quantum Field Theory.

Applying the general principles of Quantum Field Theory to the classical field theory of General Relativity, one encounters divergences that can not just be removed by the usual procedure of renormalization. One phrases this fact often by saying that General Relativity is perturbatively unrenormalizable. The number of counterterms needed in this procedure is infinite, so we are left with a quantum theory with an infinite amount of couplings, which clearly loses every predictive power as a physical theory.

A way to understand what goes wrong when trying to quantize gravity, is to look at its gauge group. The gauge group of General Relativity consists of the spacetime diffeomorphisms. This implies that a local operator $\phi(x^\mu)$, with x^μ denoting the coordinates of a spacetime point, can never be a gauge invariant operator, as the gauge group acts directly on the coordinates x^μ . While this may seem as a quite rough statement of the problems encountered in quantum gravity, many physicists now believe that it is at the core of the problem: locality should in some way be abandoned to cure the divergences of gravity at high energies.

Before looking at how string theory may be just the right theory to do that, let us first return to some of the properties of black holes, encountered in chapter 2 and their implications. The standard particle physicist is used to probe ever smaller distance scales by increasing the energy, involved in the experiment. This is also the main reason for building very large particle accelerators, such as the Large

Hadron Collider in CERN. If one would however be able to increase the energies of the colliding particles up to the Planck scale, something strange happens. The information we wish to extract from the experiment, at very small length scales, will be hidden behind a horizon, because tiny black holes are created in the collision. Increasing the energy only makes things worse: the horizon radius also increases and we are probing at larger, instead of smaller, length scales. This peculiar behaviour seems to dovetail nicely with the remark in the previous paragraph: at high energies, one needs to let go of locality. Apparently, there is a smallest length scale, beyond which the standard notions of spacetime should be altered.

This brings us quite naturally to string theory. In this theory, spacetime is not probed by point particles, which could in principle uncover spacetime properties at arbitrary resolution, but by tiny one-dimensional strings. At low energies, compared to the string scale, these strings behave like point particles and we recover the usual geometry of Quantum Field Theory. At high energies however, the length of the string, which in general increases with the energy, will become larger than the length scale you wish to study and spacetime is now swept out by a one-dimensional object, revealing all kinds of information, but not the pointlike geometry of spacetime.

In the next subsection, we will start with the Polyakov action in string theory and show how the string coupling enters the description. This is followed by a section on D-Branes, which play a vital role in this thesis. We will end our brief journey into string theory with an analysis of the low energy effective actions in string theory and an outline of the basic strategy to calculate black hole degeneracies using these tools.

For a more in-depth study of string theory and some of its applications, we refer the reader to the standard textbooks [30, 31, 32, 33, 34, 35].

3.1.1 Polyakov action and the string coupling

The study of string theory traditionally starts from the Polyakov action¹, which determines the dynamics of a two-dimensional string, with coordinates σ^0, σ^1 and worldsheet M , moving in a target spacetime with coordinates X^μ and metric $G_{\mu\nu}$:

$$S_P[X, \gamma] = -\frac{1}{4\pi\alpha'} \int_M d^2\sigma \sqrt{-\gamma} \gamma^{ab} \partial_a X^\mu \partial_b X^\nu G_{\mu\nu}, \quad (3.1)$$

where γ_{ab} is a metric on the worldsheet and γ denotes its determinant. One notices that the fields $X^\mu(\sigma)$, determining the embedding of the string in spacetime, appear as bosonic scalar fields in the worldsheet theory. The metric field $\gamma_{ab}(\sigma)$, which contains three independent components, can be used to fix the gauge degrees

¹For introductory purposes, we will restrict to the bosonic string in this section.

of freedom. A closer inspection of the action reveals that one also has three independent gauge symmetries: worldsheet reparametrization in σ^0, σ^1 and Weyl symmetry, which rescales the metric: $\gamma_{ab} \rightarrow \gamma'_{ab} = e^{2\omega} \gamma_{ab}$.

Without spoiling the aforementioned symmetries, one can add an extra term to this action, which is just the Einstein–Hilbert action for the two–dimensional worldsheet:

$$S_{EH} = -\frac{\lambda}{4\pi} \int_M d^2\sigma \sqrt{-\gamma} R, \quad (3.2)$$

where R denotes the Ricci scalar of the worldsheet metric γ_{ab} and a factor λ is included, which is a priori unknown, but will turn out to be dynamically determined. The value of the Einstein–Hilbert action turns out to be given by the topology of the two–dimensional worldsheet, much unlike the case in four dimensions, where it determines the gravitational dynamics of General Relativity. Its insertion in the path integral will only introduce a weight $e^{-\lambda\chi}$, where χ is the Euler number of the worldsheet topology. Restricting for the moment to closed strings, the worldsheet topology is completely determined by the number of handles, which is also its genus g , and the Euler characteristic is then:

$$\chi = 2 - 2g. \quad (3.3)$$

In figure 3.1, two different topologies of closed worldsheets are shown. The one on the right has one extra handle, so that the path integral receives an extra factor of $e^{2\lambda}$. Since, as the figure clearly shows, this topology corresponds to the emission and reabsorption of a closed string, one defines the string coupling to be the square root of this factor:

$$g_s \equiv e^\lambda. \quad (3.4)$$

Already at this point, we can intuitively argue why string theory should provide for a less problematic description of gravity. The infinities, encountered when one calculates amplitudes in canonically quantized General Relativity, are due to short distance divergences, also referred to as ultraviolet divergences. This happens in the perturbative picture when several interaction vertices (almost) coincide. The resolution, which is also suggested by the discussion regarding the Planck length in section 1.1, could consist of a method to spread the interaction over length scales of the order the Planck length. This could mean a drastic deviation from the classical picture of spacetime at these length scales. String theory provides a realization of this idea: as can be seen in figure 3.1, the interaction does not occur at a specific spacetime event. Depending on the inertial frame an observer uses, the splitting of the string into two strings will seem to occur at different spacetime points. This actually spreads the interaction, thereby offering the possibility to avoid the main cause of divergences in a perturbative calculation of General Relativity.

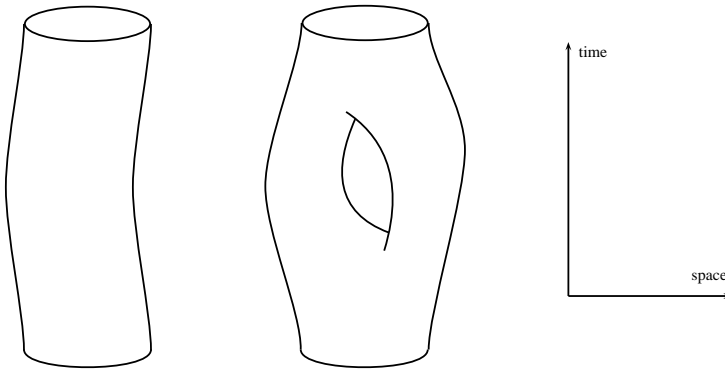


Figure 3.1: This figure shows two possibilities for the propagation of a closed string in spacetime, whereby it sweeps out a two-dimensional surface. The first figure from the left shows a free propagation of a closed string. In the second one, an interaction occurs during the propagation: a closed string is emitted and reabsorbed.

The string theory interaction mechanism has an additional advantage. In standard Quantum Field Theory, one needs to specify the particle content and their interaction terms. In string theory, one recovers the interactions automatically, if one knows the action of a free string. The reason for this is that a general Feynman diagram in string theory, such as the one in figure 3.1, can be calculated by using the free string action, evaluated on a non-trivial worldsheet topology. There are no interaction points, whose characteristics one needs to specify.

The considerations made above are all in the context of perturbative string theory, where amplitudes are calculated using the free string action, evaluated over worldsheets of different topology. The treatment also only involved closed strings, which have no boundary points. Next, we will begin exploring some non-perturbative objects in string theory, which are closely related to the existence of open strings in the theory.

Before doing so, the previously stated Polyakov action will be supplemented with some extra terms. These arise through the following arguments. The spacetime metric $G_{\mu\nu}$ in equation (3.1) should not be seen as a background, provided outside the realms of string theory. By expanding this metric around the flat one, one recovers that in the path integral, it arises as a coherent state of massless string excitations. This means that we should include also fields that arise by other string excitations. These give rise to an antisymmetric tensor field $B_{\mu\nu}$, called the Kalb-Ramond field, and the dilaton Φ . Coupling these fields in a consistent way

to the worldsheet scalars then gives rise to the following action:

$$S = \frac{1}{4\pi\alpha'} \int_M d^2\sigma \sqrt{-\lambda} \{ (\gamma^{ab} G_{\mu\nu} + i\epsilon^{ab} B_{\mu\nu}) \partial_a X^\mu \partial_b X^\nu + \alpha' \Phi R \}, \quad (3.5)$$

where ϵ^{ab} is the totally antisymmetric Levi–Civita symbol and R is the worldsheet Ricci scalar. From this formulation, one can deduce that the factor λ in equation (3.2) is actually the vacuum expectation value of the dilaton field, so we have $g_s = e^{\langle\Phi\rangle}$.

3.1.2 D–branes and open strings

By including open strings in the theory, the equations of motion, resulting from the Polyakov action (3.1), will include boundary terms. This will impose some boundary conditions on the open string endpoints, which can be of two types: Neumann or Dirichlet. For Neumann boundary conditions, the string endpoints move freely in spacetime, while in the Dirichlet case, they are fixed in spacetime. Of course, one can safely mix these two types of boundary conditions, resulting in open strings that can move freely only in certain subspaces of the bulk spacetime.

These subspaces of spacetime, to which the string endpoints are confined, give rise to the notion of D–branes. They are non–perturbative objects in string theory that encode the boundary conditions of open strings. One speaks of a D p –brane, when this object has p spacelike dimensions and one time dimension. The worldvolume of a D p –brane thus constitutes a $p+1$ –dimensional volume. The following paragraphs are meant to provide some basic results in the field of D–brane physics. For more details about D–branes in string theory, a consultation of [36, 37, 34] is highly recommended.

Worldvolume actions

In the previous description of D–branes, they were rigid objects to which the string endpoints are confined, which implies that they are infinitely massive. If they arise as solitaire states in string theory, it is however more natural if they had a finite mass and consequently, are dynamic objects that can move in spacetime themselves. To achieve this, one must find an action, describing the D–brane dynamics.

Firstly, we need to note that the worldsheet action of equation (3.5) describes closed strings, in the sense that the spacetime fields $G_{\mu\nu}$, $B_{\mu\nu}$ and Φ arise as massless closed string excitations. If one also includes the massless open string excitations, an extra bulk field A_μ appears, which couples to the string endpoints. One can thus consider this field as to live on the D–brane worldvolume, since that

is the space on which the string endpoints live. On the worldvolume, this field is a $U(1)$ gauge field.

Coupling the spacetime fields to the D-brane's embedding coordinate scalars $X^\mu(\xi_a)$ (where the ξ_a are coordinates on the worldvolume) and its gauge field A_a with field strength F_{ab} , gives the following action, which is the Dirac–Born–Infeld action for Dp-brane:

$$S_{DBI} = -T_p \int_{V_{p+1}} d^{p+1}\xi e^{-\Phi} \sqrt{\det(G_{ab} + B_{ab} + 2\pi\alpha' F_{ab})}, \quad (3.6)$$

with G_{ab} and B_{ab} the pullbacks of the respective spacetime fields to the D-brane worldvolume. The D-brane tension is given by $T_p e^{-\langle\Phi\rangle} = T_p g_s^{-1}$, with $\langle\Phi\rangle$ the dilaton vacuum expectation value, and encodes its mass density. Note that its inverse proportionality to the string coupling g_s is very natural for a non-perturbative object.

Ramond–Ramond fields

On top of the Dirac–Born–Infeld action discussed previously, there also exists a Wess–Zumino like term in the D-brane worldvolume action, which describes how the D-brane couples to the Ramond–Ramond fields that appear in type II superstring theory² (which is a supersymmetric extension of the bosonic string theory that we have used throughout the previous sections):

$$S_{WZ} = \mu_p \int_{V_{p+1}} C_{p+1}, \quad (3.7)$$

where C_{p+1} is the differential $p+1$ form that corresponds to a Ramond–Ramond potential. This straightforward action is, again, not the whole story however. It has been noted that consistency requires that the lower-dimensional Ramond–Ramond fields couple to the gauge field and curvature of the D-brane. The end result is the action:

$$S_{WZ} = \mu_p \int_{V_{p+1}} C \wedge e^{2\pi\alpha' F+B} \wedge \sqrt{\frac{\hat{A}(TV_{p+1})}{\hat{A}(NV_{p+1})}}, \quad (3.8)$$

where C denotes a polyform, containing all Ramond–Ramond potentials, \hat{A} is the A-roof genus³, TV_{p+1} and NV_{p+1} are respectively the tangent and normal bundles of the D-brane worldvolume and the integration is performed over combinations

²We now jump to a description valid for worldsheet actions with supersymmetry, although we shall only write down the results for the bosonic degrees of freedom.

³This is a characteristic class of vector bundles. In this case, the vector bundles are the tangent and normal bundles, so this term in the action encodes the coupling of Ramond–Ramond fields to gravity. For more details about characteristic classes, see for example [38].

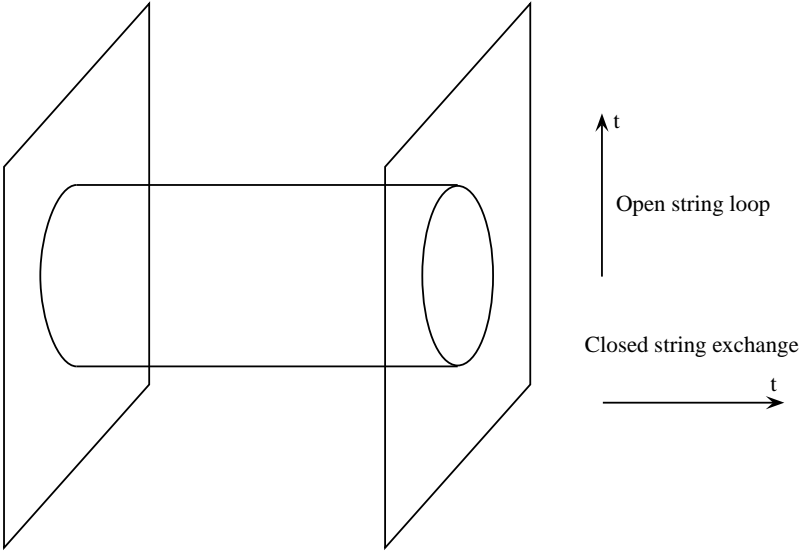


Figure 3.2: Open/closed string duality. By taking the time direction to be vertical or horizontal, we respectively get an open string loop diagram or a closed string exchange between the two D-branes.

of all these differential forms that have degree $p + 1$. This formula is related to those given appendix C, where the charges of D-branes are treated.

The prefactors $\tau_p \equiv T_p g_s^{-1}$ and μ_p can be related by considering two parallel D-branes, which are BPS. In this case, there should be no net force between them, or equivalently, the forces arising from gauge and gravitational interactions should cancel [39]. This leads to:

$$\mu_p = (2\pi)^{-p} \alpha'^{-\frac{p+1}{2}}$$

$$\tau_p = T_p g_s^{-1} = \mu_p g_s^{-1}. \quad (3.9)$$

The previous result comes from calculating a loop diagram for open strings and relating this to an exchange of a closed string between D-branes. Figure 3.2 shows how these two are related. This is an example of open/closed string duality, relating amplitudes in the open string sector to calculations in the closed string sector. Since the open string sector contains gauge interactions (from the massless open string excitation that is called the photon) and the closed string sector contains gravity, this is also an example of gauge/gravity duality.

3.1.3 Low energy effective actions

Because the masses of string excitations are all proportional to $l_s^{-1} \equiv \alpha'^{-1/2}$, it is clear that by taking $\alpha' \rightarrow 0$, while considering the theory at some fixed energy scale, will eliminate all but the massless string excitations from the spectrum. This is a result of the fact that the (very) massive excitations will not be created in physical processes at low energies. So this limit actually corresponds to a low energy limit of the string theory under consideration.

Another way of seeing this is that, in principle, one could construct an effective action by integrating out all massive string modes. Schematically, if we denote the massless modes by ϕ_0 and the massive ones by ϕ_i , the path integral is:

$$\int [\mathcal{D}\phi_0] e^{-S_{eff}[\phi_0]} \equiv \int [\mathcal{D}\phi_0][\mathcal{D}\phi_i] e^{-S[\phi_0, \phi_i]}, \quad (3.10)$$

with S_{eff} the effective action.

Just as in bosonic string theory, one could try to find the effective spacetime actions by calculating the beta functions of the different couplings in the worldsheet action, which should vanish by conformal symmetry arguments. Putting these beta functions to zero then gives the equations of motion for the spacetime fields and it is feasible to then find an action that produces exactly these equations of motion. In superstring theory however, the amount of supersymmetry uniquely determines the form of the effective spacetime actions, so there is no need to go through these awkward calculations.

For the two type II string theories, called IIA and IIB string theory, these effective actions are the ten-dimensional $\mathcal{N} = 2$ supergravity theories, which share their name with their parent string theory. Their actions will contain exactly those fields which correspond to the massless string excitations of the corresponding string theory. The unique eleven-dimensional supergravity theory, from which one can construct the type IIA supergravity theory by dimensional reduction, was first suggested in [40], which also mentioned the two ten-dimensional supergravity theories. It was then constructed in detail in [41]. The type IIB supergravity theory was first considered explicitly in [42] and further developed by [43, 44, 45].

The action of the ten-dimensional IIA supergravity theory can be formulated as⁴:

$$S_{IIA} = \frac{1}{2\kappa_0^2} \int d^{10}x \sqrt{-G} \left\{ e^{-2\Phi} \left[R + 4(\nabla\Phi)^2 - \frac{1}{2}(H_{(3)})^2 \right] - \frac{1}{2} [(F_{(2)})^2 + (F_{(4)})^2] \right\} - \frac{1}{4\kappa_0^2} \int B_{(2)} \wedge dC_{(3)} \wedge dC_{(3)}, \quad (3.11)$$

⁴To make things more readable, we will only list the bosonic fields of the actions in this section.

where $F_{(2)} = dC_{(1)}$, $F_{(4)} = dC_{(3)} + H_{(3)} \wedge C_{(1)}$, $C_{(1)}$ and $C_{(3)}$ are the Ramond–Ramond potentials and $H_{(3)} = dB$ is the field strength of the antisymmetric tensor field.

For type IIB, the action can be formulated as:

$$S_{IIB} = \frac{1}{2\kappa_0^2} \int d^{10}x \sqrt{-G} \left\{ e^{-2\Phi} \left[R + 4(\nabla\Phi)^2 - \frac{1}{2}(H_{(3)})^2 \right] - \frac{1}{2} \left[(F_{(1)})^2 + (F_{(3)})^2 + \frac{1}{2}(F_{(5)})^2 \right] \right\} - \frac{1}{4\kappa_0^2} \int C_{(4)} \wedge H_{(3)} \wedge dC_{(2)}, \quad (3.12)$$

where $F_{(1)} = dC_{(0)}$, $F_{(3)} = dC_{(2)} + H_{(3)} \wedge C_{(0)}$, $F_{(5)} = dC_{(4)} + \frac{1}{2}H_{(3)} \wedge C_{(2)} + \frac{1}{2}B_{(2)} \wedge dC_{(2)}$, $C_{(0)}$, $C_{(2)}$ and $C_{(4)}$ are the Ramond–Ramond potentials and $H_{(3)} = dB$ is the field strength of the antisymmetric tensor field. On top of the equations of motion, one must also require that the five form field strength $F_{(5)}$ is self-dual.

The reason we wish to study these low energy approximations to string theory, is that we will be interested in supersymmetric solutions of compactifications of these theories on a Calabi Yau manifold.

This concludes our lightning review of string theory and the non-perturbative D-branes it contains. We will come back to it later, when the topological B model is treated in section 4.2.

3.2 $\mathcal{N} = 2$ in various dimensions

In the last section, we showed the appearance of supergravity theories as a low energy limit of string theory. When these theories are compactified on a Calabi Yau threefold, thereby resulting in a theory with only four non-compact spacetime dimensions, we end up with a theory that exhibits $\mathcal{N} = 2$ supersymmetry (see section 3.3.1). Therefore, this section will provide a short overview of the $\mathcal{N} = 2$ algebra in four dimensions and its representations. It is largely based on [46], and we will use their conventions and notation, except that the central charge is rescaled, such that the BPS bound becomes $M \geq |Z|$.

3.2.1 The $\mathcal{N} = 2$ algebra

In this section, the $\mathcal{N} = 2$ superalgebra in four dimensions, containing the Poincaré algebra as a subalgebra, will be discussed. The Poincaré algebra in 3+1 dimensions

is determined by the following commutation relations:

$$\begin{aligned}
 [P_\mu, P_\nu] &= 0, \\
 [P_\mu, J_{\nu\sigma}] &= \eta_{\mu\nu}P_\sigma - \eta_{\mu\sigma}P_\nu, \\
 [J_{\mu\nu}, J_{\sigma\rho}] &= \eta_{\mu\rho}J_{\nu\sigma} + \eta_{\nu\sigma}J_{\mu\rho} - \eta_{\mu\sigma}J_{\nu\rho} - \eta_{\nu\rho}J_{\mu\sigma},
 \end{aligned} \tag{3.13}$$

where P_μ are the generators of spacetime translations and $J_{\mu\nu}$ are the Lorentz generators, representing infinitesimal rotations and boosts.

The $\mathcal{N} = 2$ extended superalgebra, which contains this Poincaré algebra as a subalgebra, is generated by the spinorial generators $Q_\alpha{}^I, \bar{Q}_{\dot{\alpha}J}$, which are two component Weyl spinors with $\alpha, \dot{\alpha}$ denoting the spinor indices, and the (anti)commutation relations:

$$\begin{aligned}
 \{Q_\alpha{}^I, \bar{Q}_{\dot{\beta}J}\} &= 2\sigma_{\alpha\dot{\beta}}{}^\mu P_\mu \delta^I{}_J, \\
 [P_\mu, Q_\alpha{}^I] &= [P_\mu, \bar{Q}_{\dot{\alpha}I}] = 0, \\
 \{Q_\alpha{}^I, Q_\beta{}^J\} &= 2\epsilon_{\alpha\beta}\epsilon^{IJ}Z, \\
 \{\bar{Q}_{\dot{\alpha}I}, \bar{Q}_{\dot{\beta}J}\} &= 2\epsilon_{\dot{\alpha}\dot{\beta}}\epsilon^{IJ}Z/,
 \end{aligned} \tag{3.14}$$

where $I, J \in \{1, 2\}$ (hence the notation $\mathcal{N} = 2$), σ^μ are the Pauli matrices supplemented by $\sigma^0 \equiv -1$ and Z is an operator that commutes with all the other operators. Such an operator is also called a central operator and the charge of a state under this operator will be called the central charge. Note that the commutators between $J_{\mu\nu}$ and $Q_\alpha{}^I, \bar{Q}_{\dot{\alpha}J}$ are determined by the fact that they are two component Weyl spinors.

3.2.2 Representations and BPS states

The representations of this algebra will now be discussed for eigenstates of the generators P_μ . These fall into two distinct classes: massive ($p^\mu p_\mu > 0$) and massless ($p^\mu p_\mu = 0$) states⁵. For massive states, we distinguish between representations with central charge $Z = 0$ and representations with non-trivial Z . The first thing to note is that the contraction between the Pauli matrices and the momentum vector, appearing in the anticommutator of the supercharges, can be written as:

$$\sigma_{\alpha\dot{\beta}}{}^\mu P_\mu = \begin{pmatrix} -P_0 + P_3 & P_1 - iP_2 \\ P_1 + iP_2 & -P_0 - P_3 \end{pmatrix} \tag{3.15}$$

⁵We denote by p_μ the eigenvalue of the operator P_μ .

Massive states, $Z = 0$

For massive states, we can boost to a rest frame, where $p_\mu = (-M, 0, 0, 0)$, with M the mass of the state. The supersymmetry algebra with central charge $Z = 0$ then becomes:

$$\begin{aligned} \{Q_\alpha{}^I, \bar{Q}_{\dot{\beta}J}\} &= 2M\delta_{\alpha\dot{\beta}}\delta^I{}_J, \\ \{Q_\alpha{}^I, Q_\beta{}^J\} &= \{\bar{Q}_{\dot{\alpha}I}, \bar{Q}_{\dot{\beta}J}\} = 0. \end{aligned} \quad (3.16)$$

Rescaling the generators to

$$\begin{aligned} a_\alpha{}^I &= \frac{1}{\sqrt{2M}}Q_\alpha{}^I \\ (a_\alpha{}^I)^\dagger &= \frac{1}{\sqrt{2M}}\bar{Q}_{\dot{\alpha}I}, \end{aligned} \quad (3.17)$$

the algebra of the supercharges reduces to four fermionic creation and annihilation operators. These can be used to create the following states from the Clifford vacuum⁶ $|\Omega\rangle$, which is annihilated by every annihilation operator $a_\alpha{}^I$:

$$|\alpha_1, I_1; \dots; \alpha_n, I_n; \Omega\rangle \equiv \frac{1}{\sqrt{n!}}(a_{\alpha_1}{}^{I_1})^\dagger \dots (a_{\alpha_n}{}^{I_n})^\dagger |\Omega\rangle, \quad (3.18)$$

where $\alpha_i, I_i \in \{1, 2\}$ and $0 \leq n \leq 4$. In the case the Clifford vacuum is non-degenerate (and thus spin 0), this representation is called the fundamental irreducible massive multiplet, which has dimension $2^4 = 16$. It contains 5 real scalars, 4 spin $\frac{1}{2}$ particles and one massive vector particle, for a total of 8 bosonic and 8 fermionic degrees of freedom. If the Clifford vacuum has spin different from zero, the resulting multiplet can be found by taking the tensor product of the relevant spin representation with the fundamental multiplet. Its spin decomposition then follows from the usual rules for composition of angular momenta.

Massless states

If the state is massless, we can adopt a frame where $P_\mu = (-E, 0, 0, E)$, such that⁷:

$$\begin{aligned} \{Q_\alpha{}^I, \bar{Q}_{\dot{\beta}J}\} &= 4E\delta_{\alpha\dot{\beta}}\delta^I{}_J, \\ \{Q_\alpha{}^I, Q_\beta{}^J\} &= \{\bar{Q}_{\dot{\alpha}I}, \bar{Q}_{\dot{\beta}J}\} = 0. \end{aligned} \quad (3.19)$$

⁶This Clifford vacuum can be in a non-trivial representation of the Lorentz group. In other words, it can have non zero spin.

⁷Massless states always have zero central charge. This follows from the redefinition of the generators used in the next section.

Since now the \bar{Q}_{2I} must annihilate the representation, we only need to rescale the generators with spinor index 1:

$$\begin{aligned} a^I &= \frac{1}{\sqrt{4E}} Q_{1^I} \\ (a^I)^\dagger &= \frac{1}{\sqrt{4E}} \bar{Q}_{1^I}, \end{aligned} \tag{3.20}$$

with $I \in \{1, 2\}$. They generate an algebra of two fermionic creation and annihilation operators and acting on a non-degenerate Clifford vacuum $|\Omega\rangle$, they will create the following $2^2 = 4$ states:

$$|I_1; \dots; I_n; \Omega\rangle \equiv \frac{1}{\sqrt{n}} (a^{I_1})^\dagger \dots (a^{I_n})^\dagger |\Omega\rangle, \tag{3.21}$$

where $I_i \in \{1, 2\}$ and $0 \leq n \leq 2$. If the helicity of $|\Omega\rangle$ is λ , there will be one state with helicity λ , two with $\lambda + \frac{1}{2}$ and one with $\lambda + 1$.

Central charges and BPS states

For massive states in the presence of a central charge $Z \neq 0$, we use the following redefinition of generators:

$$\begin{aligned} a_\alpha &= \frac{1}{\sqrt{2}} (Q_\alpha{}^1 + \epsilon_{\alpha\beta} (Q_\beta{}^2)^\dagger) \\ b_\alpha &= \frac{1}{\sqrt{2}} (Q_\alpha{}^1 - \epsilon_{\alpha\beta} (Q_\beta{}^2)^\dagger). \end{aligned} \tag{3.22}$$

Their anticommutators are:

$$\begin{aligned} \{a_\alpha, a_\beta^\dagger\} &= \delta_{\alpha\beta} (2M + 2Z) \\ \{b_\alpha, b_\beta^\dagger\} &= \delta_{\alpha\beta} (2M - 2Z), \end{aligned} \tag{3.23}$$

with all other anticommutators vanishing. Since the norm of state vectors in the Hilbert space should be strictly positive, this results in a bound $M \geq |Z|$, which is related to the Bogomol'nyi-Prasad-Sommerfield bound found in [47, 48], or BPS bound for short. One immediately sees that massless states always have zero central charge. In the case this bound is saturated ($M = |Z|$), half of the creation operators will actually annihilate the state, meaning that the state preserves half of the supersymmetries of the vacuum. We are thus left with only two creation and annihilation operators, relevant for the state under consideration.

The fact that BPS representations contain only half the degrees of freedom as a massive non-BPS state implies that their number is protected with respect to

continuous deformations of the theory: new BPS states can only appear in pairs by a massive non-BPS state which decays, or vice versa, they can only disappear in pairs, by forming a non-BPS state.

Since these BPS states play a fundamental role in the research presented in this thesis, let us look a little bit closer at their representations. For positive central charge⁸ ($Z > 0$), the BPS representation will have $M = Z$. From equations (3.23), we see that the state is annihilated by all generators $b_\alpha, b_\alpha^\dagger$. So we need only consider the creation and annihilation operators $a_\alpha, a_\alpha^\dagger$. Starting from a non-degenerate Clifford vacuum $|\Omega^{(0)}\rangle$, which, by definition, is annihilated by a_α and has spin 0, and by acting on this vacuum with the creation operators a_α^\dagger , we get the *fundamental BPS representation*:

$$\begin{aligned} \text{spin } 0 &: |\Omega^{(0)}\rangle, \quad a_\alpha^\dagger a_\beta^\dagger |\Omega^{(0)}\rangle \\ \text{spin } 1/2 &: a_\alpha^\dagger |\Omega^{(0)}\rangle, \end{aligned} \tag{3.24}$$

consisting of two scalars and one spin 1/2 particle, for a total of two bosonic and two fermionic degrees of freedom. We will denote this representation by $(0, 0, 1/2)$, where the numbers refer to the spin of the scalars and the spinor.

If we would act with the creation operators on a Clifford vacuum with spin j , which for ease of notation we will denote (j) , the result can be written as the tensor product of (j) with the fundamental BPS representation. The multiplet then decomposes as a Lorentz representation as follows:

$$(0, 0, 1/2) \otimes (j) = (j - 1/2) \oplus 2(j) \oplus (j + 1/2), \tag{3.25}$$

where (j) denotes an irreducible Lorentz representation with spin j .

3.3 Attractor mechanism

As already mentioned before, BPS states in $\mathcal{N} = 2$ theories are of central importance in this thesis. In a suitable limit, see section 4.1, these correspond to supersymmetric solutions of a $\mathcal{N} = 2$ supergravity theory, representing the low energy limit of string theory, compactified on a Calabi Yau threefold. When studying these supersymmetric solutions, one encounters the *attractor equations* [49, 50]. These equations imply that the moduli of the Calabi Yau manifold will be fixed to special attractor values at the black hole horizon.

In this section, we will briefly review this mechanism in the context of type IIB string theory compactified on a Calabi Yau threefold X . Because of mirror symmetry, many of the results can also be phrased in the language of type IIA

⁸The same line of argument can be used for the case when the central charge is negative.

	Type IIA	Type IIB
Vector multiplets	$h^{1,1}$	$h^{2,1}$
Hypermultiplets	$h^{2,1} + 1$	$h^{1,1} + 1$

Table 3.1: Vector- and hypermultiplets in type II theories

string theory on the mirror Calabi Yau \tilde{X} . Some applications of the attractor mechanism can be found in [51, 52, 53].

3.3.1 Type IIB on $M_4 \times X$

We start by considering type IIB string theory on $M_4 \times X$, where M_4 is a non-compact four-dimensional spacetime, which is asymptotically Minkowski and X is a Calabi Yau threefold⁹. These compactifications were first described in [54, 55] for type I, and in [56] for type II superstring theory. For type II string theories, they result in a low energy $\mathcal{N} = 2$ supergravity theory. This result comes from the fact that by setting the supersymmetry variations of the gravitino to zero, one obtains the condition that there should exist a covariantly constant spinor on the internal manifold. This is a strong condition, because this implies:

$$[\nabla_m, \nabla_n]\zeta = \frac{1}{4}R_{mnpq}\Gamma^{pq}\zeta = 0, \quad (3.26)$$

where R_{mnpq} is the Riemann tensor and Γ^{pq} is an antisymmetrized product of Dirac matrices. This equation effectively restricts the components of Γ^{pq} from a general $SO(6)$ rotation to a subgroup $SU(3)$, which is the holonomy group of a Calabi Yau. The two 16-dimensional spinorial supersymmetry parameters of the ten-dimensional type II supergravity theory will then decompose into two spinorial supersymmetry parameters in the four-dimensional theory, with their six-dimensional counterpart given by the covariantly constant spinor ζ . This gives a $\mathcal{N} = 2$ supergravity theory in four dimensions.

The number of vector- and hypermultiplets is determined by the Hodge numbers of the compactification geometry and is summarized in table 3.1.

To see the appearance of these multiplets in the case of type IIB string theory, we will once more focus our attention to the bosonic field content. This content is directly related to the presence of harmonic forms on the Calabi Yau manifold. The counting of these forms is summarized in the Hodge diamond, see appendix A. We now enumerate the resulting multiplets.

Let us first set our notation: capital Latin indices range over all 10 dimensions, Greek indices denote 4-dimensional spacetime directions and lowercase Latin

⁹More information on the geometry of Calabi Yau threefolds is provided in appendix A.

indices are internal directions of the Calabi Yau. For these internal coordinates, the indices i, j, k, \dots and $\bar{i}, \bar{j}, \bar{k}, \dots$ are associated with holomorphic and antiholomorphic coordinates respectively.

The massless bosonic fields of type IIB string theory are: graviton g_{MN} , anti-symmetric tensor field b_{MN} , dilaton ϕ and Ramond–Ramond gauge fields c, c_{MN}, c_{MNOP} .

From the four-dimensional perspective, these fields can be identified with the following multiplets:

- Supergravity multiplet: spin 2 field $g_{\mu\nu}$ and vector $c_{\mu ijk}$;
- Universal hypermultiplet: scalars $a \sim b_{\mu\nu}$, $a' \sim c_{\mu\nu}$, ϕ and c , where a, a' denote two axions, dual to the antisymmetric two-forms $b_{\mu\nu}, c_{\mu\nu}$;
- $h^{1,1}$ hypermultiplets: for each harmonic $(1, 1)$ -form that exists on the Calabi Yau, there is a multiplet that consists of the following four real scalar fields: $g_{i\bar{j}}, b_{i\bar{j}}, c_{i\bar{j}}, c_{\mu\nu i\bar{j}}$, where $c_{\mu\nu i\bar{j}}$ again denotes the dual scalar;
- $h^{2,1}$ vector multiplets: there is one vector $c_{\mu i j \bar{k}}$ and two scalars $g_{i\bar{j}\bar{k}}, g_{i j \bar{k}}$ for each harmonic $(2, 1)$ -form. Here we have used $g_{i\bar{j}\bar{k}} \equiv g_{im} G^{m\bar{l}} \Omega_{\bar{l}\bar{j}\bar{k}}$, with $G_{i\bar{j}}$ and $\Omega_{\bar{i}\bar{j}\bar{k}}$ respectively the metric and the unique harmonic $(0, 3)$ -form¹⁰, and similarly for $g_{i j \bar{k}}$.

For the remainder of this thesis, we will be dealing only with the supergravity and vector multiplets. The hypermultiplet fields can thus be thought of as set to zero. In ungauged $\mathcal{N} = 2$ supergravity, this is a consistent truncation of the theory because the hypermultiplets decouple from the supersymmetry variations and equations of motion for the vector multiplets.

A similar structure appears in the low energy limit of type IIA string theory on $M_4 \times X$ but, as table 3.1 shows, with the roles of $(1, 1)$ - and $(2, 1)$ -forms interchanged. This observation is closely related to mirror symmetry: the mirror partner of a Calabi Yau manifold has the same Hodge numbers, but $h^{(1,1)}$ and $h^{(2,1)}$ are exchanged.

3.3.2 BPS states

As shown in the previous section, there are $h^{2,1} + 1$ $U(1)$ gauge vectors in the low energy theory, one as being part of the supergravity multiplet, the other $h^{(2,1)}$ living in vector multiplets. The one-particle Hilbert space \mathcal{H} will then be graded by the quantized charges of these $U(1)$ groups. Since every vector descends from the

¹⁰This harmonic $(0, 3)$ -form is unique, up to a complex factor.

self-dual Ramond–Ramond five-form F_{MNOPQ} in ten dimensions, at low energy these charges can be found from:

$$\int_{S^2} F = \Gamma \in H^3(X), \quad (3.27)$$

where the integration is performed over a two-sphere at spatial infinity. This gives the direct sum decomposition $\mathcal{H} = \bigoplus_{\Gamma} \mathcal{H}_{\Gamma}$, where \mathcal{H}_{Γ} denotes the part of the Hilbert space with charge Γ .

By using a symplectic basis α^I, β_J of $H^3(X)$, such that $\int_X \alpha^I \wedge \beta_J = \delta^I_J$, these charges can be written as $\Gamma = p^I \beta_I + q_I \alpha^I$, where we call the p^I and q_I magnetic and electric charges respectively¹¹.

Since a vacuum state is characterized by constant (in M_4) moduli fields, the Hilbert space \mathcal{H} will depend on boundary conditions of these moduli at spatial infinity, denoted collectively by t_{∞} . The central charge in the $\mathcal{N} = 2$ algebra depends on both the boundary conditions of the moduli and on the charge of the state, so we have $Z = Z(t_{\infty}, \Gamma)$. It can be explicitly calculated as

$$Z(t, \Gamma) = e^{K/2} \int_X \Omega \wedge \Gamma, \quad \text{with } e^{-K} = i \int_X \Omega \wedge \bar{\Omega}, \quad (3.28)$$

and Ω a generator¹² of $H^{(3,0)}(X)$. The dependence of Z on the moduli t is due to the fact that the Hodge decomposition of the harmonic three-forms

$$H^3(X) = H^{(3,0)}(X) \oplus H^{(2,1)}(X) \oplus H^{(1,2)}(X) \oplus H^{(0,3)}(X), \quad (3.29)$$

depends on the complex structure of X . The relevant moduli are thus the complex structure moduli of the Calabi Yau X . Our main object of study then, is the BPS sector of $\mathcal{H}_{\Gamma}(t_{\infty})$, or in other words, the states in $\mathcal{H}_{\Gamma}(t_{\infty})$, satisfying the BPS bound

$$M = |Z(t_{\infty}, \Gamma)|. \quad (3.30)$$

This sector will be denoted by $\mathcal{H}_{\Gamma}^{BPS}(t_{\infty})$. As we will see in the next sections, for these BPS states, the moduli are driven to a stationary point of $|Z(t, \Gamma)|^2$ at the horizons of their, possibly multiple, centers.

¹¹Note that this crucially depends on a choice of basis. In the IIA picture, where the charges live in the even cohomology groups of the Calabi Yau, this choice of basis can be taken as follows: the magnetic charges represent D6 and D4 brane charges, while the electric charges represent D2 and D0 brane charges. This is natural, since these D-branes couple magnetically, respectively electrically, to the Ramond–Ramond gauge fields c_M and c_{MNO} of the type IIA theory.

¹²Since the redefinition of Ω with an extra complex factor does not alter the result of (3.28), unless otherwise stated, we will take Ω to depend holomorphically on the complex structure moduli of X .

3.3.3 Supersymmetric black holes

In this section, field configurations satisfying the equations of motion of the $\mathcal{N} = 2$ supergravity theory will be considered, with the extra requirement that they preserve half of the supersymmetry. These correspond semiclassically to the aforementioned BPS sector of the Hilbert space of states. We will first look at static, spherically symmetric solutions, corresponding to single center black holes. This setting most clearly demonstrates the implications of the attractor mechanism for supersymmetric black holes, first described in [49, 50]. Then, we will briefly review the generalization to multicentered black holes [57, 58, 59, 60].

The bosonic part of the $\mathcal{N} = 2$ action, containing the relevant terms for the supergravity and vectormultiplets, can be written as:

$$S = \frac{1}{16} \int_{M_4} d^4x \sqrt{-G} R - 2g_{a\bar{b}} dz^a \wedge *d\bar{z}_{\bar{b}} - \pi \int_{M_4} F^I \wedge G_I. \quad (3.31)$$

Here, z, \bar{z} are the vector multiplet scalars, sitting in a special Kähler manifold with metric $g_{a\bar{b}}$; $G_{\mu\nu}$ and R are the four-dimensional spacetime metric and Ricci scalar respectively and the self-dual five-form field has been decomposed, using a symplectic basis $\alpha^I, \beta_I \in H^3(x)$:

$$F = F^I \wedge \beta_I - G_I \wedge \alpha^I. \quad (3.32)$$

Single centered BPS black holes

To find supersymmetric solutions to the equations of motion, one makes an Ansatz for the metric and vector fields. In the present case, single centered black holes, we look for static, spherically symmetric solutions. The line element can then be written as:

$$ds^2 = -e^{2U(r)} dt^2 + e^{-2U(r)} [dr^2 + r^2(d\theta^2 + \sin^2\theta d\phi^2)]. \quad (3.33)$$

We also make the following Ansatz for the vector fields:

$$F = \Gamma \sin\theta d\theta \wedge d\phi + \tilde{\Gamma} e^{2U(r)} dt \wedge dr, \quad (3.34)$$

where $\tilde{\Gamma}$ is determined by the self-duality of F .

We will then try to find supersymmetric solutions with vanishing Fermi fields¹³. In this case, the supersymmetry variation of the bosonic fields, which is linear in the fermionic fields, is automatically zero. For supersymmetry to be (partially)

¹³Lorentz invariance forbids vacuum expectation values for Fermi fields ψ . The only condensates allowed are scalar combinations of fields, like for example a $\langle \bar{\psi}\psi \rangle$ expectation value, which appears in superconducting phases.

preserved, we still need to impose that the supersymmetry variations of the fermionic fields vanish for some spinorial variation parameters ζ . This will result in first order equations in the bosonic fields. Using the Ansatz for the metric and vector fields, these equations can be succinctly denoted as:

$$\begin{aligned} \text{Gravitino: } \dot{U} &= -e^U |Z|, \\ \text{Gaugino: } z^a &= -2e^U g^{a\bar{b}} \partial_{\bar{b}} |Z|, \end{aligned} \quad (3.35)$$

where a dot denotes the derivative with respect to $\rho = 1/r$. Defining $\mu = e^{-U(\rho)}$, they can also be written as:

$$\begin{aligned} \text{Gravitino: } \dot{\mu} &= |Z|, \\ \text{Gaugino: } \mu \frac{dz^a}{d\mu} &= -g^{a\bar{b}} \partial_{\bar{b}} \log |Z|^2. \end{aligned} \quad (3.36)$$

It thus follows that μ increases monotonically for $\rho \rightarrow \infty$, which is equivalent to sending $r \rightarrow 0$. Going from spatial infinity to the horizon, where $G^{rr} = \mu^{-2} = 0$, the gaugino variation then implies that the moduli z^a flow to a minimum of $|Z|^2$. Using

$$|Z(t, \Gamma)|^2 = \frac{\int_X \Omega \wedge \Gamma \cdot \int_X \bar{\Omega} \wedge \Gamma}{i \int_X \Omega \wedge \bar{\Omega}}, \quad (3.37)$$

we have

$$\partial_a |Z(t, \Gamma)|^2 = \int_X \left(\partial_a \Omega - \frac{\int_X \partial_a \Omega \wedge \bar{\Omega}}{\int_X \Omega \wedge \bar{\Omega}} \Omega \right) \wedge \Gamma \cdot \frac{\int_X \bar{\Omega} \wedge \Gamma}{i \int_X \Omega \wedge \bar{\Omega}}, \quad (3.38)$$

and similarly for the $\partial_{\bar{b}}$ derivative. Note that here we used the freedom to define Ω as depending holomorphically on the complex structure moduli. Putting these partial derivatives to zero, we can distinguish two cases:

- $Z(t, \Gamma) = 0$: This clearly only happens when $\Gamma \in H^{(2,1)}(X) \oplus H^{(1,2)}(X)$.
- $Z(t, \Gamma) \neq 0$: Since infinitesimal deformations of the holomorphic three-form Ω are $\partial_a \Omega \in H^{(2,1)}(X)$, this implies that $\Gamma \in H^{(3,0)}(X) \oplus H^{(0,3)}(X)$.

Since the equations (3.36) can run into problems when $|Z| = 0$ at a regular point in moduli space (where the metric $g_{a\bar{b}}$ is nondegenerate), we will, for now, focus on the second case. The equation $\Gamma \in H^{(3,0)}(X) \oplus H^{(0,3)}(X)$ is the famous attractor equation, formulated as a condition on the Hodge structure of the Calabi Yau. Since Γ is real, or, as a consequence of charge quantization, $\Gamma \in H^3(X, \mathbb{Z})$, the attractor equation can also be formulated as

$$2 \operatorname{Im}(C\Omega) = \Gamma, \quad (3.39)$$

with C a complex constant. Because of the presence of this constant, this equation can also be used with a $(3, 0)$ -form Ω that does not depend holomorphically on the complex structure moduli.

At last, yet another form of the attractor equations, derived using the Bogomol'nyi trick of completing the squares in the action, was given in [57]:

$$2 \operatorname{Im}(e^{-U} e^{-i\alpha} \Omega_n) = -\Gamma\tau + 2 \operatorname{Im}(e^{-U} e^{-i\alpha} \Omega_n)_{\tau=0}, \quad (3.40)$$

where $\alpha \equiv \arg Z$ and Ω_n denotes the normalized $(3, 0)$ -form:

$$\Omega_n = \left(i \int_X \Omega \wedge \bar{\Omega} \right)^{-1/2} \Omega, \quad (3.41)$$

with Ω now an arbitrary generator of $H^{(3,0)}(X)$. As was noted in [57], this form of the equations should only be used when a specific three-cycle in $H_3(X)$ is not vanishing. Points in moduli space where cycles shrink to zero are singular, so the use of this equation is allowed at regular points.

Related to the comment of the last paragraph is the question of what happens when Z becomes zero at a specific point in moduli space. If this point is regular, no single flow can exist in an open neighborhood of this point. If it did exist, the state would be a massless BPS particle, which causes a singularity of the metric in moduli space [61, 62, 51], contradicting our assumption that the point is a regular point of moduli space.

Multicentered BPS black holes

The restriction to static, spherically symmetric solutions is actually too severe to produce a correspondence between supergravity solutions and BPS states in the compactified string theory. The description of this correspondence is postponed to section 4.1. Here, we prepare for this correspondence by discussing a generalization of single centered black holes to multicentered black holes, as developed in [63, 57, 58, 59, 60]. In this case, a less restrictive Ansatz is used for the metric. The metric of time independent BPS configurations can be cast into the form [64]:

$$ds^2 = -e^{2U} (dt + \omega)^2 + e^{-2U} dx^i dx^i, \quad (3.42)$$

where U and the one-form ω are now space dependent through their dependence on the moduli fields. Using the symplectic product of three-forms $\langle \Gamma_1, \Gamma_2 \rangle \equiv \int_X \Gamma_1 \wedge *_X \Gamma_2$, with $*_X$ the Hodge star operator on the Calabi Yau manifold X , the generalization of (3.40) for the stationary case was found to be [57]:

$$\begin{aligned} 2 \operatorname{Im}(e^{-U} e^{-i\alpha} \Omega_n) &= H, \\ *_3 d\omega &= \langle dH, H \rangle, \end{aligned} \quad (3.43)$$

with $*_3$ the Hodge star operator on \mathbb{R}^3 , α a real function and H a $H^3(X)$ -valued harmonic function on \mathbb{R}^3 (the space part, with coordinates x^i). For N centers with charges Γ_i at locations \mathbf{x}_i , it is given by:

$$H = - \sum_{i=1}^N \Gamma_i \tau_i + 2 \operatorname{Im}(e^{-i\alpha} \Omega_n)|_{r=\infty}, \quad (3.44)$$

with $\tau_i \equiv 1/|\mathbf{x} - \mathbf{x}_i|$. Whereas a single centered black hole is described by the harmonic function $H = h + Q/r$, with Q denoting its charge, equation (3.44) is seen to represent a sum of such terms, corresponding to charges located at N distinct ‘centers’. Contrary to the situation in Einstein’s theory of General Relativity, the positions of these point charges are fixed: the different forces that would tend to set them in motion exactly compensate.

The equations imply that for $r \rightarrow \infty$, α goes asymptotically to $\arg Z(\sum_i \Gamma_i)$, while for $\mathbf{x} \rightarrow \mathbf{x}_i$, one has $\alpha \rightarrow \arg Z(\Gamma_i)$. For a solution of (3.43) to exist, an important integrability condition must be satisfied. This condition can be stated, for each charge center i , as:

$$\sum_{i \neq j=1}^N \frac{\langle \Gamma_i, \Gamma_j \rangle}{|\mathbf{x}_i - \mathbf{x}_j|} = 2 \operatorname{Im}(e^{-i\alpha} Z(\Gamma_i))|_{r=\infty}, \quad (3.45)$$

which for two centers reduces to the following equation for the distance between the centers:

$$|\mathbf{x}_i - \mathbf{x}_j| = \frac{\langle \Gamma_i, \Gamma_j \rangle}{2} \cdot \frac{|Z|}{\operatorname{Im}(Z_1 \bar{Z}_2)} \Big|_{r=\infty}, \quad (3.46)$$

implying the integrability condition

$$\langle \Gamma_i, \Gamma_j \rangle \operatorname{Im}(Z_1 \bar{Z}_2)|_{r=\infty} > 0. \quad (3.47)$$

3.4 Split flow trees

Solutions of the attractor equations (3.43) will have a very specific asymptotical behaviour at infinity and near the charge centers. As was already stated for the real field $\alpha(\mathbf{x})$, at infinity, the flow in moduli space will look like an ordinary single flow for a spherically symmetric solution with total charge $\Gamma \equiv \sum_i \Gamma_i$. This can be understood from the fact that in this limit, the τ_i can be taken equal to $\tau \equiv 1/r$. On the other hand, if we move close to a specific center with charge Γ_i , the flow equations will be dominated by the contribution of this charge and, consequently, the flow will behave very much like a single center flow for a total charge Γ_i .

To see what happens in between these two limiting cases, consider for simplicity a two-center state with charges Γ_1, Γ_2 . As the integrability condition (3.45) shows, the centers will move infinitely far apart from each other when the moduli at infinity approach a point where the phases of $Z(\Gamma_1)$ and $Z(\Gamma_2)$ align. This alignment of phases defines a real codimension one hypersurface in moduli space, separating the region where the two center solution exists and where it does not. It is called a wall of marginal stability, for reasons that will become clear at the end of this section.

If we slowly move the moduli at spatial infinity from a fixed starting value downstream¹⁴ until it crosses the wall of marginal stability at t_{split} , this particular flow tree should disappear. It is therefore natural to picture the complete flow as a single flow for the total charge Γ from the moduli at spatial infinity up to the wall of marginal stability, followed by two separate single flows, using the individual charges Γ_1 and Γ_2 , starting from t_{split} on the wall to the individual charge centers. This is pictured in figure 3.3.

Note however that in reality, the flow tree should represent the values of the moduli fields at every point in space. Without spherical symmetry, these fields will also depend on the angular coordinates. This means that the flow tree will look more like a fat line, particularly at the split point t_{split} .

In [65], the presence of a (split) flow tree in the supergravity regime was conjectured to be an existence criterion for a BPS D-brane state in string theory, generalizing the partial correspondence found in [51, 52] for single center solutions.

Let us now make some comments on the issue of marginal stability. The central charge is a linear function of the charges, so at each point in moduli space, we have:

$$Z \equiv Z(\Gamma_{total}) = Z(\Gamma_1) + Z(\Gamma_2) \equiv Z_1 + Z_2, \quad (3.48)$$

where we defined shorthand notations for the central charges. Since the mass, or equivalently the energy, of a BPS state equals the modulus of its central charge, we have

$$|M| = |Z| = |Z_1 + Z_2| \leq |Z_1| + |Z_2| = |M_1| + |M_2|, \quad (3.49)$$

implying that the state with charge Γ_{total} is always at least as stable as the combination of the two charges Γ_1 and Γ_2 ¹⁵. When the phases of Z_1 and Z_2 align, this bound is saturated, meaning that the total charge can decompose into its constituents. Energetically, this process is only marginally possible, because the two configurations have exactly the same energy. This explains why this locus in moduli space is called a wall of marginal stability.

¹⁴The flow direction from spatial infinity to the charged centers will be referred to as *downstream*. Note that for the single center attractor flow, this corresponds to increasing τ .

¹⁵Of course, this statement only makes sense when the total charge state exists. At the other side of the wall of marginal stability, this may not be the case.

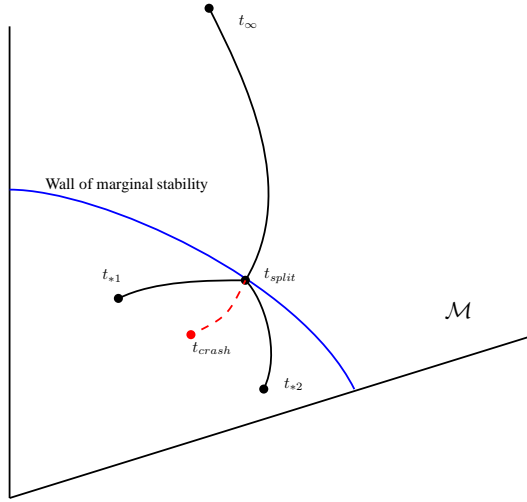


Figure 3.3: Split flow tree. The flow through moduli space \mathcal{M} starts from the value at spatial infinity t_{∞} and follows a single flow until the wall of marginal stability is encountered (blue line). From this point (t_{split}) on, two separate flows continue to the two respective attractor points t_{*1} and t_{*2} . If the flow would not split, it would reach a zero of $|Z|$ at a regular point in moduli space t_{crash} , indicated by the red line. As remarked in section 3.3.3, such a flow does not correspond to a BPS state.

3.5 Elliptic genera

In this section, we will outline the construction of an *elliptic genus* for black holes. To count the degeneracy of a supersymmetric solution with specific charges and mass, we will use a supersymmetric index, which is a quantity that is protected from most of the continuous deformations of the action. This allows us to calculate this index in a suitable limit, where the calculations become more tractable. The elliptic genus is then a formal partition sum containing these indices for a specific ensemble of different charges. The specific choice of ensemble we use, gives rise to particular transformation properties of the partition sum¹⁶ under the modular group $SL(2, \mathbb{Z})$. These transformation properties will then allow us to determine all coefficients in the partition sum from the knowledge of only a finite number of them.

¹⁶These transformation properties are also responsible for making this partition sum an *elliptic genus*. Mathematically, these are multiplicative cobordism invariants, valued in a ring of modular forms. We will however only be interested in their modular properties.

The arguments, presented in this section, are mainly based on the discussion of the elliptic genus in [65].

Let us start by saying a few words about the ensemble of charges that will be used in the partition sum. We will use the framework of type IIA string theory, compactified on a Calabi Yau threefold. As stated in section 3.3.2, in this framework, we can split the charges into magnetic and electric charges. The ensemble, used for the construction of the elliptic genus, will then consist of all charges with a fixed, and thus specified, magnetic charge. This means that the elliptic genus sums over all electric charges, while keeping the magnetic charges fixed.

The index we will try to calculate in the next chapter is the *second helicity supertrace* of the BPS sector of the theory. For a state with charges $(p, q) \equiv (p^I, q_I)$, it is defined by

$$\Omega(p, q; t) \equiv -2 \operatorname{Tr}_{\mathcal{H}_{BPS}(p, q; t)} (-1)^{2J_3} J_3^2, \quad (3.50)$$

with $\mathcal{H}_{BPS}(p, q; t)$ the BPS sector of the one-particle Hilbert space with fixed charges (p, q) and moduli t and where J_3 is a generator of angular momentum in a fixed direction. The exponent of J_3 in this supertrace, being two, explains why this index is called the *second helicity* supertrace. Since every BPS representation contains a half hypermultiplet factor (see section 3.2.2), we can decompose its representation as:

$$|\Psi\rangle = (0, 0, 1/2) \otimes |\Psi'\rangle, \quad (3.51)$$

where $(0, 0, 1/2)$ denotes the fundamental BPS representation, as in section 3.2.2. The one-particle Hilbert space of BPS solutions $\mathcal{H}_{BPS}(p, q; t)$ then also factorizes as

$$\mathcal{H}_{BPS}(p, q; t) = (0, 0, 1/2) \otimes \mathcal{H}'_{BPS}(p, q; t). \quad (3.52)$$

The index can then be rewritten as a supertrace over this reduced Hilbert space:

$$\Omega(p, q; t) \equiv \operatorname{Tr}_{\mathcal{H}'_{BPS}(p, q; t)} (-1)^{2J'_3}, \quad (3.53)$$

where J'_3 is the reduced angular momentum.

With these indices, one can construct a formal partition sum by summing over the electric charges:

$$Z_{BH}(\phi, t) \equiv \sum_q \Omega(p, q; t) e^{2\pi\phi^\Lambda q_\Lambda}, \quad (3.54)$$

where the ϕ^Λ denote the electric potentials.

Now consider a D4-D2-D0 state, with a D4 wrapped on a holomorphic surface in an ample divisor class $P \equiv P^A D_A$ of the Calabi Yau X , with D_A a basis in $H_4(X)$.

The lower-dimensional charges are created by turning on a flux $F \in H^2(P)$ and by putting in N $\overline{D0}$'s. The total D2 brane charge then reads:

$$q_A = D_A \cdot F, \quad (3.55)$$

where the product is defined as the integral over the wedge product in P . The total D0 brane charge is

$$q_0 = -N + \frac{1}{2}F^2 + \frac{\chi(P)}{24}, \quad (3.56)$$

with $\chi(P)$ the Euler characteristic of P . With these definitions, the partition sum (3.54) can be rewritten as:

$$Z_{BH}(\phi, t) = \sum_{F, N} d(F, N) \exp\left(2\pi\phi^0\left[-N + \frac{1}{2}F^2 + \frac{\chi(P)}{24}\right] + 2\pi\phi \cdot F\right). \quad (3.57)$$

In this formula, $d(F, N)$ is now the index for states of fixed flux and added $\overline{D0}$ brane charge N .

By adding a Boltzmann factor $\exp(-\beta H)$ into this partition sum, which removes the divergences [66], and using the large radius limit of the central charge (which by the BPS condition is proportional to the energy), we arrive at

$$Z_{D4}(\tau, C, B) = \sum_{F, N} d(F, N) \exp\left(2\pi i\tau\left[N - \frac{1}{2}\mathcal{F}_-^2 - \frac{\chi(P)}{24}\right] - 2\pi i\tau\left[\frac{1}{2}\mathcal{F}_+^2 - 2\pi i\mathcal{F} \cdot \left(C + \frac{P}{2}\right)\right]\right), \quad (3.58)$$

where we used the following definitions: $\mathcal{F} = F - B$, \mathcal{F}_+ and \mathcal{F}_- are the self-dual and anti self-dual parts of the flux \mathcal{F} and $\tau = C_0 + \frac{i\beta}{g_s}$. We also substituted the electric potentials with corresponding Ramond-Ramond potentials: $C_1 \equiv C_0 \cdot dt/\beta \equiv i\phi^0 \cdot dt/\beta$ and $C_3 \equiv C \wedge dt/\beta \equiv (i\phi - P/2) \wedge dt/\beta$.

The transformation properties of this partition sum can be investigated by performing a T-duality, an S-duality and again a T-duality (commonly referred to as a TST duality). This results in

$$Z_{D4}(\tau, C, 0) = \omega_S^{-1} \tau^{-w} \bar{\tau}^{-\bar{w}} \exp\left(\pi i C_-^2/\tau + \pi i C_+^2/\bar{\tau}\right) Z_{D4}\left(-\frac{1}{\tau}, \frac{C}{\tau}, 0\right). \quad (3.59)$$

A careful analysis reveals the following values for the parameters in this equation: $\omega_S = -\exp\left(i\pi(P^3/6 + c_2(X) \cdot P/12) + i\pi(w - \bar{w})/2 + i\pi P^2/2\right)$, $w = -3/2$ and $\bar{w} = 1/2$. This completes the description of the behaviour of the partition sum Z_{D4} under the transformation $\tau \rightarrow -1/\tau$.

Under the transformation $\tau \rightarrow \tau + 1$, the partition sum receives an extra factor of $\omega_T = \exp(2\pi i c_2(X) \cdot P/24)$. These two transformations generate the special linear group $SL(2, \mathbb{Z})$ and we see that our partition sum transforms in a special way under these modular transformations. This will be used next to decompose Z_{D_4} into theta functions and formulate a very important result that states that one can calculate the whole partition sum from the knowledge of its polar terms.

The fluxes $F \in H^2(P)$ can be decomposed as follows. First, we have the fluxes that are pulled back from the Calabi Yau fluxes and which form the lattice $L_X \equiv i_P^* H^2(X)$. We also have the fluxes that are orthogonal to L_X and whose lattice is denoted L_X^\perp . The metric on the resulting flux lattice is in general not unimodular and is given by $D_{AB} = D_{ABC} P^C$, where D_{ABC} are the intersection numbers of the cycles $D_A \in H_4(X)$. The quotient of the total flux lattice $H^2(P)$ by $L_X \oplus L_X^\perp$ is a finite group \mathcal{D} of fluxes, called glue vectors $\gamma \in \mathcal{D}$. If we also include the half-integer flux $P/2$, needed to cancel the Freed–Witten anomaly [67], we have:

$$F = \frac{P}{2} + f^\parallel + f^\perp + \gamma, \quad (3.60)$$

with $f^\parallel + f^\perp$ denoting the decomposition of part of the flux in $L_X \oplus L_X^\perp$.

The previous decomposition of the flux then allows to decompose the partition function in theta functions as follows:

$$Z_{D_4}(\tau, C, 0) = \sum_{\gamma} \Psi_{\gamma}(\tau, \bar{\tau}, C) Z_{\gamma}(\tau), \quad (3.61)$$

where the Ψ_{γ} are known Siegel–Narain theta functions. This implies that all the non trivial information of the partition function is contained in the function $Z_{\gamma}(\tau)$.

Because the pullback fluxes in L_X are automatically of type $(1, 1)$ (note that $H^{(2,0)}(X) = H^{(0,2)}(X) = 0$), these fluxes do not alter the BPS conditions of supersymmetric configurations, which for the flux is $F \in H^{(1,1)}(P)$ (see [68] for a derivation of this BPS condition on the flux). As a consequence, the indices can not depend on this part of the flux. We can then write

$$Z_{\gamma}(\tau) \equiv \sum_{f^\perp, N} d\left(\frac{P}{2} + \gamma + f^\perp\right) \exp(-2\pi i \tau \hat{q}_0(F, N)), \quad (3.62)$$

with $\hat{q}_0 \equiv q_0 - Q^2/2$. By using equivalence classes of charges, defined as

$$[\gamma, \hat{q}_0] \equiv \left\{ (0, P, Q, q_0) \mid q_0 - \frac{Q^2}{2} = \hat{q}_0 \quad \text{and} \quad Q = \frac{P}{2} + f^\parallel + \gamma^\parallel \right\}, \quad (3.63)$$

for some $f^\parallel \in L_X$, we can regroup terms of equation (3.62), giving

$$Z_{\gamma}(\tau) \equiv \sum_{\hat{q}_0} \Omega([\gamma, \hat{q}_0]) \exp(-2\pi i \tau \hat{q}_0). \quad (3.64)$$

In [69, 70, 71], the vector of modular forms $Z_\gamma(\tau)$ was shown to be holomorphic in τ , to have no singularities in the upper half plane and to transform with weight $-\frac{b_2}{2} - 1$, where b_2 is the second Betti number of the Calabi Yau X . This resulted in an asymptotic expansion which is completely fixed by its *polar part*. For a fixed glue vector γ , the vector component looks like

$$Z_\gamma(q) = q^{-\hat{q}_0, max} (a_0 + a_1q + a_2q^2 + \dots) , \tag{3.65}$$

where we introduced $q \equiv \exp(2\pi i\tau)$, \hat{q}_0, max is the maximal value of \hat{q}_0 for the given γ and the a_i are integer numbers, corresponding to the indices $\Omega([\gamma, \hat{q}_0])$. The polar part of this function is then defined as the terms with a negative exponent of q .

To illustrate how this polar part could possibly reproduce the whole modular form, let us start with the simpler case of a single modular form $Z(\tau)$ with weight w :

$$Z(\tau) = \sum_{n \geq 0} d(n) \exp(2\pi i\tau(n - A)) , \tag{3.66}$$

where A is some positive constant. By definition, the modular form $Z(\tau)$ transforms under modular transformations as

$$Z(\tau) = Z\left(\frac{a\tau + b}{c\tau + d}\right) (c\tau + d)^{-w} , \tag{3.67}$$

and has poles at $0 = q \equiv \exp(2\pi i\tau)$ and its images under the modular group $\Gamma \equiv SL(2, \mathbb{Z})$. We can then construct the whole partition function with the Rademacher formula:

$$Z(\tau) = \sum_{\alpha \in \Gamma/\Gamma_\infty} Z^-\left(\frac{a\tau + b}{c\tau + d}\right) (c\tau + d)^{-w} , \tag{3.68}$$

where $Z^-(\tau)$ is the polar part of the modular form $Z(\tau)$ and Γ_∞ is the subgroup of Γ that leaves $\tau = i\infty$ invariant. That this should be correct, can be seen from the fact that this expansion will have the same poles and weight as $Z(\tau)$, which completely determines a modular form.

In the more general case, which we need to construct $Z_\gamma(\tau)$ from its polar part, the formula becomes:

$$Z_\gamma(\tau) = \sum_{\alpha \in \Gamma/\Gamma_\infty} M(\alpha)_\gamma^\mu H_\mu^- \left(\frac{a\tau + b}{c\tau + d}\right) (c\tau + d)^{-w} , \tag{3.69}$$

where $M(\alpha)$ is a faithful representation of the modular group, which can be deduced from the transformation properties of $Z_{D_4}(\tau, C, 0)$.

It is interesting to note that the modularity of the generalized elliptic genus suggests a dual conformal field theory description. It is also in this context that

the Farey Tail expansion, which produces the partition sum from its polar part, has been derived in [69, 70, 71]. The extremality of the black hole solutions gives rise to an anti de Sitter factor in the near horizon region, which, through the AdS/CFT correspondence [72, 73, 74]¹⁷, leads to exactly such a description.

3.6 D–particle microstates from split flow trees

We now have collected enough material to make a first step in calculating black hole degeneracies. As shown in the previous section, all we need to do is to calculate the indices of the polar states, which then determine the whole elliptic genus. The first thing to do then is to identify the polar charges, which form the polar part of the partition sum. This is a relatively easy task, as one just has to look for charge states with positive \hat{q}_0 .

For each polar charge state, we can then use the split flow tree classification to enumerate the possible flow trees corresponding to this state. In the large radius limit, it is easy to show that polar states will never correspond to single flow trees, as there will always be a zero of $|Z|$ in moduli space.

If one has a prescription for calculating the index of the polar charges corresponding to these flow trees, which will be the subject of the next chapter, one can just sum up these indices for a fixed polar charge state, thereby arriving at the total index for this state.

Once we have all the indices of the polar charge states, we can use equation (3.69) to generate $Z_\gamma(\tau)$ completely, which can then be used in equation (3.61) to generate the whole partition sum.

As a side remark, if we do have a prescription for calculating indices of flow trees, we could verify this prescription by calculating non–polar state degeneracies and comparing them with the prediction from the modular expansion of the elliptic genus. This verification will be performed in the next chapter, yielding very convincing evidence that our index computation is correct.

3.7 Summary

We started by introducing the reader to string theory by providing the perturbative formulation in terms of the Polyakov action. Two aspects of this formulation should be stressed: first, the coupling of strings to each other is determined by the theory itself and is given by the vacuum expectation value of the dilaton and

¹⁷For a nice review on this correspondence, see [75].

secondly, string interactions can be calculated by using only the free string action, evaluated on non-trivial worldsheet topologies.

The introduction of open strings in the spectrum then led to higher-dimensional objects to which the string endpoints are attached. These objects, called D-branes, are solitonic states of the theory and as such, they incorporate non-perturbative aspects of string theory. They are also the (only) sources for the Ramond-Ramond fields that are present in type II superstring theory.

To end the brief overview of string theory, we looked at spacetime actions that correspond to the type II string theories in the limit of small string length l_s , or equivalently, at low energy. The resulting effective theory is one of the previously known supergravity theories.

Because the theory we will be interested in, type II string theory compactified on a Calabi Yau threefold, exhibits $\mathcal{N} = 2$ supersymmetry, some properties of the corresponding algebra and its representations are presented. Most importantly, BPS representations, which saturate a certain mass bound $M \geq |Z|$, where Z represents the central charge of the representation, were introduced. These states preserve half of the supersymmetries and together form the BPS sector of the theory, which is the sector in which we will be interested in the next chapter.

Then we discussed the field content of Calabi Yau compactifications of type IIB supergravity, which was related to the harmonic differential forms on the Calabi Yau manifold. The attractor mechanism, an important tool for studying supersymmetric black holes in the resulting $\mathcal{N} = 2$ supergravity theory, was shown to fix the moduli values at the horizon. First, for spherically symmetric black holes, this mechanism was shown to have a formulation in terms of the Hodge structure of the Calabi Yau, which encodes the space of harmonic forms. Then, the formalism was generalized to include also multicentered configurations. In the latter case, an integrability constraint should be satisfied for the solution to exist in the supergravity picture.

Related to the attractor equations for, possibly multicentered, black holes in $\mathcal{N} = 2$ supergravity in four dimensions, is the notion of flow trees, representing how the moduli of the compactification manifold vary from spatial infinity to their attractor values at the center(s) of the solution. In this context, the notion of walls of marginal stability was introduced, marking the locus in moduli space where certain BPS states can decay and consequently, the index of BPS states could jump.

In the next section, we constructed a formal partition sum out of the indices of BPS states with fixed magnetic and variable electric charges. This elliptic genus was then decomposed into theta functions and a holomorphic part that contained all the non-trivial information of the partition sum, denoted $Z_\gamma(\tau)$. The transformation properties of the latter under the modular group $SL(2, \mathbb{Z})$ implied that knowledge of its polar part, which constitutes only a finite number

of terms, is sufficient to determine the whole modular vector $Z_\gamma(\tau)$. Since this in turn determines the complete partition sum, this means that one only needs the indices contained in the polar part to derive the indices of all charge states in the partition sum.

Finally, the concepts and techniques, introduced in this chapter, enabled us to state the general methodology to calculate degeneracies of BPS states in type II string compactifications on a Calabi Yau threefold, which will be the subject of the next chapter.

Chapter 4

A refined calculation of the index for BPS D–particles

In the present chapter, a detailed treatment of our results in [18, 19] will be given. By looking at the correspondence between BPS solutions in supergravity and branes in the topological B model, we were able to exactly calculate the degeneracies of small charge BPS states.

Unlike the expectation from the wall crossing formula of [65], the index does not completely factorize into Donaldson–Thomas invariants [76, 77, 78].

It turns out that some brane configurations are perceived differently by the open string states binding the constituent branes together. The index of the open string states, which become tachyonic at the stable side of the wall of marginal stability, ‘jumps’ at these special configurations. To calculate the index exactly, one must first identify these special configurations and then calculate the index of open string states in these configurations. As we will show, these jumps in the tachyon index are very natural from the viewpoint of the topological B model, which, as we will argue, can be used to describe BPS brane states in the limit of zero string coupling.

In the first section, the reader will find a description of the correspondence between BPS solutions in supergravity and B branes in the topological B model. We also make an attempt to provide an intuitive description of what happens when taking the limit of zero string coupling, which as far as we know is new. The next section contains a treatment of B branes in the topological B model, which will form an important tool in our refined calculation of the indices. The last section then contains the calculations and results of [18, 19], which forms a significant part of the authors own research.

4.1 Supergravity/B brane correspondence

Before delving into the computation of degeneracies of BPS states, let us first see how the correspondence between supergravity and the topological B model works.

The gravitational constant in ten dimensions behaves like $G_{10} \approx g_s^2 l_s^8 = l_p^8$, with g_s the string coupling, l_s the string length and l_p the Planck length. If we fix the string length l_s and decrease the string coupling g_s , then also the gravitational constant and the Planck length will decrease. In four dimensions, the Newton constant is $G_4 = G_{10}/V_6$, where V_6 denotes the volume of the compactification manifold and G_d is the gravitational constant in d dimensions. Measuring the compactification volume in string units $V_* \equiv V_6/l_s^6$, we obtain $l_4^2 = G_4 \approx g_s^2 l_s^2/V_*$, with l_4 the four-dimensional Planck length.

The supergravity approximation is expected to break down when curvature invariants at the horizon become of the order the string length l_s . This happens when $r_H \sim l_s$. The condition for the supergravity approximation to be valid is thus $G_4 M \gg l_s$ or equivalently $M \gg V_*/l_s g_s^2$, with M the mass of the black hole. Since the horizon area, and thus the entropy, will be a function of the dimensionless combination $M l_4 = M \sqrt{G_4}$, we need to keep this constant while sending $g_s \rightarrow 0$, when we investigate black hole entropy. This means that the mass will scale as $M \sim 1/g_s$. Note that in that case, the condition $M \gg V_*/l_s g_s^2$ will still break down for small enough g_s .

Since the index is protected by supersymmetry, it will remain fixed during this procedure. Clearly, at some point, the string length will become big, compared to the Planck length. At this point, the supergravity approximation is no longer valid, since this approximation rests on the assumption that at low energies, gravity dominates compared to physics at the scale of the string length. The supergravity solution will slowly change into a string solution and by taking the limit $g_s \rightarrow 0$, this stringy solution does not receive higher genus corrections. The physics of this model can thus be described by a two-dimensional conformal field theory on a worldsheet with the disk topology (for open strings).

Because the charges of the BPS states under investigation are the charges of D-branes, the solution will then correspond to a D-brane configuration, which is pointlike in the four-dimensional non-compact spacetime. These D-branes can thus only wrap internal cycles of the Calabi Yau geometry. Stability, which results from the preservation of part of the supersymmetry, then also implies that the branes are BPS in the reduced two-dimensional sigma model with target space the Calabi Yau¹.

The next step consists of twisting this sigma model, such that it becomes a topological model. This can be done in two ways, without spoiling the BPS brane

¹Note that the inverse statement is not necessarily correct.

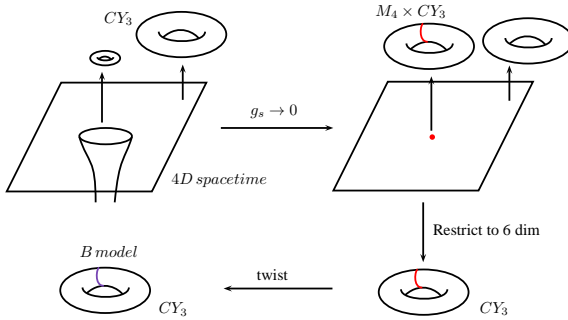


Figure 4.1: Correspondence between supergravity BPS solutions and B branes in the topological model. Starting on the top left, a BPS black hole in supergravity is pictorially represented in the ten-dimensional spacetime. The plane represents the four-dimensional non-compact spacetime M_4 , while the torus represents the internal Calabi Yau geometry CY_3 , which varies over M_4 . By taking the limit $g_s \rightarrow 0$, the horizon shrinks to zero and we are left with a pointlike D-brane state, wrapping an internal cycle of the Calabi Yau. The BPS D-brane is represented by the red curve. In the next step, we restrict to the six-dimensional description of this D-brane in the Calabi Yau threefold. And at last, a topological twist is performed, so as to arrive at a B brane in the topological B model, defined on the same Calabi Yau. See also section 4.2 for more information on these B branes. To distinguish between D-branes and B branes, the latter have a purple color.

content of the theory. One finally arrives at a description of the BPS states as a configuration of B branes² in the topological B model. A cartoon of this procedure is drawn in figure 4.1.

The correspondence, as sketched in the previous paragraph, is not so straightforward however. It is a priori not clear what happens to the supergravity solution in going to the limit $g_s \rightarrow 0$, since the supergravity description breaks down at a certain point. The correspondence between, possibly multicentered, BPS solutions of supergravity and BPS D-brane states in string theory therefore remains a conjecture [65].

We will now present a possible scenario that provides some more intuition of this limiting procedure. Let us first recall the attractor equations of supergravity for

²For evident reasons, branes in the topological B model are called B branes. We will use this naming convention to distinguish between D-branes in an untwisted sigma model or string theory and the B branes we describe in the B model.

a single centered solution, see equations (3.36):

$$\begin{aligned} \dot{\mu} &= |Z|, \\ \mu \frac{dz^a}{d\mu} &= -g^{a\bar{b}} \partial_{\bar{b}} \log |Z|^2, \end{aligned} \quad (4.1)$$

where $\mu = e^{-U(r)}$ denotes a radial parameter that starts from the value 1 at infinity and increases monotonically when approaching the horizon. The radial component of the metric is just μ^2 , so at the horizon, we have $\mu \rightarrow \infty$. From the second attractor equation, one then sees that the moduli will flow to a minimum of $|Z|^2$. Now lets think what will happen if we decrease the string coupling, while keeping the string length fixed. At a certain point, the horizon radius will become of the order of l_s and we can certainly no longer trust the supergravity description. In this case, it seems no longer right to speak about a horizon. What is left, is a stringy state without horizon [79]. If we would still use the attractor equations, which we are strictly speaking not allowed to, then the moduli will still flow towards a minimum, but they will never reach it, since μ is now bounded from above.

In the flow tree picture, the modulus at the point where the stringy solution lives, which is where the horizon was in the supergravity approximation, climbs up the flow tree. Equivalently, the flow tree stops before reaching the minimum value of $|Z|$. It is plausible that this will continue all the way up to the point where the modulus becomes a constant, equal to its value at infinity.

In this way, we recover a spacetime which is a direct product of flat Minkowski space and a Calabi Yau, with moduli fixed at the original values at infinity. The existence of such a state is then equivalent to the existence of a D-brane state on just the Calabi Yau threefold with the specified values of the moduli. The last step, towards a topological field model, then easily follows. Figure 4.2 shows a visualization of this scenario.

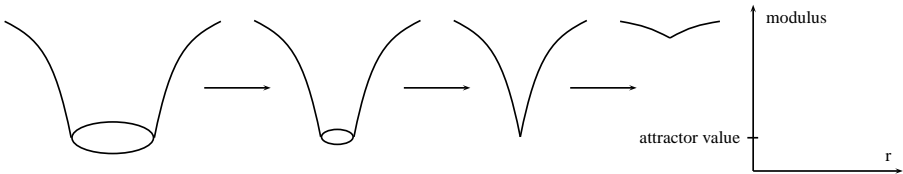


Figure 4.2: Moduli profile at decreasing string coupling. For the first three situations, the horizon radius decreases, but the moduli will still attain the attractor value. The third situation is a limiting case where the horizon radius reaches the string length scale. In the last situation, there is no horizon left and the moduli will not reach the attractor point. One sees that the moduli profile tends to flatten out as we decrease the string coupling.

For multicentered configurations, the distance between the centers, which is fixed by the attractor equations, scales like the Planck length. Decreasing the string coupling would thus result in not only decreasing the horizon size, but also the distance between different charge centers. At a certain point, where supergravity is no longer valid, they will merge. Again, this situation is very reminiscent of the split flow tree picture: each center climbs up its own flow tree until they meet at a split point, where they merge and continue upstream on the single flow.

Whereas this scenario, both for single and split flows, does provide an intuitive picture of the correspondence between the supergravity solutions and D-brane states in string theory, it should not be taken to be proven. The use of the attractor equations beyond the supergravity regime has not been justified.

A confirmation of how the black hole solution in supergravity gets deformed to a flat space solution with D-branes, can be found by looking at the deviations of the metric from the flat one. These are, in four dimensions, $\delta G_{\mu\nu} \sim G_4 M/r$. By sending $g_s \rightarrow 0$, the combination $G_4 M$ also goes to zero, resulting in a flat metric at fixed r . In fact, the same reasoning can be applied to all the other fields present in the supergravity theory, since they generically all depend on harmonic functions that look like $H = 1 + q/r$, where q depends on the mass and charges and will go to zero at zero string coupling.

4.2 Branes and the topological B model

The correspondence, described in the previous section, suggests that, given a supergravity solution with specific total charge, one can investigate some of its properties by studying the corresponding B branes in the topological model, assuming these properties do not change under the operation of varying the string coupling constant. Therefore, in the present section we will give an overview of how these B branes can be represented and provide some examples of these B branes that are relevant in the following computations.

We will start by describing how BPS D-branes in a two-dimensional sigma model with a Calabi Yau target space map to B branes in the topological B model, which is the last step in the correspondence of figure 4.1. In [80, 81], the reader can find a more detailed introduction to the construction of topological string models.

4.2.1 A supersymmetric non-linear sigma model

Consider a worldsheet sigma model with target manifold X and fields $\phi : \Sigma \rightarrow X$ describing the embedding of the two-dimensional string worldsheet Σ into the target manifold. In the current section, the target manifold will always be a

complex manifold with complex dimension three, thereby anticipating to restrict attention to Calabi Yau threefolds. One can then define the action of the non-linear sigma model as

$$S_\sigma = \frac{i}{8\pi\alpha'} \int_\Sigma d^2z g_{IJ} \frac{\partial\phi^I}{\partial z} \frac{\partial\phi^J}{\partial\bar{z}}. \quad (4.2)$$

In the following, for ease of notation, we will use $\partial \equiv \frac{\partial}{\partial z}$ and $\bar{\partial} \equiv \frac{\partial}{\partial\bar{z}}$.

If X is also Kähler, we can construct a $\mathcal{N} = (2, 2)$ supersymmetric extension of this sigma model, with action:

$$\begin{aligned} S_{(2,2)} = & \frac{i}{4\pi\alpha'} \int_\Sigma d^2z \left\{ g_{i\bar{j}} (\partial\phi^i \bar{\partial}\phi^{\bar{j}} + \bar{\partial}\phi^i \partial\phi^{\bar{j}}) + iB_{i\bar{j}} (\partial\phi^i \bar{\partial}\phi^{\bar{j}} - \bar{\partial}\phi^i \partial\phi^{\bar{j}}) \right. \\ & \left. + ig_{i\bar{j}}\psi_-^{\bar{j}} D\psi_-^i + ig_{i\bar{j}}\psi_+^{\bar{j}} \bar{D}\psi_+^i + R_{i\bar{j}j\bar{i}}\psi_+^i\psi_+^{\bar{j}}\psi_-^j\psi_-^{\bar{i}} \right\}, \end{aligned} \quad (4.3)$$

The fermion fields are sections of the tensor product of the square root of the (anti)canonical bundle³ (denoted $K^{\frac{1}{2}}$ and $K^{-\frac{1}{2}}$ respectively) with the pullback of the (anti)holomorphic tangent bundle (denoted $\phi^*(T_X)$ and $\phi^*(\bar{T}_X)$), depending on their index structure. Since this theory has $\mathcal{N} = (2, 2)$ supersymmetry, the supersymmetry transformations will in general depend on four fermionic parameters α_\pm and $\tilde{\alpha}_\pm$.

4.2.2 The topological B model

In this section, we will deform the $\mathcal{N} = (2, 2)$ sigma model of the previous section, in order to obtain a topological field theory. More precisely, we will end up with a theory that contains a generator Q that squares to zero ($Q^2 = 0$). Similar to what happens in BRST quantization, we will then restrict the physical spectrum to Q -closed states: $Q|\Psi\rangle = 0$. The theory becomes a topological one if the vacuum preserves the symmetry generated by Q and the energy momentum tensor is Q -exact ($T_{\mu\nu} = \{Q, G_{\mu\nu}\}$, for some operator $G_{\mu\nu}$). The condition of preserved Q -symmetry implies that expectation values of operator products involving a Q -exact operator will vanish. The condition on the energy momentum tensor renders expectation values independent of the metric, as can be seen by taking the

³The canonical bundle of a manifold of dimension n is defined as the n th exterior power of the cotangent bundle. For complex manifolds, it is also the determinant bundle of holomorphic n -forms.

variational derivative of such an expectation value with respect to the metric:

$$\begin{aligned}
 \frac{\delta}{\delta g^{\mu\nu}} \langle \mathcal{O}_1 \cdots \mathcal{O}_n \rangle &= \frac{\delta}{\delta g^{\mu\nu}} \int [\mathcal{D}\phi] \mathcal{O}_1 \cdots \mathcal{O}_n e^{iS[\phi]} \\
 &= i \int [\mathcal{D}\phi] \mathcal{O}_1 \cdots \mathcal{O}_n \frac{\delta S}{\delta g^{\mu\nu}} e^{iS[\phi]} \\
 &= i \langle \mathcal{O}_1 \cdots \mathcal{O}_n T_{\mu\nu} \rangle = 0,
 \end{aligned} \tag{4.4}$$

At this point, the reader might wonder why we need to deform the theory to obtain a topological theory. After all, in the original theory, the supersymmetry generators do square to zero and one could find a vacuum which preserves this symmetry. Why does that not define a topological theory then? The answer is that we still need the correlation functions to be independent of the metric.

Clearly, we then need to be able to at least *define* the generator Q , independently from the metric. For a fermionic generator, this implies that we are able to find a covariantly constant spinor, which acts as the parameter for the generator Q . But for an arbitrary metric on the worldsheet, such a covariantly constant supersymmetry parameter will in general not exist. The only way to assure its existence is by making it a scalar, which renders the aforementioned condition rather trivial as one can always define a constant scalar on any manifold.

We are now ready to change the bundles in which the fermions live, to obtain such a topological model [82]. Take $\psi_{\pm}^{\bar{j}}$ to be sections of $\phi^*(\bar{T}_X)$, ψ_{+}^j of $K \otimes \phi^*(T_X)$ and ψ_{-}^j a section of $\bar{K} \otimes \phi^*(T_X)$, where K denotes the canonical bundle on Σ and ϕ^* is the pullback map, defined by the embedding ϕ . This procedure is called a *twisting* of the fermion bundles.

From these, one can then define the scalars

$$\begin{aligned}
 \eta^{\bar{j}} &\equiv \psi_{+}^{\bar{j}} + \psi_{-}^{\bar{j}} \\
 \theta_i &\equiv g_{i\bar{j}}(\psi_{+}^{\bar{j}} - \psi_{-}^{\bar{j}}),
 \end{aligned} \tag{4.5}$$

and the one-forms $\rho^j \equiv \rho_z^j dz + \rho_{\bar{z}}^j d\bar{z} \equiv \psi_{+}^j dz + \psi_{-}^j d\bar{z}$. Because of the twisting, the supersymmetry parameters will no longer be all fermionic. One then defines a particular combination of the supersymmetry generators that now have a scalar parameter, as Q , which (still) squares to zero. The action can then be written as:

$$S_B = i \int_{\Sigma} \{Q, V\} + U, \tag{4.6}$$

with

$$\begin{aligned}
 V &= g_{i\bar{j}} \left(\rho_z^i \bar{\partial} \phi^{\bar{j}} + \rho_z^{\bar{i}} \partial \phi^j \right) \\
 U &= \int_{\Sigma} \left(-\theta_i D \rho^i - \frac{i}{2} R_{i\bar{i}j\bar{j}} \rho^i \wedge \rho^{\bar{j}} \eta^{\bar{i}} \theta_k g^{k\bar{j}} \right). \tag{4.7}
 \end{aligned}$$

To eliminate the chiral anomaly that is present in this theory, one can restrict to a Calabi Yau, which will be our main concern anyway⁴.

By restricting the physical spectrum to Q -closed states, we now have a topological field theory⁵. Since the expectation values of operator products containing a Q -exact operator vanish, the spectrum is more precisely restricted to Q cohomology classes. For this reason, such topological field theories are also called *cohomological* field theories.

The important thing to remember from this construction is that supersymmetric D-brane states in the non-linear sigma model will survive this construction. Without going into too much details here⁶, the result is that these BPS D-branes will wrap holomorphically embedded submanifolds of X , which forces their dimension to be even.

Because there is also a gauge field living on a D-brane, we are led to think that B branes should be classified by holomorphic vector bundles over holomorphically embedded submanifolds of X . However, as it turns out, the reality is much more complex, and the category of B branes is actually the *derived category of coherent sheaves*. The interested reader can consult the previously given references, which contain the arguments leading to this statement. For more information on categories and sheaves and how one constructs a derived category, we refer the reader to appendix B.

In the following, we will try to provide some general intuition of how to work with the objects in this fascinating category and also give some basic examples.

4.2.3 B branes and examples

As already conjectured in [83], B branes can be described as objects in the derived category of coherent sheaves $D(X)$. The objects in this category are

⁴The origin of this anomaly is that the twisting procedure mixes the supersymmetry transformation with the axial R-symmetry of the model. It is this R-symmetry which suffers from an anomaly. This anomaly vanishes when $\int_{\phi(\Sigma)} c_1(X) = 0$, which is clearly satisfied for Calabi Yau manifolds X , since $c_1(X) = 0$.

⁵Actually, we have not shown that the energy momentum tensor is Q -exact. This is however the case, see for example [80].

⁶The reader can consult [81] for more information.

complexes of coherent sheaves. The need for coherent sheaves, instead of locally free sheaves, arises from the fact that we will need the cohomologies of these complexes, something which is really only well defined in an abelian category. Thus, the category of locally free sheaves is enlarged by adding (co)kernels inside the category of \mathcal{O}_X modules. An example of such a B brane is:

$$\dots \rightarrow 0 \rightarrow \mathcal{E}^{-1} \xrightarrow{d_{-1}} \mathcal{E}^0 \xrightarrow{d_0} \mathcal{E}^1 \xrightarrow{d_1} 0 \rightarrow \dots, \quad (4.8)$$

where \mathcal{E}^i denotes a coherent sheaf on X and the d_i are morphisms obeying $d_{n+1} \circ d_n = 0$. Following the notation in the literature, this complex will be denoted as \mathcal{E}^\bullet .

The morphisms in the derived category consist of chain maps between the complexes, which are a set of $f_n : \mathcal{E}^n \rightarrow \mathcal{F}^n$, such that every square commutes (actually, the morphisms are chain maps modulo chain homotopy, but this will not interfere with our discussion here). On top of these morphisms, one defines the notion of a quasi-isomorphism: chain maps that induce an isomorphism between the cohomologies of the complexes. In such a case, one also adds their inverse as a morphism. Complexes linked by quasi-isomorphisms are then considered to be isomorphic. The set of (coherent) sheaf complexes and these morphisms then form the derived category of B branes.

In the next subsections, examples of objects in the derived category we will encounter are discussed. To shorten the notation we will indicate a brane of dimension p as Dp and the corresponding anti-brane as \overline{Dp} , revealing our eventual interest in describing D-branes.

6-branes with flux

The representation of (anti-)6-branes with $U(1)$ -flux as a sheaf complex is rather straightforward. Since the brane is spacefilling, the sheaf is locally free and corresponds to a holomorphic line bundle. In homogeneous coordinates, the transition functions can be represented by a homogeneous degree d polynomial. In this case, the corresponding sheaf will be denoted by $\mathcal{O}(d)$. We will also sometimes write $\mathcal{O}(dH) \equiv \mathcal{O}(d)$, with H a basis element of $H^2(X)$. If the manifold, on which the sheaf is defined, needs to be specified, we will denote it in a subscript, e.g. $\mathcal{O}_X(d)$.

Note that the complex

$$0 \rightarrow 0 \rightarrow \mathcal{O} \xrightarrow{Id_{\mathcal{O}}} \mathcal{O} \rightarrow 0, \quad (4.9)$$

with $Id_{\mathcal{O}}$ the identity morphism, is exact, indicating a quasi-isomorphism between the zero complex and $\mathcal{O} \xrightarrow{Id_{\mathcal{O}}} \mathcal{O}$. The two 6-branes can thus annihilate each other.

This observation suggests that anti-branes are represented by the same complex, but shifted by one position. This turns out to be correct, so the anti-brane of \mathcal{E}^\bullet is $\mathcal{E}^\bullet[1]$, where $\mathcal{E}^\bullet[n]$ indicates the complex \mathcal{E}^\bullet shifted by n places to the left.

Adding 0-branes

Adding an $\overline{\text{D0}}$ to a D6 can be done in the following way. In a neighborhood of the position of the $\overline{\text{D0}}$, we use the inhomogeneous complex coordinates (x, y, z) and define a morphism from $\mathcal{O}^{\oplus 3}$ to \mathcal{O} by $(f_1, f_2, f_3) \xrightarrow{x, y, z} xf_1 + yf_2 + zf_3$. The cokernel object of this morphism is called the skyscraper sheaf and has support equal to the origin. For a more general point $p \in X$, denote this sheaf as \mathcal{O}_p . The D6 plus $\overline{\text{D0}}$ at the point p can then be represented as the following complex:

$$\cdots \rightarrow 0 \rightarrow \mathcal{O} \rightarrow \mathcal{O}_p \rightarrow 0 \rightarrow \cdots, \quad (4.10)$$

where the only non-trivial morphism takes a holomorphic function to its value in p . In terms of the coordinate ring, the polynomial ring $\mathbb{C}[x, y, z]$ gets quotiented out by the maximal ideal generated by the three linear functions (f_1, f_2, f_3) . This leaves the ring \mathbb{C} , representing constant functions, exactly as one would have expected for the function ring over a point.

By adding the kernel of this morphism and its object, one can construct a short exact sequence:

$$0 \rightarrow \mathcal{I}_p \rightarrow \mathcal{O} \rightarrow \mathcal{O}_p \rightarrow 0, \quad (4.11)$$

where \mathcal{I}_p is called the ideal sheaf in p . The short exact sequence implies a quasi-isomorphism between \mathcal{I}_p and $\mathcal{O} \rightarrow \mathcal{O}_p$. So we may equally well consider the ideal sheaf as representing a D6 with one $\overline{\text{D0}}$.

The construction of 6-branes with more $\overline{\text{D0}}$'s is very similar. To include two $\overline{\text{D0}}$'s, instead of considering three linear functions mapping $\mathcal{O}^{\oplus 3}$ to \mathcal{O} , we now take one quadratic function and two linear functions. For simplicity, we take the morphism defined by multiplication with $x^2 - a^2$, y and z respectively. The support of the cokernel sheaf will then be restricted to the two points $(a, 0, 0)$ and $(-a, 0, 0)$. For $a \neq 0$, the sheaf looks like two isolated points with fiber \mathbb{C} . When $a = 0$ however, we are faced with a single point as support and a coordinate ring different from \mathbb{C} (quotienting out by the three functions, we are left with functions of the form $ag + b$, with $a, b \in \mathbb{C}$ and g a linear function, determined, up to a constant factor, by the three defining functions).

Physically, it is very natural to include these states as multiple branes on the same position. Mathematically, the inclusion of multiplicities will force us to use the notion of a scheme, rather than a variety. In algebraic geometry, this is also closely related to the notion of a blowup procedure: putting two points on the same locus,

the degrees of freedom are the locus of these points plus the direction from which they approach each other (in three dimensions, the direction, or as we have seen, the extra linear polynomial lives in $\mathbb{C}\mathbb{P}^2$).

The sheaf complex, corresponding to a D6 with two $\overline{D0}$'s at loci p_1, p_2 will be denoted as:

$$0 \rightarrow \mathcal{O} \rightarrow \mathcal{O}_{p_1, p_2} \rightarrow 0. \quad (4.12)$$

The only non-trivial morphism in this complex generically maps a holomorphic function to its two values at p_1 and p_2 . When the two $\overline{D0}$'s coincide however, this morphism will send the holomorphic function to its value at p and its derivative at p in the direction determined by the linear function g . This can be shown by analyzing the coordinate rings of the two different schemes (\mathcal{O} and \mathcal{O}_{2p} , the latter representing two $\overline{D0}$'s at p).

The reader who is unfamiliar with the language of schemes, can consult appendix B or [84] or just think of these as describing (sub)varieties with multiplicity.

Adding 2-branes

Finally, we will look at D6 $\overline{D2D0}$ states. As an example, take a curve defined by the zero locus of the ideal generated by the functions x and y (as in the previous examples, we work in local coordinates (x, y, z)). This is just the z -axis. To this curve we add a point, defined by the three functions $x, y - a$ and z . The union of these two varieties will be defined as the zero locus of the intersection of the two aforementioned ideals. This new ideal will be generated by the functions $x, y(y - a)$ and yz . The coordinate ring consists of the direct sum of polynomial functions in z (denoted $\mathbb{C}[z]$) and the constant functions \mathbb{C} . This is directly related to the functions on the curve and the point. If $a \rightarrow 0$, the point will be located on the curve. As a variety, the zero locus is just the curve. But as a scheme, the point is not 'lost', as we can see from the coordinate ring. This ring consists of $\mathbb{C}[z] \oplus \mathbb{C} \cdot y$. In general, the coordinate ring consists of the direct sum of the coordinate ring on the curve and \mathbb{C} times a linear function that is perpendicular to the curve. The blowup procedure in this case thus includes a $\mathbb{C}\mathbb{P}^1$ of normal directions. This $\mathbb{C}\mathbb{P}^1$ encodes the directions normal to the curve in a three-dimensional complex manifold.

4.3 Refined index calculation for three models

This section provides the main results of the author concerning the refined index calculation method⁷. In a first part, the general strategy for finding such an

⁷The adjective 'refined' refers to the method. We are thus not calculating a 'refined' index.

index for a specific BPS charge state will be outlined. This is followed by explicit calculations on three different Calabi Yau threefolds, which demonstrate, through verification with modular predictions, the correctness of this method.

4.3.1 General strategy

The overview of the general strategy on using the refined index calculation will proceed in two steps. In the first step, this method is outlined for states that correspond to split flow trees in the supergravity regime. This was the method used in [18]. A generalization of this method, which is also able to deal with single flows in supergravity and which was found by the author [19], will form the second part.

In order not to obscure the following description of the refined index calculation, in the next paragraphs, the split flows we will consider will be of the simplest type: we only consider the first split point of the flow tree. In a real calculation, one should check if the two constituent charges will not have inequivalent realizations as split flows themselves. The generalization of the present discussion to more complex flow trees is however straightforward.

The index for split flows

Suppose that for a certain charge state Γ , no single flows in supergravity exist, because they will all crash at a regular zero of the central charge Z in moduli space. In this case, all realizations of this state in supergravity should be split flow trees. The first thing to do then, is to find all possible split flow trees. Figure 4.3 clarifies a necessary criterion for the existence of a given split flow tree: the wall of marginal stability in moduli space should separate the modulus at infinity and the crash point (or minimum of $|Z|^2$ in moduli space). Otherwise, the flow would reach the regular zero before it could split into the given constituents. This criterion is conjectured to be also sufficient by the split attractor flow conjecture [65].

In practice, to find split or single flows for specific charge states, the Mathematica code, written and provided by Frederik Denef, was used. It includes a numerical approximation to the central charge in moduli space, thereby enabling one to find minima and walls of marginal stability.

To calculate the index for a specific split flow tree, one argues that changing the modulus at infinity, while keeping it inside the region of moduli space where this state is stable, does not influence its index. This means that we could bring the modulus very close to the wall of marginal stability, where, by equation (3.46), the distance between the centers goes to infinity. In this case it is natural to

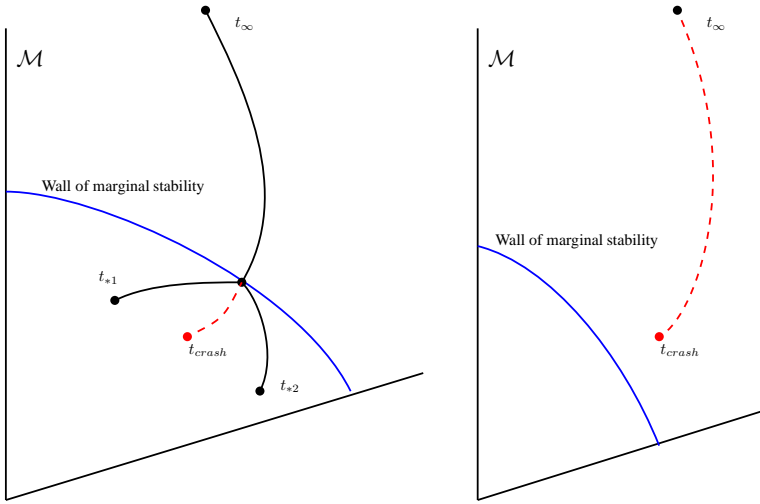


Figure 4.3: Existence of split flows. At the left the wall of marginal stability sits in between the modulus at infinity t_∞ and the regular point in moduli space t_{crash} , where the central charge, for the total charge Γ , becomes zero. In this case, a split flow exists, assuming the two different centers are separately stable. On the right, the crash point t_{crash} lies in front of the wall of marginal stability. No split flow exists, because the flow will never reach the wall of marginal stability.

assume that the degeneracy of the state factorizes into the degeneracies of the two constituent states.

There is an important caveat however. Because non-local charges, for which $\langle \Gamma_1, \Gamma_2 \rangle \neq 0$, have a non-trivial angular momentum, associated to their gauge field configuration, an extra factor representing this angular momentum appears. In the language of the B model branes, this factor represents the index of the tachyon field that binds the two constituent states together. One then arrives at a factorization that is equivalent to saying that the moduli space of such a state has a product structure:

$$\mathcal{M}_{\text{total}} = \mathcal{M}_1 \times \mathcal{M}_T \times \mathcal{M}_2, \quad (4.13)$$

where \mathcal{M}_i denotes the moduli space of configurations of the charge constituent Γ_i and \mathcal{M}_T is the tachyon moduli space.

As it turns out, not every state of the individual charges is perceived equally by the tachyon field: for some configurations, the index of this field ‘jumps’ between different constituent configurations. The refined calculation is intended to deal with this issue, by distinguishing parts of the moduli space of configurations where

the tachyon index has a non-generic value. The examples in the next subsections will clarify this procedure by showing how this is done in practice. Figure 4.4 shows an example of a situation where the tachyon index jumps between different configurations of the constituent charge states.

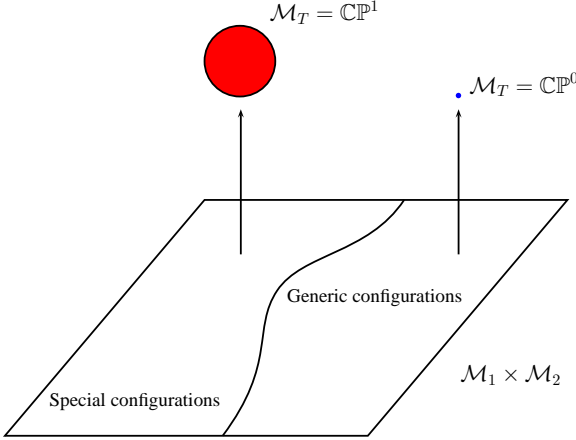


Figure 4.4: A fibered moduli space. This figure depicts how the total moduli space of configurations for a specific split state could look like. The tachyon moduli space is generically a $\mathbb{C}\mathbb{P}^0$, which is a point, but is enlarged to a $\mathbb{C}\mathbb{P}^1$ for special configurations of the constituent charge states.

For a BPS state with N inequivalent split flow trees, the total index is then $\Omega = \sum_{i=1}^N \Omega^{(i)}$, where $\Omega^{(i)}$ denotes the index of the split flow tree, indexed by i . According to the previous discussion, the individual indices for the split flow trees can be written as

$$\Omega^{(i)} = \sum_{j=1}^M \Omega_j(\Gamma_1^{(i)}) \Omega_j(\Gamma_2^{(i)}) \Omega(T_j^{(i)}), \quad (4.14)$$

where $\Omega(T_j^{(i)})$ denotes the index of the tachyon field for a subset of charge configurations that have indices $\Omega_j(\Gamma_1^{(i)})$ and $\Omega_j(\Gamma_2^{(i)})$.

In the case the constituent charges consist of a single (anti-)D6 brane, possibly with extra D2 and D0 charges, the total index of such a constituent state is given by a Donaldson–Thomas invariant. We must then have

$$\sum_j \Omega_j(\Gamma_1^{(i)}) = N_{DT}(\beta, n), \quad (4.15)$$

where β and n encode the lower-dimensional brane charges on the (anti-)D6 brane with charge $\Gamma_1^{(i)}$. In the examples of the following subsections, we will always consider this situation to be the case.

In [16, 85], a geometric interpretation is developed which provides some intuition into the analogy between the moduli space of D4-D2-D0 BPS states and the moduli space of D6- $\overline{\text{D6}}$ states and the tachyon field between them. In this geometric picture, which is reviewed in [65], one starts with the observation that a D4 brane on a divisor Σ in the class $P \in H_4(X)$ with flux $F \in H^2(\Sigma)$, which induces D2 brane charge, and n pointlike instantons, representing D0 brane charge, has a moduli space that is roughly a fiber bundle over \mathcal{M}_P with fiber the Hilbert scheme of points on P , denoted $\text{Hilb}^n P$. Here, \mathcal{M}_P denotes the moduli space of deformations of effective divisors in the class P . These deformations are generically obstructed by the supersymmetry requirement, stating that $F \in H^{1,1}(\Sigma)$. Only in the case the flux is pulled back from fluxes on the Calabi Yau, $F = \iota^* S$ with $S \in H^2(X)$, this is automatically satisfied⁸.

The condition $F \in H^{1,1}(\Sigma)$ is equivalent to demanding that the Poincaré dual of F in Σ is a holomorphic two-cycle $[C] \in H_2(\Sigma)$. We could thus just as well start by fixing these curve classes in the Calabi Yau X , together with n pointlike instantons and look for the divisors that contain these curves and points. In this way, we are actually fixing D2 and D0 brane charges in the Calabi Yau X and calculating the moduli space of divisors that contain the respective curves and points. This is very similar to making a bound state of D6 and $\overline{\text{D6}}$ branes, containing these curves and points, and calculating the tachyon moduli space that bounds them. The tachyon moduli space corresponds in this geometric picture to the moduli space of divisors that contain the curves and points.

The index for general flows

The procedure, as outlined in the previous paragraphs, can be generalized by turning our attention to the B model side of the correspondence. In this description, the moduli are not fields, but parameters determining the topological field theory. Regardless of the existence of a split flow, one could argue that varying this modulus inside a stable region of moduli space should never influence the index of the state under investigation. In figure 4.5 this is shown for a state with a single flow in the supergravity picture. Although the supergravity flow never reaches the wall of marginal stability, one can tune the modulus in the B model picture to a value on this wall, without affecting the index of the corresponding state. At marginal stability, the state looks like a superposition of the constituent

⁸Here $\iota: \Sigma \rightarrow X$ denotes the embedding map of the divisor Σ into the Calabi Yau X

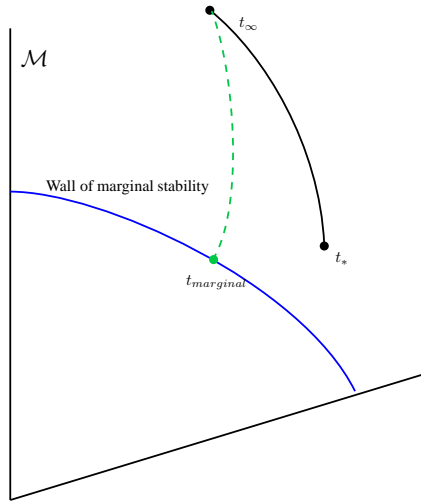


Figure 4.5: The marginal limit in the B model. This figure represents a state for which the supergravity flow reaches a minimum (at t_*) before hitting the wall of marginal stability. In the B model however, one could tune the modulus to a value on this wall (t_{marginal}) without changing the corresponding index. This is represented by the dashed green line.

charge states. Again, this allows us to find its index by calculating the indices of the constituent states and of the massless string states that bind them⁹.

The refinement, as explained above in the case of split flow trees, can then be carried out in exactly the same way: one identifies constituent configurations for which the index of the tachyon field (or massless open string fields at marginal stability) jumps. The formula in equation (4.14) will then remain valid. One should realize however that a given single flow in supergravity could correspond to multiple bound states in the B model (with each its own wall of marginal stability). The B model picture thus gives a more refined partitioning of charge states: for each split flow tree in supergravity, one has exactly one bound state in the B model; but for single flows in supergravity, one can possibly have multiple inequivalent¹⁰ bound states in the B model.

To clarify the difference between the supergravity and B model picture, their main characteristics are repeated here:

⁹These massless open string states become tachyonic at the stable side of the wall of marginal stability. After these tachyonic states have condensed, one is left with a bound state that no longer looks like an exact superposition of constituent states.

¹⁰This equivalence is defined in the derived category of B branes by (quasi-)isomorphisms. See appendix B for more details.

Supergravity. The moduli space denotes the space in which the scalars of the vector multiplets live. The moduli are thus fields that can vary over spacetime. The value of these moduli at infinity defines the vacuum in which the corresponding BPS states are investigated. Moving this value at spatial infinity in the direction of a wall of marginal stability, causes the constituent charges to move apart. At marginal stability, their separation will go to infinity, justifying the assumption that the total index factorizes, up to subtleties concerning the interaction of their gauge fields.

B model. Here, each point in moduli space denotes a specific topological field theory. The moduli are just parameters of the theory. Tuning this value to one that lies on a wall of marginal stability, will result in the B brane being described by a simple superposition of the constituent branes. Again, this justifies a (partial) factorization of its index.

4.3.2 Example 1: the sextic

We will define¹¹ the sextic X_6 as a degree six hypersurface in the weighted projective space $W\mathbb{C}P^4_{11112}$. For practical purposes, the degree six polynomial will be taken of the form:

$$p^{(6)} = x_5^3 + f^{(6)}(x_1, x_2, x_3, x_4), \quad (4.16)$$

with $f^{(6)}$ a homogeneous polynomial of degree 6 in the given coordinates and $(x_1, x_2, x_3, x_4, x_5)$ are homogeneous coordinates with weights $(1, 1, 1, 1, 2)$ in $W\mathbb{C}P^4_{11112}$.

Its main properties are:

- Total Chern class: $c(X_6) = \frac{(1+H)^4(1+2H)}{1+6H} = 1 + 14H^2 - 68H^3$.
- Euler character: $\chi(X_6) = -204$.

Here, H denotes a basis element of the second cohomology group of X_6 ($H \in H^2(X_6)$) and one has $\int_{X_6} H^3 = 3$, indicating that the weak Jacobi form will be three-dimensional¹²:

$$Z(q, \bar{q}, z) = \sum_{k=0}^2 Z_k(q) \Theta_k(\bar{q}, z), \quad (4.17)$$

¹¹For more information about the example Calabi Yau's and some of their properties, the reader is referred to appendix A.

¹²See section 3.5 for more details about the decomposition of the elliptic genus into theta functions. Also note that $Z_k(q)$ denotes the same function as $Z_\gamma(\tau)$ in section 3.5, but as a function of $q \equiv e^{2\pi i\tau}$.

which means that we only have to determine Z_0 and Z_1 .

We will adopt the following notation:

- As in [86], charge systems are labeled by their deviation in D2 brane charge Δq and D0 brane charge Δq_0 as measured from the most polar state. In the ‘charge shift’ notation the most polar state is thus denoted as $\Delta q = 0, \Delta q_0 = 0$.
- As explained in [65], various charges are related by flux shifts. Charge equivalence classes contain the same entropy, and they can be labeled by the (flux) gluing vector (see section 3.5), as well as the reduced D0 brane charge \hat{q}_0 . A charge equivalence class is then labeled by $[\gamma, \hat{q}_0]$.
- For a D6-D4-D2-D0 brane system, we denote the charges as (p_0, p, q, q_0) , such that a polyform using our basis can be written as

$$\Gamma = p_0 + pH + \frac{q}{\mathcal{H}}H^2 + \frac{q_0}{\mathcal{H}}H^3, \tag{4.18}$$

where $\mathcal{H} := \int_{X_6} H^3$. We also use the vector notation: $\Gamma \equiv (p_0, p, q, q_0)$.

In what follows, the calculation of charge vectors from the knowledge of the flux and added $\overline{\text{D0}}$ ’s will be based on the equations, given in appendix C.

Using the relation between Gopakumar–Vafa and Donaldson–Thomas invariants (see appendix A), one can calculate the latter. These are found to be:

Donaldson–Thomas invariants: sextic				
	n = 0	n = 1	n = 2	n = 3
$\beta = \mathbf{0}$	1	204	20’298	1’311’584
$\beta = \mathbf{1}$	0	7884	1’592’568	156’836’412
$\beta = \mathbf{2}$	7884	7’636’788	1’408’851’522	136’479’465’324

As reviewed in section 3.5, the modular properties of the elliptic genus imply that knowledge of the indices for the polar states is sufficient to determine the whole elliptic genus. In a first part, we will calculate these polar indices. In a second part, the calculation of some non-polar indices will provide non-trivial evidence for the correctness of the refined index calculation method.

Polar states

The polar states, or more precisely representatives of classes of states $[\gamma, \hat{q}_0]$ with positive \hat{q}_0 , can be found by gradually adding $\overline{\text{D0}}$ charges to a pure D4 brane, possibly with flux along a gluing vector. For each of these representatives (of different classes $[\gamma, \hat{q}_0]$), the different flow trees and their index calculation is given.

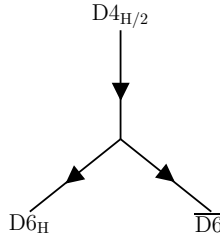
1. $\Delta \mathbf{q} = \mathbf{0}, \Delta \mathbf{q}_0 = \mathbf{0}, \quad [0, \frac{45}{24}]$:

The pure D4 brane carries half a unit of flux to ensure anomaly cancellation, which we denote by $D4_{H/2}$, and has total charge $\Gamma = H + \frac{H^2}{2} + (\frac{\chi(P)}{24} + \frac{1}{2}F^2)\omega = H + \frac{1}{2}H^2 + \frac{3}{4}H^3 = (0, 1, \frac{3}{2}, \frac{9}{4})$. This is the most polar state and represents the class $[0, \frac{45}{24}]$.

One finds just one split flow tree with two centers:

- a D6 with flux H , denoted $D6_H$, with charge $\Gamma_1 = (1, 1, \frac{13}{4}, \frac{9}{4})$;
- a pure $\overline{D6}$: $\Gamma_2 = (-1, 0, -\frac{7}{4}, 0)$.

Schematically, the flow tree looks as follows:



This state can be represented in the B model as the following sheaf complex:

$$0 \rightarrow \mathcal{O} \xrightarrow{\times f_1} \mathcal{O}(H) \rightarrow 0,$$

where $\xrightarrow{\times f_1}$ denotes the morphism defined by multiplication with a degree one polynomial. This morphism also encodes the tachyon field and as can be seen from the sheaf complex, no refinement can occur. The BPS index then reads

$$\Omega = (-1)^{|\langle \Gamma_1, \Gamma_2 \rangle| - 1} |\langle \Gamma_1, \Gamma_2 \rangle| N_{DT}(0, 0) \cdot N_{DT}(0, 0) = (-1)^3 \cdot 4 \cdot 1 \cdot 1 = -4. \quad (4.19)$$

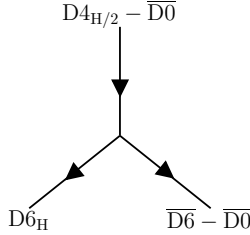
Note that the intersection number between Γ_1 and Γ_2 nicely corresponds with the index of the moduli space of the hyperplanes $H \subset X$, which are defined by the choice of a degree one polynomial f_1 . This moduli space is a $\mathbb{C}\mathbb{P}^3$ because the coordinate with weight 2 can of course not be used to define a hyperplane: $\chi(\mathbb{C}\mathbb{P}^3) = |\langle \Gamma_1, \Gamma_2 \rangle| = 4$.

 2. $\Delta \mathbf{q} = \mathbf{0}, \Delta \mathbf{q}_0 = -1, \quad [0, \frac{21}{24}]$:

Adding one $\overline{D0}$, one gets the state $D4_{H/2} - \overline{D0}$. It has total charge $(0, 1, \frac{3}{2}, \frac{5}{4})$, and reduced D0-brane charge $\hat{q}_0 = \frac{21}{24}$. One finds one split flow tree with two centers (depending on the side of the threshold stability wall from which one starts, the $\overline{D0}$ could also be initially bound to the $D6_H$ constituent):

- a D6 with flux H , denoted $D6_H$, with charge $\Gamma_1 = (1, 1, \frac{13}{4}, \frac{9}{4})$;
- a $\overline{D6}$ with one added $\overline{D0}$, denoted $\overline{D6} - \overline{D0}$: $\Gamma_2 = (-1, 0, -\frac{7}{4}, -1)$.

The flow tree looks like



This state can be represented in the B model as the following sheaf complex:

$$0 \rightarrow \mathcal{O} \xrightarrow{\times f_1} \mathcal{O}(H) \rightarrow \mathcal{O}_p \rightarrow 0,$$

with \mathcal{O}_p the skyscraper sheaf of the $\overline{D0}$ at point p . One sees that a necessary condition on f_1 , the tachyon field, is that it should vanish at p . In the case at hand, every locus p will give one constraint to f_1 , reducing its moduli space to $\mathbb{C}\mathbb{P}^2$. The BPS index then becomes

$$\Omega = (-1)^{|\langle \Gamma_1, \Gamma_2 \rangle| - 1} |\langle \Gamma_1, \Gamma_2 \rangle| N_{DT}(0, 0) \cdot N_{DT}(0, 1) = (-1)^2 \cdot 3 \cdot 1 \cdot 204 = 612, \quad (4.20)$$

where we again have $\chi(\mathbb{C}\mathbb{P}^2) = |\langle \Gamma_1, \Gamma_2 \rangle| = 3$.

3. $\Delta \mathbf{q} = \mathbf{1}, \Delta \mathbf{q}_0 = -\mathbf{1}, \quad [\gamma_1, \frac{5}{24}]$:

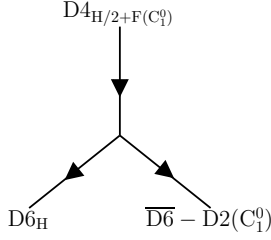
One can now consider a flux, along the gluing vector γ_1 . According to our intuition, this means turning on an extra flux dual to a degree one rational curve, denoted $D4_{H/2+F}(C_1^0)$. This leads to the total charge $(0, 1, \frac{5}{2}, \frac{5}{4})$, and to the reduced D0-brane charge $\hat{q}_0 = \frac{5}{24}$: thus, there is only one polar state in this γ_1 -class. One finds the split flow tree with the following constituents:

- a D6 with flux H , denoted $D6_H$, with charge $\Gamma_1 = (1, 1, \frac{13}{4}, \frac{9}{4})$;
- a $\overline{D6}$ with one added D2 along the curve C_1^0 , denoted $\overline{D6} - D2(C_1^0)$: $\Gamma_2 = (-1, 0, -\frac{3}{4}, -1)$.

The flow tree looks like

This state can be represented in the B model as the following sheaf complex:

$$0 \rightarrow \mathcal{O} \xrightarrow{\times f_1} \mathcal{O}(H) \rightarrow \mathcal{O}_{C_1^0} \rightarrow 0,$$



with $\mathcal{O}_{C_1^0}$ denoting the coherent sheaf, representing the D2 brane on the curve C_1^0 . The constraints on the tachyon map, i.e. its vanishing at the curve, reduce the moduli space from $\mathbb{C}\mathbb{P}^3$ to $\mathbb{C}\mathbb{P}^1$. The BPS index is calculated according to

$$\Omega = (-1)^{|\langle \Gamma_1, \Gamma_2 \rangle| - 1} |\langle \Gamma_1, \Gamma_2 \rangle| N_{\text{DT}}(0, 0) \cdot N_{\text{DT}}(1, 1) = (-1)^1 \cdot 2 \cdot 1 \cdot 7'884 = -15'768. \quad (4.21)$$

And again we have $\chi(\mathbb{C}\mathbb{P}^1) = |\langle \Gamma_1, \Gamma_2 \rangle| = 2$.

Using a basis for modular forms of the right weight¹³, one can use these numbers to determine the modular form to be given by

$$Z_0(q) = q^{-\frac{45}{24}} (-4 + 612q - 40'392q^2 + 146'464'860q^3 \dots) \quad (4.22)$$

$$Z_1(q) = Z_2(q) = q^{-\frac{29}{24}} (-15'768q + 7'621'020q^2 + \dots). \quad (4.23)$$

This agrees with the findings of [87] (up to an overall sign), which is expected, given that the small number of polar states supporting split flow tree realizations apparently do not involve subtleties and so do not require a refinement.

Non-polar state: $\Delta \mathbf{q} = 0, \Delta \mathbf{q}_0 = -2, \quad [0, -\frac{1}{8}]$

This state, denoted $D4_{H/2} - 2\overline{D0}$, has total charge $(0, 1, \frac{3}{2}, \frac{1}{4})$, and reduced D0-brane charge $\hat{q}_0 = -\frac{1}{8}$. One finds the split flow tree with the following constituents:

- a D6 with flux H , denoted $D6_H$, with charge $\Gamma_1 = (1, 1, \frac{13}{4}, \frac{9}{4})$;
- a $\overline{D6}$ with two added $\overline{D0}$'s, denoted $\overline{D6} - 2\overline{D0}$: $\Gamma_2 = (-1, 0, -\frac{7}{4}, -2)$.

The flow tree looks like

¹³See the appendix of [87] for more details on how this is done.

$$\begin{array}{ccc}
 & D4_{\text{H}/2} - 2\overline{D0} & \\
 & \downarrow & \\
 & \swarrow \quad \searrow & \\
 D6_{\text{H}} & & \overline{D6} - 2\overline{D0}
 \end{array}$$

This state can be represented in the B model as the following sheaf complex:

$$0 \rightarrow \mathcal{O} \xrightarrow{\times f_1} \mathcal{O}(H) \rightarrow \mathcal{O}_{p_1, p_2} \rightarrow 0,$$

with \mathcal{O}_{p_1, p_2} the coherent sheaf representing two $\overline{D0}$'s at locations p_1, p_2 .

A naive index calculation would give

$$\begin{aligned}
 \Omega_{\text{naive}} &= (-1)^{|\langle \Gamma_1, \Gamma_2 \rangle| - 1} |\langle \Gamma_1, \Gamma_2 \rangle| N_{\text{DT}}(0, 0) \cdot N_{\text{DT}}(0, 2) \\
 &= (-1)^1 \cdot 2 \cdot 1 \cdot 20'298 = -40'596,
 \end{aligned} \tag{4.24}$$

which obviously differs from the exact index, which is given by the elliptic genus in equation (4.22) to be $\Omega_{\text{exact}} = -40'392$. This can be cured using the refined calculation, as will be shown in the next paragraphs.

A general tachyon field is described by the degree one polynomial f_1 , which in the homogeneous coordinates of $W\mathbb{CP}_{11112}^4$ has the form:

$$f_1 = a_1 x_1 + a_2 x_2 + a_3 x_3 + a_4 x_4. \tag{4.25}$$

Since a general rescaling of (a_1, a_2, a_3, a_4) can be absorbed in the scaling of the homogeneous coordinates, the moduli space of these maps is a \mathbb{CP}^3 . For the sheaf complex to be a complex, this map has to vanish on the loci of the two $\overline{D0}$'s, denoted p_1 and p_2 in the sheaf complex. This puts a number of independent constraints on this map, given by

$$\text{rank} \begin{pmatrix} x_1 & x_2 & x_3 & x_4 \\ y_1 & y_2 & y_3 & y_4 \end{pmatrix}, \tag{4.26}$$

with x_i, y_i the homogeneous coordinates of the points p_1 and p_2 respectively.

For general positions p_1, p_2 , this rank will be two, reducing the moduli space from \mathbb{CP}^3 to a \mathbb{CP}^1 . This is where the intersection number $|\langle \Gamma_1, \Gamma_2 \rangle| = \chi(\mathbb{CP}^1) = 2$ comes from.

Now we are ready to search for cases where the number of constraints is different, resulting in a jump in the tachyon index. We will proceed in two steps. First,

the case $p_1 \neq p_2$ will be investigated. Then, the configurations where the $\overline{D0}$'s sit at the same location will be analyzed. In this last case, one needs to perform a blowup, possibly resulting in an extra constraint from the tangent direction (see section 4.2.3).

1. $\mathbf{p}_1 \neq \mathbf{p}_2$

In this case, since $(x_1, x_2, x_3, x_4) = (0, 0, 0, 0)$ is not a point on the sextic X_6 , we have to look for two different points p_1, p_2 with $(x_1, x_2, x_3, x_4) = \lambda(y_1, y_2, y_3, y_4)$. By looking at equation (4.16), we see that there are three solutions with given (x_1, x_2, x_3, x_4) . We could also use the adjunction formula to calculate the number of points p_2 which satisfy the requirement $(x_1, x_2, x_3, x_4) = \lambda(y_1, y_2, y_3, y_4)$. For a given p_1 , this locus is given by three independent linear constraints (for example, set three independent determinants of the matrix in equation (4.26) to zero). The index of this locus is

$$\int_{X_6} H^3 = 3, \quad (4.27)$$

as was expected from the more direct calculation before. Two of these three points will be different than p_1 , so we have, for each p_1 , two different points $p_2 \neq p_1$ for which the rank in equation (4.26) is one instead of two.

2. $\mathbf{p}_1 = \mathbf{p}_2$

As discussed in section 4.2.3, when the two $\overline{D0}$'s sit at the same location, one needs to perform a blowup procedure, resulting in an extra tangent direction along which the tachyon field should also vanish. If we parametrize this direction by the homogeneous components X^i , the jump of the tachyon index occurs when:

$$\text{rank} \begin{pmatrix} x_1 & x_2 & x_3 & x_4 \\ X^1 & X^2 & X^3 & X^4 \end{pmatrix} \neq 2, \quad (4.28)$$

One can distinguish between two cases:

- $x_5 \neq 0$: This means one can choose affine coordinates with $x_5 = 1$. Thus, in these coordinates, one knows that $X^5 = 0$ for the tangent vector (and hence the case $X^1 = \dots = X^4 = 0$ is ruled out and only the case $X^i = \lambda x_i$, $i = 1, \dots, 4$ remains). The tangent vectors should be tangent to the Calabi Yau X_6 (meaning $\nabla_X p^{(6)} = 0$), which leads to $6\lambda f^{(6)} = 0$. Since $\lambda \neq 0$, this means $p^{(6)} = 0$, so $x_5 = 0$ upon plugging this into the defining equation of the sextic (4.16), which contradicts our assumption. So if $x_5 \neq 0$, no jump in tachyon index occurs.
- $x_5 = 0$: In this case, without loss of generalization, fix $x_1 = 1$. This means $X^1 = 0$ for the tangent vector. The condition for a jump in

the tachyon index is then $X^1 = \dots = X^4 = 0$. This happens when the tangent vector equals $X^5\partial_5$, which, at the locus $x_5 = 0$, is tangent to the Calabi Yau. Note that there is *one* tangent direction and *one* locus ($x_5 = 0$) for which this happens.

From this information, one can now calculate the index, by treating each of these special configurations separately. Note that we use the following notations and definitions:

- The Euler character of the sextic $\chi(X_6) = -204$ is the index of the moduli space of a pointlike $\overline{D0}$ on the Calabi Yau and will just be denoted χ .
- The locus $x_5 = 0$ is denoted by X_0 and its Euler characteristic by $\chi_0 = 108$.

The index receives the following contributions:

- $\frac{1}{2}(\chi^2 - 3\chi + 2\chi_0) \cdot \chi(\mathbb{CP}^1)$: this is the generic case, where the two particles are separated and the locus where $x_i = y_i$ for $i = 1, 2, 3, 4$ has been subtracted. Note that one has to be careful not to subtract the locus where the first four coordinates are identical and $x_5 = 0$ more than once. This has been taken into account with the $+2\chi_0$ term. The factor $\frac{1}{2}$ accounts for the fact that interchanging the two particles gives the same configuration.
- $(\chi - \chi_0) \cdot \chi(\mathbb{CP}^2) \cdot \chi(\mathbb{CP}^1)$: this accounts for the case when the two $\overline{D0}$'s coincide, and $x_5 \neq 0$. Note that the $\chi(\mathbb{CP}^2)$ results from the blowup of a codimension 3 locus.
- $2 \cdot \frac{1}{2}(\chi - \chi_0) \cdot \chi(\mathbb{CP}^2)$: this takes into account the case when $(x_1, x_2, x_3, x_4) = \lambda(y_1, y_2, y_3, y_4)$ and $p_1 \neq p_2$ (hence the overall factor of two). Note that the tachyon index has jumped to $\chi(\mathbb{CP}^2)$.
- $\chi_0 \cdot (\chi(\mathbb{CP}^2) - 1) \cdot \chi(\mathbb{CP}^1)$: here, the locus $p_1 = p_2$ and $x_5 = 0$ is dealt with. In principle, one just has to do a blowup of a codimension 3 locus (hence a factor of $\chi(\mathbb{CP}^2)$). After the blowup, there is a special tangent direction however, which must be treated separately. So this tangent direction is subtracted.
- $\chi_0 \cdot 1 \cdot \chi(\mathbb{CP}^2)$: this is the case $p_1 = p_2$, $x_5 = 0$ and tangent direction $X = X^5\partial_5$. For this one blowup direction (for which the 1 stands for its index), the tachyon index jumps to $\chi(\mathbb{CP}^2)$.

Collecting all the pieces linked to the value 2 or 3 for the tachyon index (up to a sign), one can state the correct index in the form

$$\Omega_{\text{exact}} = -2 \cdot (20'502) - 3 \cdot (-204) = -40'392, \quad (4.29)$$

which exactly matches the modular prediction in equation (4.22). One can now define the *Donaldson–Thomas partitions* $\mathcal{N}_{\text{DT}}^{(g,s)}(0, 2)$ for the sextic:

$$\mathcal{N}_{\text{DT}}^{(g)}(0, 2) = 20'502, \quad (4.30)$$

$$\mathcal{N}_{\text{DT}}^{(s)}(0, 2) = -204. \quad (4.31)$$

$\mathcal{N}_{\text{DT}}^{(g)}(0, 2)$ counts the generic configurations of two $\overline{\text{D0}}$'s on the $\overline{\text{D6}}$, for which the tachyon index is $\chi(\mathbb{C}\mathbb{P}^1)$, and $\mathcal{N}_{\text{DT}}^{(s)}(0, 2)$ counts the special configurations, for which the tachyon index jumps to $\chi(\mathbb{C}\mathbb{P}^2)$. Note that there is a sign difference between these indices. The total number of configurations just equals the standard Donaldson–Thomas invariant, as it should be:

$$N_{\text{DT}}(0, 2) = \mathcal{N}_{\text{DT}}^{(g)}(0, 2) + \mathcal{N}_{\text{DT}}^{(s)}(0, 2) = 20'502 - 204 = 20'298. \quad (4.32)$$

4.3.3 Example 2: the octic

The octic Calabi Yau X_8 is defined as a degree eight hypersurface in the weighted projective space $W\mathbb{C}\mathbb{P}_{11114}^4$. We take the defining polynomial to be of the form:

$$p^{(8)} = x_5^2 + f^{(8)}(x_1, x_2, x_3, x_4), \quad (4.33)$$

with $f^{(8)}$ a homogeneous polynomial of degree 8 in the given coordinates and where $(x_1, x_2, x_3, x_4, x_5)$ again denote homogeneous coordinates of $W\mathbb{C}\mathbb{P}_{11114}^4$.

The properties that we will mostly use are:

- Total Chern class: $c(X_8) = \frac{(1+H)^4(1+4H)}{1+8H} = 1 + 22H^2 - 148H^3$.
- Euler character: $\chi(X_8) = -296$.

In these formulas, H denotes a basis element of the second cohomology group of X_8 ($H \in H^2(X_8)$) and $\int_{X_8} H^3 = 2$, indicating that the weak Jacobi form is two-dimensional:

$$Z(q, \bar{q}, z) = \sum_{k=0}^1 Z_k(q) \Theta_k(\bar{q}, z), \quad (4.34)$$

which means that we have to determine Z_0 and Z_1 .

The Donaldson–Thomas invariants are again calculated from the knowledge of the Gopakumar–Vafa invariants and are found to be:

Donaldson–Thomas invariants: octic				
	n = 0	n = 1	n = 2	n = 3
$\beta = 0$	1	296	43'068	4'104'336
$\beta = 1$	0	29'504	8'674'176	1'253'300'416
$\beta = 2$	564'332	204'456'696	45'540'821'914	6'127'608'486'208

Polar states

The calculation of the polar state indices is quite analogous to the case of the sextic. One has the following polar states:

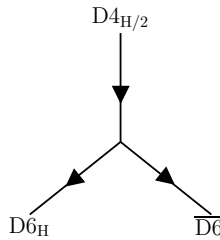
1. $\Delta \mathbf{q} = 0, \Delta \mathbf{q}_0 = 0, \quad [0, \frac{23}{12}]$:

The pure D4 brane carries half a unit of flux to ensure anomaly cancellation, which we denote by $D4_{H/2}$, and has total charge $(0, 1, 1, \frac{13}{6})$. This is the most polar state and represents the class $[0, \frac{23}{12}]$.

One finds just one split flow tree with two centers:

- a D6 with flux H , denoted $D6_H$, with charge $\Gamma_1 = (1, 1, \frac{17}{6}, \frac{13}{6})$;
- a pure $\overline{D6}$: $\Gamma_2 = (-1, 0, -\frac{11}{6}, 0)$.

Schematically, the flow tree looks as follows:



This state can be represented in the B model as the following sheaf complex:

$$0 \rightarrow \mathcal{O} \xrightarrow{\times f_1} \mathcal{O}(H) \rightarrow 0,$$

where $\xrightarrow{\times f_1}$ denotes the morphism defined by multiplication with a degree one polynomial. This morphism also encodes the tachyon field and as can be seen from the sheaf complex, no refinement can occur. The BPS index then reads

$$\Omega = (-1)^{|\langle \Gamma_1, \Gamma_2 \rangle| - 1} |\langle \Gamma_1, \Gamma_2 \rangle| N_{DT}(0, 0) \cdot N_{DT}(0, 0) = (-1)^3 \cdot 4 \cdot 1 \cdot 1 = -4.$$

(4.35)

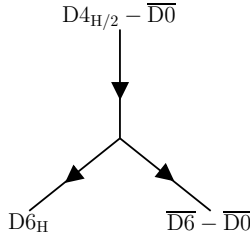
Note again that the intersection number between Γ_1 and Γ_2 nicely corresponds with the index of the moduli space of the hyperplanes $H \subset X$, which is a $\mathbb{C}\mathbb{P}^3$ because the coordinate with weight 4 can not be used to define the hyperplane: $\chi(\mathbb{C}\mathbb{P}^3) = |\langle \Gamma_1, \Gamma_2 \rangle| = 4$.

2. $\Delta \mathbf{q} = \mathbf{0}, \Delta \mathbf{q}_0 = -\mathbf{1}, \quad [0, \frac{11}{12}]$:

Adding one $\overline{\text{D0}}$, one gets the state $\text{D4}_{\text{H}/2} - \overline{\text{D0}}$. It has total charge $(0, 1, 1, \frac{7}{6})$, and reduced D0-brane charge $\hat{q}_0 = \frac{11}{12}$. One finds one split flow tree with two centers:

- a D6 with flux H , denoted D6_H , with charge $\Gamma_1 = (1, 1, \frac{17}{6}, \frac{13}{6})$;
- a $\overline{\text{D6}}$ with one added $\overline{\text{D0}}$, denoted $\overline{\text{D6}} - \overline{\text{D0}}$: $\Gamma_2 = (-1, 0, -\frac{11}{6}, -1)$.

The flow tree looks like



This state can be represented in the B model as the following sheaf complex:

$$0 \rightarrow \mathcal{O} \xrightarrow{\times f_1} \mathcal{O}(H) \rightarrow \mathcal{O}_p \rightarrow 0,$$

with \mathcal{O}_p the skyscraper sheaf of the $\overline{\text{D0}}$ at point p . One sees that a necessary condition on f_1 , the tachyon field, is that it should vanish at p . In the case at hand, every locus p will give one constraint to f_1 , reducing its moduli space to $\mathbb{C}\mathbb{P}^2$. The BPS index then becomes

$$\Omega = (-1)^{|\langle \Gamma_1, \Gamma_2 \rangle| - 1} |\langle \Gamma_1, \Gamma_2 \rangle| N_{\text{DT}}(0, 0) \cdot N_{\text{DT}}(0, 1) = (-1)^2 \cdot 3 \cdot 1 \cdot 296 = 888,$$

(4.36)

where we again have $\chi(\mathbb{C}\mathbb{P}^2) = |\langle \Gamma_1, \Gamma_2 \rangle| = 3$.

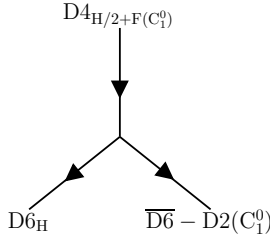
3. $\Delta \mathbf{q} = \mathbf{1}, \Delta \mathbf{q}_0 = -\mathbf{1}, \quad [\gamma_1, \frac{1}{6}]$:

One can now consider a flux, along the gluing vector γ_1 . As seen previously for the sextic, this means turning on an extra flux dual to a degree one rational curve, denoted $\text{D4}_{\text{H}/2+\text{F}(\mathbb{C}^1)}$. This leads to the total charge

$(0, 1, 2, \frac{7}{6})$, and to the reduced D0-brane charge $\hat{q}_0 = \frac{1}{6}$: thus, there is again only one polar state in this γ_1 -class. One finds the split flow tree with the following constituents:

- a D6 with flux H , denoted $D6_H$, with charge $\Gamma_1 = (1, 1, \frac{17}{6}, \frac{13}{6})$;
- a $\overline{D6}$ with one added D2 along the curve C_1^0 , denoted $\overline{D6} - D2(C_1^0)$: $\Gamma_2 = (-1, 0, -\frac{5}{6}, -1)$.

The flow tree looks like



This state can be represented in the B model as the following sheaf complex:

$$0 \rightarrow \mathcal{O} \xrightarrow{\times f_1} \mathcal{O}(H) \rightarrow \mathcal{O}_{C_1^0} \rightarrow 0,$$

with $\mathcal{O}_{C_1^0}$ denoting the coherent sheaf, representing the D2 brane on the curve C_1^0 . The constraints on the tachyon map, i.e. its vanishing at the curve, reduce the moduli space from $\mathbb{C}\mathbb{P}^3$ to $\mathbb{C}\mathbb{P}^1$. The BPS index is calculated according to

$$\Omega = (-1)^{|\langle \Gamma_1, \Gamma_2 \rangle| - 1} |\langle \Gamma_1, \Gamma_2 \rangle| N_{DT}(0, 0) \cdot N_{DT}(1, 1) = (-1)^1 \cdot 2 \cdot 1 \cdot 29'504 = -59'008. \quad (4.37)$$

And again we have $\chi(\mathbb{C}\mathbb{P}^1) = |\langle \Gamma_1, \Gamma_2 \rangle| = 2$.

Using a basis for modular forms of the right weight, one can use these numbers to determine the modular form to be given by

$$Z_0(\tau) = q^{-\frac{23}{12}} (-4 + 888q - 86'140q^2 + 131'940'136q^3 \dots) \quad (4.38)$$

$$Z_1(\tau) = q^{-\frac{7}{6}} (-59'008q + 8'615'168q^2 + \dots) \quad (4.39)$$

This again agrees with the findings of [87] (up to an overall sign).

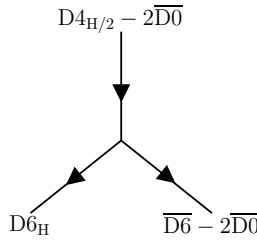
Non-polar states on the octic

1. The state $\Delta \mathbf{q} = \mathbf{0}, \Delta \mathbf{q}_0 = -2, \left[\mathbf{0}, -\frac{1}{12} \right]$

This state, denoted $D_{4H/2} - 2\overline{D0}$, has total charge $(0, 1, 1, \frac{1}{6})$, and reduced D0-brane charge $\hat{q}_0 = -\frac{1}{12}$. One finds the split flow tree with the following constituents:

- a D6 with flux H , denoted $D6_H$, with charge $\Gamma_1 = (1, 1, \frac{17}{6}, \frac{13}{6})$;
- a $\overline{D6}$ with two added $\overline{D0}$'s, denoted $\overline{D6} - 2\overline{D0} : \Gamma_2 = (-1, 0, -\frac{11}{6}, -2)$.

The flow tree looks like



This state can be represented in the B model as the following sheaf complex:

$$0 \rightarrow \mathcal{O} \xrightarrow{\times f_1} \mathcal{O}(H) \rightarrow \mathcal{O}_{p_1, p_2} \rightarrow 0,$$

with \mathcal{O}_{p_1, p_2} the coherent sheaf representing two $\overline{D0}$'s at locations p_1, p_2 .

A naive index calculation would give

$$\begin{aligned} \Omega_{\text{naive}} &= (-1)^{|\langle \Gamma_1, \Gamma_2 \rangle| - 1} |\langle \Gamma_1, \Gamma_2 \rangle| N_{\text{DT}}(0, 0) \cdot N_{\text{DT}}(0, 2) \\ &= (-1)^1 \cdot 2 \cdot 1 \cdot 43'068 = -86'136, \end{aligned} \quad (4.40)$$

which obviously differs from the exact index, which is given by the elliptic genus in equation (4.38) to be $\Omega_{\text{exact}} = -86'140$. This can be cured using the refined method, as will be shown in the next paragraphs.

A general tachyon field is described by the degree one polynomial f_1 , which in the homogeneous coordinates of $W\mathbb{C}\mathbb{P}_{11114}^4$ has the form:

$$f_1 = a_1 x_1 + a_2 x_2 + a_3 x_3 + a_4 x_4. \quad (4.41)$$

The moduli space, prior to imposing the constraints, is again a $\mathbb{C}\mathbb{P}^3$. For the sheaf complex to be a complex, this map has to vanish on the loci of the two $\overline{D0}$'s, denoted p_1 and p_2 in the sheaf complex. This puts a number of independent constraints on this map, given by

$$\text{rank} \begin{pmatrix} x_1 & x_2 & x_3 & x_4 \\ y_1 & y_2 & y_3 & y_4 \end{pmatrix}, \quad (4.42)$$

with x_i, y_i the homogeneous coordinates of the points p_1 and p_2 respectively. For general positions p_1, p_2 , this rank will be two, reducing the moduli space from $\mathbb{C}\mathbb{P}^3$ to a $\mathbb{C}\mathbb{P}^1$. This is where the intersection number $|\langle \Gamma_1, \Gamma_2 \rangle| = \chi(\mathbb{C}\mathbb{P}^1) = 2$ comes from.

Just as we did for the sextic, the refined calculation will proceed in two steps. First, the case $p_1 \neq p_2$ will be investigated. Then, the configurations where the $\overline{\text{D0}}$'s sit at the same location will be analysed. In this last case, one needs to perform a blowup, possibly resulting in an extra constraint from the tangent direction.

(a) $\mathbf{p}_1 \neq \mathbf{p}_2$

In this case, since $(x_1, x_2, x_3, x_4) = (0, 0, 0, 0)$ is not a point on the octic X_8 , we have to look for two different points p_1, p_2 with $(x_1, x_2, x_3, x_4) = \lambda(y_1, y_2, y_3, y_4)$. By looking at equation (4.33), we see that there are two solutions with given (x_1, x_2, x_3, x_4) . We could also use the adjunction formula to calculate the number of points p_2 which satisfy the requirement $(x_1, x_2, x_3, x_4) = \lambda(y_1, y_2, y_3, y_4)$. For a given p_1 , this locus is given by three independent linear constraints (for example, set three independent determinants of the matrix in equation (4.42) to zero). The index of this locus is

$$\int_{X_8} H^3 = 2, \quad (4.43)$$

as was expected from the more direct calculation before. One of these points will be different than p_1 , so we have, for each p_1 , one point $p_2 \neq p_1$ for which the rank in equation (4.42) is one instead of two. Also observe that when $x_5 = 0$, this point coincides with p_1 , so this case needs to be treated separately. This can also be seen by using the adjunction formula: the locus $x_5 = 0$ in $W\mathbb{C}\mathbb{P}^4_{11114}$ is just a $\mathbb{C}\mathbb{P}^3$. Three linear constraints in this $\mathbb{C}\mathbb{P}^3$ give just one intersection point, instead of two on the Calabi Yau, since $\int_{\mathbb{C}\mathbb{P}^3} H^3 = 1$.

(b) $\mathbf{p}_1 = \mathbf{p}_2$

As discussed previously, when the two $\overline{\text{D0}}$'s sit at the same location, one needs to perform a blowup procedure, resulting in an extra tangent direction along which the tachyon field should also vanish. If we parametrize this direction by the homogeneous components X^i , the jump of the tachyon index occurs when:

$$\text{rank} \begin{pmatrix} x_1 & x_2 & x_3 & x_4 \\ X^1 & X^2 & X^3 & X^4 \end{pmatrix} \neq 2, \quad (4.44)$$

One distinguishes between two cases:

- $x_5 \neq 0$: This means one can choose affine coordinates with $x_5 = 1$. Thus, in these coordinates, one knows that $X^5 = 0$ for the tangent vector (and hence the case $X^1 = \dots = X^4 = 0$ is ruled out and only the case $X^i = \lambda x_i$, $i = 1, \dots, 4$ remains). The tangent vectors should be tangent to the Calabi Yau X_8 (meaning $\nabla_X p^{(8)} = 0$), which leads to $8\lambda f^{(8)} = 0$. Since $\lambda \neq 0$, this means $p^{(8)} = 0$, so $x_5 = 0$ upon plugging this into the defining equation of the octic (4.33), which contradicts our assumption. So if $x_5 \neq 0$, no jump in the tachyon index occurs.
- $x_5 = 0$: In this case, without loss of generalization, fix $x_1 = 1$. This means $X^1 = 0$ for the tangent vector. The condition for a jump in the tachyon index is then $X^1 = \dots = X^4 = 0$. This happens when the tangent vector equals $X^5 \partial_5$, which, at the locus $x_5 = 0$, is tangent to the Calabi Yau. Note that there is *one* tangent direction and *one* locus ($x_5 = 0$) for which this happens.

From this information, one can now calculate the index, by treating each of these special configurations separately. Note that we use the following notations and definitions:

- The Euler character of the octic $\chi(X_8) = -296$ is the index of the moduli space of a pointlike $\overline{D0}$ on the Calabi Yau and will just be denoted χ .
- The locus $x_5 = 0$ is denoted by X_0 and its Euler characteristic by $\chi_0 = 304$.

The index receives similar contributions as in the case of the sextic, but the calculation is slightly simpler:

- $\frac{1}{2}(\chi^2 - 2\chi + \chi_0) \cdot \chi(\mathbb{CP}^1)$: this is again the generic case, but as in this case only two points share the same first four homogeneous coordinates, one subtracts two instead of three loci with index χ . Instead of subtracting the locus $x_5 = 0$ three times, one does this twice, and needs to compensate once. In this case, $\chi_0 = 304$.
- $(\chi - \chi_0) \cdot \chi(\mathbb{CP}^2) \cdot \chi(\mathbb{CP}^1)$: this accounts for the case when the two $\overline{D0}$ s coincide, without the locus $x_5 = 0$. Note that the $\chi(\mathbb{CP}^2)$ results from the blowup of a codimension 3 locus.
- $\frac{1}{2}(\chi - \chi_0) \cdot \chi(\mathbb{CP}^2)$: this takes into account the case when $p_1 \neq p_2$ and $(x_1, x_2, x_3, x_4) = \lambda(y_1, y_2, y_3, y_4)$. This is again a locus where the tachyon index has jumped.
- $\chi_0 \cdot (\chi(\mathbb{CP}^2) - 1) \cdot \chi(\mathbb{CP}^1)$: here, the locus $x_5 = 0$ and other coordinates equal is dealt with. In principle one just has to do a blowup (hence a factor of $\chi(\mathbb{CP}^2)$). As was the case with the sextic, one needs to subtract the one tangent direction we found above, because one loses

one of the two constraints on the tachyon field. This tangent direction is taken into account on the next line.

- $\chi_0 \cdot 1 \cdot \chi(\mathbb{CP}^2)$: for this one blowup direction, the tachyon index has jumped.

Collecting all the pieces linked to the value 2 or 3 for the tachyon index, one can state the correct index in the form

$$\Omega_{\text{exact}} = -2 \cdot (43'064) - 3 \cdot (+4) = -86'140, \quad (4.45)$$

which exactly matches the modular prediction in equation (4.38). One can now define the *Donaldson–Thomas partitions* $\mathcal{N}_{\text{DT}}^{(g,s)}(0, 2)$ for the octic:

$$\mathcal{N}_{\text{DT}}^{(g)}(0, 2) = 43'064, \quad (4.46)$$

$$\mathcal{N}_{\text{DT}}^{(s)}(0, 2) = 4. \quad (4.47)$$

$\mathcal{N}_{\text{DT}}^{(g)}(0, 2)$ counts the generic configurations of two $\overline{\text{D0}}$'s on the $\overline{\text{D6}}$, for which the tachyon index is $\chi(\mathbb{CP}^1)$, and $\mathcal{N}_{\text{DT}}^{(s)}(0, 2)$ counts the special configurations, for which the tachyon index jumps to $\chi(\mathbb{CP}^2)$. The total number of configurations just equals the standard Donaldson–Thomas invariant, as it should be:

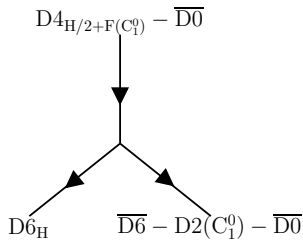
$$N_{\text{DT}}(0, 2) = \mathcal{N}_{\text{DT}}^{(g)}(0, 2) + \mathcal{N}_{\text{DT}}^{(s)}(0, 2) = 43'064 + 4 = 43'068. \quad (4.48)$$

2. The state $\Delta \mathbf{q} = \mathbf{1}$, $\Delta \mathbf{q}_0 = -\mathbf{2}$, $[\gamma_1, -\frac{5}{6}]$

This state, denoted $\text{D4}_{\text{H}/2+\text{F}(\text{C}_1^0)} - \overline{\text{D0}}$, has total charge $(0, 1, 2, \frac{1}{6})$, and reduced D0–brane charge $\hat{q}_0 = -\frac{5}{6}$. One finds the split flow tree with the following constituents:

- a D6 with flux H , denoted D6_{H} , with charge $\Gamma_1 = (1, 1, \frac{17}{6}, \frac{13}{6})$;
- a $\overline{\text{D6}}$ with two added $\overline{\text{D0}}$'s, denoted $\overline{\text{D6}} - 2\overline{\text{D0}}$: $\Gamma_2 = (-1, 0, -\frac{5}{6}, -2)$.

The flow tree looks like



This state can be represented in the B model as the following sheaf complex:

$$0 \rightarrow \mathcal{O} \xrightarrow{\times f_1} \mathcal{O}(H) \rightarrow \mathcal{O}_{C_1^0, p} \rightarrow 0,$$

with $\mathcal{O}_{C_1^0, p}$ the coherent sheaf representing the D2 charge on the curve C_1^0 and $\overline{D0}$ charge at the point p .

The index without refinement would be

$$\begin{aligned} \Omega_{\text{naive}} &= (-1)^{|\langle \Gamma_1, \Gamma_2 \rangle| - 1} |\langle \Gamma_1, \Gamma_2 \rangle| N_{\text{DT}}(0, 0) \cdot N_{\text{DT}}(1, 2) \\ &= (-1)^0 \cdot 1 \cdot 1 \cdot 8'674'176 = 8'674'176, \end{aligned} \quad (4.49)$$

which differs from the modular prediction in equation (4.38): $8'615'168$. So a refinement is necessary. As can be seen from the sheaf complex, the tachyon field, defined by the degree one polynomial f_1 , should vanish at the curve and the point p .

A degree one rational curve on the octic can be represented as a degree one map from a $\mathbb{C}\mathbb{P}^1$, parametrized by the homogeneous coordinates (s, t) to the Calabi–Yau. Consider for example the map

$$(s, t) \rightarrow (s, e^{\frac{i\pi}{8}} s, t, e^{\frac{i\pi}{8}} t, 0). \quad (4.50)$$

This imposes two constraints on the tachyon field, reducing its moduli space to a $\mathbb{C}\mathbb{P}^1$. Adding an extra $\overline{D0}$ will then reduce this moduli space to a $\mathbb{C}\mathbb{P}^0$ (a point), unless something special happens:

- The particle ($\overline{D0}$) does not sit on the curve, but nevertheless produces no extra constraint. It is easy to verify that this cannot possibly happen for this example.
- The $\overline{D0}$ lies on the curve, which means that a blowup needs to be performed in the directions normal to the curve. Again, one might encounter special tangent directions, which do not impose an extra constraint on the tachyon field. Following a similar procedure as in the previous examples, one can indeed verify that this is the case for the direction $X^5 \partial_5$, which is clearly normal to the curve. As the points on the curve satisfy $x_5 = 0$ by equation (4.50), this direction is also automatically tangent to the octic. This means that, for each point p on the curve, there is one special tangent direction for which the tachyon index jumps.

From this information, one can now calculate the index, by treating each of these special configurations separately. Note that we use the following notations and definitions:

- The Euler character of the octic $\chi(X_8) = -296$ is the index of the moduli space of a pointlike $\overline{D0}$ on the Calabi Yau and will just be denoted χ .
- The curve C_1^0 has Euler characteristic $\chi_C = 2$, because it is a rational curve.

The various contributions to the exact index according to the refined prescription read:

- $-n_1^0(\chi - \chi_C)\chi(\mathbb{CP}^0)$. where $n_1^0 = 29'504$ is the Gopakumar–Vafa invariant, counting the number of rational curves of degree one on the octic (see appendix A). The extra minus sign comes from the expansion of Donaldson–Thomas invariants in terms of Gopakumar–Vafa invariants. This term deals with the case, when the $\overline{D0}$ is placed at a point $p \notin C_1^0$, thereby reducing the tachyon moduli space to a \mathbb{CP}^0 .
- $-n_1^0\chi_C[\chi(\mathbb{CP}^1) - 1]\chi(\mathbb{CP}^0)$, dealing with the case that the $\overline{D0}$ is located on the curve, but the blowup tangent direction leads to an extra constraint on the tachyon.
- $-n_1^0\chi_C \cdot 1 \cdot \chi(\mathbb{CP}^1)$, which deals with the case, when the $\overline{D0}$ lies on the curve and a blowup is performed leading to a special tangent direction. In this case, the tachyon field moduli space remains a \mathbb{CP}^1 .

In total, this leads to the index

$$\Omega_{\text{exact}} = 1 \cdot (8'733'184) + 2 \cdot (-59'008) = 8'615'168. \quad (4.51)$$

Spectacularly, by comparing this number to the prediction from modularity (equation (4.38)), one finds exact agreement! One can thus state the *Donaldson–Thomas partitions* $\mathcal{N}_{\text{DT}}(1, 2)$ for the octic:

$$\mathcal{N}_{\text{DT}}^{(g)}(1, 2) = 8'733'184, \quad (4.52)$$

$$\mathcal{N}_{\text{DT}}^{(s)}(1, 2) = -59'008. \quad (4.53)$$

Again, the total number of configurations of the degree one rational curve plus an extra $\overline{D0}$ equals the standard Donaldson–Thomas invariant, as it should be:

$$N_{\text{DT}}(1, 2) = \mathcal{N}_{\text{DT}}^{(g)}(1, 2) + \mathcal{N}_{\text{DT}}^{(s)}(1, 2) = 8'733'184 - 59'008 = 8'674'176. \quad (4.54)$$

4.3.4 Example 3: the decantic

As a last example, we will consider the decantic Calabi Yau. This example is very interesting for two reasons:

1. The index of the polar states receives corrections from the refined calculation method. This means that a new prediction for its elliptic genus is found.
2. On this Calabi Yau, an exact calculation of the index is made for a state that has a single flow realization in supergravity. The refined index calculation for single flows can thus be verified in this case.

The decantic Calabi Yau X_{10} is defined as a degree ten hypersurface in the weighted projective space $W\mathbb{C}P^4_{11125}$. We take the defining polynomial to be of the form:

$$p^{(10)} = x_5^2 + x_4^5 + f^{(10)}(x_1, x_2, x_3), \tag{4.55}$$

with $f^{(10)}$ a homogeneous polynomial of degree 10 in the given coordinates and where $(x_1, x_2, x_3, x_4, x_5)$ again denote homogeneous coordinates of $W\mathbb{C}P^4_{11125}$.

Its main properties are:

- Total Chern class: $c(X_{10}) = \frac{(1+H)^3(1+2H)(1+5H)}{1+10H} = 1 + 34H^2 - 288H^3$.
- Euler character: $\chi(X_{10}) = -288$.

In these formulas, H denotes a basis element of the second cohomology group of X_{10} ($H \in H^2(X_{10})$) and $\int_{X_{10}} H^3 = 1$, indicating that the weak Jacobi form is one-dimensional:

$$Z(q, \bar{q}, z) = Z_0(q) \Theta_0(\bar{q}, z), \tag{4.56}$$

which means that we only have to determine Z_0 .

The Donaldson–Thomas invariants are again calculated from the knowledge of the Gopakumar–Vafa invariants and are found to be:

Donaldson–Thomas invariants: decantic				
	n = 0	n = 1	n = 2	n = 3
$\beta = \mathbf{0}$	1	288	40'752	3'774'912
$\beta = \mathbf{1}$	1150	435'827	89'103'872	11'141'118'264

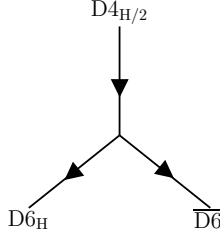
Polar states

One has the following polar states:

1. $\Delta\mathbf{q} = \mathbf{0}, \Delta\mathbf{q}_0 = \mathbf{0}, \quad [0, \frac{35}{24}]$:
 The pure D4 brane carries half a unit of flux to ensure anomaly cancellation, which we denote by $D4_{H/2}$, and has total charge $(0, 1, \frac{1}{2}, \frac{19}{12})$. This is the most polar state and represents the class $[0, \frac{35}{24}]$.
 One finds just one split flow tree with two centers:

- a D6 with flux H , denoted $D6_H$, with charge $\Gamma_1 = (1, 1, \frac{23}{12}, \frac{19}{12})$;
- a pure $\overline{D6}$: $\Gamma_2 = (-1, 0, -\frac{17}{12}, 0)$.

Schematically, the flow tree looks as follows:



This state can be represented in the B model as the following sheaf complex:

$$0 \rightarrow \mathcal{O} \xrightarrow{\times f_1} \mathcal{O}(H) \rightarrow 0,$$

where $\xrightarrow{\times f_1}$ denotes the morphism defined by multiplication with a degree one polynomial. This morphism also encodes the tachyon field and as can be seen from the sheaf complex, no refinement can occur. The BPS index then reads

$$\Omega = (-1)^{|\langle \Gamma_1, \Gamma_2 \rangle| - 1} |\langle \Gamma_1, \Gamma_2 \rangle| N_{DT}(0, 0) \cdot N_{DT}(0, 0) = (-1)^2 \cdot 3 \cdot 1 \cdot 1 = 3. \quad (4.57)$$

Note again that the intersection number between Γ_1 and Γ_2 nicely corresponds with the index of the moduli space of the hyperplanes $H \subset X$, which is a \mathbb{CP}^2 because the coordinates with weight 2 and 5 can not be used to define the hyperplane: $\chi(\mathbb{CP}^2) = |\langle \Gamma_1, \Gamma_2 \rangle| = 3$.

2. $\Delta \mathbf{q} = \mathbf{0}, \Delta \mathbf{q}_0 = -1, \quad [0, \frac{11}{24}]$:

The next polar state is the D4 brane with one added $\overline{D0}$ brane, which again carries half a unit of flux to ensure anomaly cancellation. It is denoted $D4_{H/2} - \overline{D0}$, and has total charge $(0, 1, \frac{1}{2}, \frac{7}{12})$. This is the most polar state and represents the class $[0, \frac{11}{24}]$.

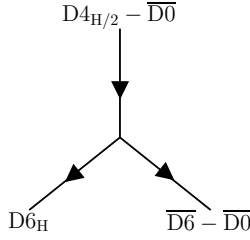
One finds just one split flow tree with two centers:

- a D6 with flux H , denoted $D6_H$, with charge $\Gamma_1 = (1, 1, \frac{23}{12}, \frac{19}{12})$;
- a $\overline{D6}$ with one added $\overline{D0}$: $\Gamma_2 = (-1, 0, -\frac{17}{12}, -1)$.

Schematically, the flow tree looks as follows:

This state can be represented in the B model as the following sheaf complex:

$$0 \rightarrow \mathcal{O} \xrightarrow{\times f_1} \mathcal{O}(H) \rightarrow \mathcal{O}_p \rightarrow 0,$$



where \mathcal{O}_p denotes the skyscraper sheaf of the $\overline{D0}$ at point p . This time, a refinement becomes necessary. The naive index would be

$$\begin{aligned} \Omega_{\text{naive}} &= (-1)^{|\langle \Gamma_1, \Gamma_2 \rangle| - 1} |\langle \Gamma_1, \Gamma_2 \rangle| N_{\text{DT}}(0, 0) \cdot N_{\text{DT}}(0, 1) \\ &= (-1)^1 \cdot 2 \cdot 1 \cdot 288 = -576. \end{aligned} \quad (4.58)$$

Note again that the intersection number between Γ_1 and Γ_2 nicely corresponds with the index of the moduli space of the hyperplanes $H \subset X$, which, for generic configurations of the $\overline{D0}$ brane, is a \mathbb{CP}^1 : $\chi(\mathbb{CP}^1) = |\langle \Gamma_1, \Gamma_2 \rangle| = 2$.

The tachyon field, which is determined by a degree one polynomial:

$$T = a_1 x_1 + a_2 x_2 + a_3 x_3, \quad (4.59)$$

needs to vanish at the point p . When $(x_1, x_2, x_3) = (0, 0, 0)$ however, this does not put any constraint on this map, so the tachyon moduli space is a \mathbb{CP}^2 in this case, rather than a \mathbb{CP}^1 . One can easily see that this locus is just a point on the decantic Calabi Yau, denoted X_{123} and so we have $\chi_{123} \equiv \chi(X_{123}) = 1$. The refined BPS index then receives the following contributions:

- $(\chi - \chi_{123})\chi(\mathbb{CP}^1)$: this is the general case, where the tachyon moduli space is reduced to a \mathbb{CP}^1 .
- $\chi_{123}\chi(\mathbb{CP}^2)$: this deals with the case when the point p is defined by $(x_1, x_2, x_3) = (0, 0, 0)$. The tachyon moduli space is a \mathbb{CP}^2 here.

Again, we used $\chi \equiv \chi(X_{10})$. The index can thus be written as:

$$\Omega_{\text{exact}} = (-2) \cdot (289) + (-3) \cdot (-1) = -575, \quad (4.60)$$

and the Donaldson–Thomas partitions are:

$$\mathcal{N}_{\text{DT}}^{(g)}(0, 1) = 289, \quad (4.61)$$

$$\mathcal{N}_{\text{DT}}^{(s)}(0, 1) = -1. \quad (4.62)$$

Again, the total number of configurations of the $\overline{D0}$ equals the standard Donaldson–Thomas invariant:

$$N_{DT}(0, 1) = \mathcal{N}_{DT}^{(g)}(0, 1) + \mathcal{N}_{DT}^{(s)}(0, 1) = 289 - 1 = 288. \tag{4.63}$$

These two polar state degeneracies determine the elliptic genus of the decantic to be:

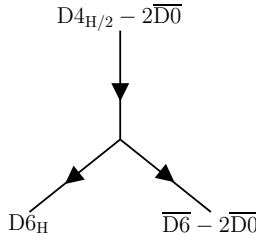
$$Z_0(q) = q^{-\frac{35}{24}}(3 - 575q + 271'955q^2 + 206'406'410q^3 + 21'593'817'025q^4 \dots). \tag{4.64}$$

Non-polar state: $\Delta\mathbf{q} = \mathbf{0}, \Delta\mathbf{q}_0 = -2, \quad [0, -\frac{13}{24}]$

The total charge for this system reads $\Gamma = (0, 1, \frac{1}{2}, -\frac{5}{12})$, which implies $\hat{q}_0 = -\frac{13}{24}$: this is thus a non-polar state. One finds a split flow tree with the centers

- a D6 with flux H , denoted $D6_H$, with charge $\Gamma_1 = (1, 1, \frac{23}{12}, \frac{19}{12})$;
- a $\overline{D6}$ with two added $\overline{D0}$'s, denoted $\overline{D6} - 2\overline{D0}$: $\Gamma_2 = (-1, 0, -\frac{17}{12}, -2)$.

The flow tree looks like



This state can be represented in the B model as the following sheaf complex:

$$0 \rightarrow \mathcal{O} \xrightarrow{\times f_1} \mathcal{O}(H) \rightarrow \mathcal{O}_{p_1, p_2} \rightarrow 0,$$

with \mathcal{O}_{p_1, p_2} the coherent sheaf representing two $\overline{D0}$'s at locations p_1, p_2 .

A naive index calculation would give

$$\begin{aligned} \Omega_{\text{naive}} &= (-1)^{|\langle \Gamma_1, \Gamma_2 \rangle| - 1} |\langle \Gamma_1, \Gamma_2 \rangle| N_{DT}(0, 0) \cdot N_{DT}(0, 2) \\ &= (-1)^0 \cdot 1 \cdot 1 \cdot 40'752 = 40'752. \end{aligned} \tag{4.65}$$

This index needs refinement because, just as in the case where there is only one $\overline{D0}$, the points p_1, p_2 could be at the special locus where $(x_1, x_2, x_3) = (0, 0, 0)$.

Furthermore, as we will show, there are other configurations that exhibit an enhanced tachyon moduli space.

Similarly as in the previously discussed cases, the number of constraints on the tachyon field is given by

$$\text{rank} \begin{pmatrix} x_1 & x_2 & x_3 \\ y_1 & y_2 & y_3 \end{pmatrix}, \tag{4.66}$$

with (x_1, x_2, x_3) and (y_1, y_2, y_3) the homogeneous coordinates of weight one of the points p_1 and p_2 respectively.

The special point $(x_1, x_2, x_3) = (0, 0, 0)$ will be treated first and denoted by X_{123} . Its Euler characteristic is just $\chi_{123} = 1$, as would be expected for a single point. If one of the $\overline{D0}$'s sits in X_{123} , the number of constraints is clearly just one, instead of two for general positions of the $\overline{D0}$'s. If both are in X_{123} , we have to perform a blowup and it is easy to see that the full set of blowup directions ($\mathbb{C}P^2$) does give an extra constraint.

For the remaining set of points $X \setminus X_{123}$, suppose we fix a constraint by putting one $\overline{D0}$. From (4.66), we see that constraint loss ($\text{rank} < 2$) occurs for a second $\overline{D0}$ whose coordinates satisfy two degree one equations (whose coefficients are determined by (x_1, x_2, x_3)). Additivity of the Chern class then determines

$$c(X_{cl}(x_i)) = \frac{c(X)}{(1+H)^2} = 1 - 2H, \tag{4.67}$$

where $X_{cl}(x_i)$ denotes the locus with constraint loss (which depends on the coordinates x_i of the first $\overline{D0}$). Its Euler characteristic is $\int_{X_{cl}} -2H = \int_X -2H^3 = -2$. However, the special point X_{123} , which we already treated in the previous paragraph, will always be a solution to the two degree one equations (the trivial solution), so the index of ‘parallel’ solutions on $X \setminus X_{123}$ is $\chi_{\parallel} = -2 - 1 = -3$. This index counts the number of solutions for the first $\overline{D0}$ in general position, so one has to check if special situations can occur. For (y_1, y_2, y_3) fixed, up to scaling, the only possibility for this to happen would be when $p^{(10)}(y_1, y_2, y_3) = 0$. In this case, one still has ‘-3 solutions’ where $(y_4, y_5) \neq (0, 0)$, but there is also an extra solution for which $(y_4, y_5) = (0, 0)$. The index for such a set thus becomes $\chi_{\parallel} + 1 = -2$. Since each point with $(y_4, y_5) = (0, 0)$ will have an inequivalent set of degree one coordinates (y_1, y_2, y_3) with $p^{(10)}(y_1, y_2, y_3) = 0$, this locus counts the number of inequivalent classes of points that satisfy $p^{(10)}(y_1, y_2, y_3) = 0$. Define X_{45} as the locus $x_4 = x_5 = 0$, then

$$c(X_{45}) = \frac{c(X)}{(1+2H)(1+5H)} = 1 - 7H, \tag{4.68}$$

and $\chi_{45} \equiv \chi(X_{45}) = \int_{X_{45}} -7H = \int_X 2H \wedge 5H \wedge (-7H) = -70$. As each of these classes denotes a set with index -2 , the total index of this set of points is

$\chi_{special} \equiv (-70)(-2) = 140$. For each of these, there are $\chi_{||} + 1 = -2$ solutions that result in a constraint loss.

Finally, one has to calculate the number of constraints in the case of a blowup in $X \setminus X_{123}$. Since $(x_1, x_2, x_3) \neq (0, 0, 0)$, one can fix one of these coordinates to 1, meaning that constraint loss will only occur for tangent directions $X^i \partial_i$ with $X^1 = X^2 = X^3 = 0$. The condition for the direction to lie in the tangent space of the Calabi–Yau hypersurface then becomes

$$2X^5x_5 + 5X^4x_4 = 0. \quad (4.69)$$

If $(x_4, x_5) \neq (0, 0)$, this gives one direction with constraint loss. In the case $(x_4, x_5) = (0, 0)$, there is a \mathbb{CP}^1 of directions with constraint loss.

Now we have all we need to calculate the index of the $D6_H - 2\overline{D0}$, $\overline{D6}$ state. It has the following contributions without constraint loss:

- $\frac{1}{2} [(\chi - \chi_{123})^2 - (\chi - \chi_{123} - \chi_{special})\chi_{||} - \chi_{special}(\chi_{||} + 1)] = 41'257$: This counts the generic situation with two $\overline{D0}$'s in different location and giving two independent constraints. Note that $\chi - \chi_{123}$ is the index of $X \setminus X_{123}$.
- $(\chi - \chi_{123} - \chi_{45}) [\chi(\mathbb{CP}^2) - 1] + \chi_{45} [\chi(\mathbb{CP}^2) - \chi(\mathbb{CP}^1)] = -508$: The index for a blowup in $X \setminus X_{123}$, without constraint loss. The locus X_{45} is dealt with separately, because of the enlarged set of directions with constraint loss (a \mathbb{CP}^1).

These indices sum up to 40'749.

The index contributions where constraint loss occurs are given by:

- $\frac{1}{2}(\chi - \chi_{123} - \chi_{special})(\chi_{||} - 1) = 858$: This index denotes the situation where one $\overline{D0}$ is in a generic location ($X \setminus (X_{123} \cup X_{special})$) and the other gives constraint loss. The '-1' in the last factor subtracts the situation where a blowup needs to be performed.
- $\frac{1}{2}\chi_{special}(\chi_{||} + 1 - 1) = -210$: This index refers to a similar situation as in the previous item, but with an extra point giving constraint loss (hence, the '+1' in the last factor).
- $\chi_{123}(\chi - \chi_{123}) = -289$: The index of the situation where one $\overline{D0}$ has $(x_1, x_2, x_3) = (0, 0, 0)$ and the other sits in $X \setminus X_{123}$.
- $(\chi - \chi_{123} - \chi_{45}) \cdot 1 + \chi_{123} \cdot \chi(\mathbb{CP}^2) + \chi_{45} \cdot \chi(\mathbb{CP}^1) = -356$: These are the blowup situations with constraint loss. Three different cases are distinguished: 'general' point, $x_1 = x_2 = x_3 = 0$ and $x_4 = x_5 = 0$.

The index of the constraint loss situations totals 3.

In total, this leads to the index

$$\Omega_{\text{exact}} = 1 \cdot 40'749 + 2 \cdot 3 = 40'755. \tag{4.70}$$

We then have the following *Donaldson–Thomas partitions* $\mathcal{N}_{\text{DT}}(0, 2)$ for the decantic:

$$\mathcal{N}_{\text{DT}}^{(g)}(0, 2) = 40'749, \tag{4.71}$$

$$\mathcal{N}_{\text{DT}}^{(s)}(0, 2) = 3. \tag{4.72}$$

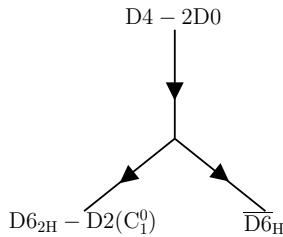
Again, the total number of configurations of two $\overline{\text{D0}}$'s equals the standard Donaldson–Thomas invariant:

$$N_{\text{DT}}(0, 2) = \mathcal{N}_{\text{DT}}^{(g)}(0, 2) + \mathcal{N}_{\text{DT}}^{(s)}(0, 2) = 40'749 + 3 = 40'752. \tag{4.73}$$

On top of the previous state, corresponding to a split flow tree, one also finds a D6 with a degree one rational curve and flux $2H$ plus a $\overline{\text{D6}}$ with flux H . The individual charges of these constituents are:

- a D6 with flux $2H$ and one added D2 along the curve C_1^0 denoted $\text{D6}_{2H} - \text{D2}(C_1^0)$, with charge $\Gamma_1 = (1, 2, \frac{29}{12}, \frac{7}{6})$;
- a $\overline{\text{D6}}$ with flux H , denoted $\overline{\text{D6}}_H : \Gamma_2 = (-1, -1, -\frac{23}{12}, -\frac{19}{12})$.

The flow tree looks like



This state can be represented in the B model as the following sheaf complex:

$$0 \rightarrow \mathcal{O}(H) \xrightarrow{\times f_1} \mathcal{O}(2H) \rightarrow \mathcal{O}_{C_1^0} \rightarrow 0,$$

with $\mathcal{O}_{C_1^0}$ denoting the coherent sheaf, representing the D2 brane on the curve C_1^0 .

This state corresponds to a single flow tree, as the flow in moduli space reaches its attractor value before crossing the wall of marginal stability. To calculate its

index, the extension of the refined index calculation is necessary. As stated before however, this does not affect the calculation itself very much, as this state could be moved in moduli space to the wall of marginal stability without changing its index. We are therefore in a position to calculate the index as in the case of split flows.

The curve on the D6 will completely fix the tachyon field (this is very similar to the case of rational curves on the octic), implying that the total index will equal the number of degree one rational curves, which can be found to be $231'200$ (see for example [88]).

Adding up the contributions from the split and the single flow, the result is $40'755 + 231'200 = 271'955$, which exactly matches the modular prediction in (4.64)!

Furthermore, the Donaldson–Thomas invariant $\mathcal{N}_{DT}(1, 1) = 435'827$ consists of contributions from these degree one rational curves and degree one curves with genus one and two, with added $\overline{D0}$ charges. This means that, by using only the contribution from the rational curves, this index also results from a refined calculation.

Note that the modular prediction itself was also a result of a refined calculation. The remarkable correspondence between this calculation and the modular prediction therefore provides strong support to both the refined index calculation method as to the new elliptic genus in equation (4.64).

4.3.5 Discussion of the results

The refined calculation method is based on the observation that the tachyon moduli space can differ for different configurations of D6 and $\overline{D6}$ brane states. It calculates the index of the total moduli space, which does not constitute a simple fibration of the tachyon moduli space over the moduli space of D6 and $\overline{D6}$ configurations, by treating these different components of the tachyon moduli space separately. In the beginning of this chapter, this procedure was argued to follow simply from the structure of these brane states in the topological B model, where the tachyon field is represented as a morphism between coherent sheaves.

The results of this refined method for three example Calabi Yau threefolds leads to the following observations:

1. For the sextic and octic Calabi Yau, the calculation for the polar state indices results in the same index as would be expected from an unrefined computation. This implies that the elliptic genus is found to be the exact same one as in [87].

2. Applying the method to calculate some non-polar state indices for these two Calabi Yau threefolds, shows that, unlike the calculation in [87], we obtain the exact same numbers as expected from the modular expansion of the elliptic genus. This provides strong support for the correctness of the refined calculation.
3. On the decantic Calabi Yau, the refined calculation results in a different elliptic genus as in [87], since the index of a polar state was shown to receive corrections, originating from a $\overline{D0}$ configuration that is perceived differently by the tachyon field.
4. By analyzing the index of some non-polar states on the decantic, the newly found elliptic genus was found to agree with these refined computations. Furthermore, as one of these non-polar states had a realization as a single flow in the supergravity picture, the generalization of the method to single flow states could be verified. The result turned out to be positive: the calculated index perfectly agreed with the modular prediction from the new elliptic genus.

These observations can be succinctly summarized by saying that the results provide strong evidence of the correctness of our refined calculation and also give rise to new elliptic genera in specific cases. The latter point should be stressed, because it implies the necessity of the refinement: if it only affected non-polar states, one could use the unrefined method to calculate the polar state indices and then the modular expansion to find the non-polar indices.

Finally, as any nice result in physics, it also raises some questions. Here, we want to state two of these: the relation of the refined method to the wall crossing formulas and Π -stability of single flow realizations in the B model.

Let us first state the wall crossing behaviour of BPS states, found in [65]. As was already indicated in the beginning of this chapter, if one tunes the moduli at spatial infinity to a value close to the wall of marginal stability, the constituent charge states' position tend to diverge from one another until they become infinitely separated. If the wall is crossed, this specific flow tree ceases to exist and a jump in the index occurs. The amount of this jump, which is just the difference in the index on either side of the wall of marginal stability, is exactly what one tries to capture with a wall crossing formula. In [65], they found the following formula, which was later confirmed in the more general setting of [89, 90]:

$$\Delta\Omega|_{t_{ms}} = (-1)^{\langle\Gamma_1, \Gamma_2\rangle - 1} |\langle\Gamma_1, \Gamma_2\rangle| \Omega(\Gamma_1)|_{t_{ms}} \Omega(\Gamma_2)|_{t_{ms}}, \quad (4.74)$$

where $\Delta\Omega|_{t_{ms}}$ denotes the jump in the index by crossing a wall of marginal stability at the moduli value t_{ms} and $\Omega(\Gamma_i)|_{t_{ms}}$ is the index of the constituent charge Γ_i at moduli value t_{ms} .

One first notes that this jump is exactly the value of an unrefined calculation of the index (referred to by Ω_{naive} in the preceding sections of this thesis).

Although the total index, calculated by our refined computation scheme has been confirmed by the modular expansion of the elliptic genus, it does not seem to capture this wall crossing behaviour, as a straightforward application of it would seem to contradict equation (4.74). However, they do not need to contradict one another, as there is an important distinction between a total index computation and a jump of this index at a wall of marginal stability. If both descriptions, the refined calculation of the index and the wall crossing formula of equation (4.74), are assumed to be correct, this would only imply that at the other side of the wall of marginal stability, some residual states survive. It would surely be very interesting to study this issue from the viewpoint of the topological B model, in which our calculations find their *raison d'être*.

The second open question concerns the stability of a bound state in the B model, representing a single flow in the supergravity description. The integrability constraint of equation (3.47) can be shown to be violated at the attractor value of a single flow, for every possible split into constituent states Γ_1, Γ_2 . Of course, since the state in supergravity is realized as a single flow, this does not pose any problem for its existence. But in the B model approach, where we represent the corresponding state by a bound state of two constituents, this raises the question: can this bound state be stable at the attractor value of the single flow?

Although this issue remains to be elucidated, we can already provide a remark that may point to its clarification. The supergravity constraint on the state's stability is not necessarily applicable in the B model approach, where a more complex criterion of stability should be applied, called Π -stability. It would be interesting to investigate this type of stability for the single flow state realization we found on the decantic. Furthermore, this could provide for a clear criterion of which bound states should be included in the computation of the index of a single flow state in supergravity.

These two subjects clearly deserve to be treated in more detail in future research.

4.4 Summary

We started this chapter by discussing the correspondence between BPS solutions in supergravity and B branes in the topological B model. By tuning the string coupling constant to zero, in the parent string theory of which the supergravity theory is a low-energy approximation, we arrived at D-brane states that are localized at a point in the non-compact four-dimensional part of spacetime. Furthermore, the moduli profile in these four non-compact directions was argued

to be flat. This allowed the discussion of these brane states in a topologically twisted version of a $\mathcal{N} = (2, 2)$ sigma model.

The topological B model was then briefly introduced, with an emphasis on examples of B branes that are used throughout the remainder of the chapter. The representation of these B branes as complexes of coherent sheaves, turning them into objects of the renowned derived category of coherent sheaves, enabled us to pinpoint the need for a refined procedure to calculate their indices. The origin of this refinement was shown to be the non-trivial fibration structure of the tachyon field moduli space over the moduli space of D6 and $\overline{\text{D6}}$ brane configurations. This tachyon field is represented in the derived category as a morphism between coherent sheaves and the jump in its index is a result of the requirement that the bound state is still a complex, implying that the image of a morphism should be in the kernel of the next morphism.

The major part of this chapter constituted a discussion of the results of [18, 19], obtained by the author and collaborators. In this part, the refined calculation method is used to find BPS indices for three different Calabi Yau compactifications. As mentioned in section 4.3.5, these results confirm the correctness of the refined method and also provide for a new elliptic genus in the case of the decantic Calabi Yau. Furthermore, the extension of the technique to single flow states was confirmed by an index calculation of a non-polar state on the decantic.

The chapter concluded with a short discussion of the results, found in [18, 19]. Apart from the successes of the refined technique, some open questions were mentioned. More specifically, the relation of the refined method to wall crossing and the use of Π -stability for single flows were put forward as subjects that require future attention.

Chapter 5

Conclusion

Despite the remarkable successes of Quantum Field Theory and General Relativity, which are two major achievements of twentieth century theoretical physics, some issues remain to be solved. Their fundamentally different formulations, one as a quantum theory of relativistic fields, the other as a classical field theory, raises questions as to how they should be reconciled with one another. This question becomes all the more important when considering physical situations that require both approaches.

In our introduction, we showed that in different physical regimes, different physical theories should be applied. More precisely, in some limits, simpler models can be used to describe physics. For example, when the speed of the particles in a given system is low, as compared to the speed of light, one does not need a relativistic description of the system and, in the case quantum mechanical effects are also negligible, one can use classical mechanics to describe its dynamics with high accuracy. This all seems to suggest one overarching theory, a so-called *theory of everything*, of which all other known physical theories are just limits.

The need for such a unified description of physical phenomena becomes clear when considering systems that require both a quantum mechanical treatment and a general relativistic one. In particular, this happens at the Planck scale, where gravity should be described as a quantum theory. The most obvious of examples are the starting point of our universe, the Big Bang, and black holes.

In the first chapter, some distinctive properties of black holes were discussed. In General Relativity, or generalizations thereof that include gauge theories, black holes are characterized by the presence of an event horizon, which forms the boundary of trapped light rays (and a fortiori, of every timelike worldline). We showed this causal structure by using Penrose diagrams and used these also to

argue that the horizon is a global feature, as opposed to something that could be measured locally. One of the implications of this observation is that locally, there is nothing special about the horizon. For large black holes, the tidal effects at the horizon become increasingly small, justifying the Rindler approximation of the near horizon region. The Rindler coordinate system describes flat Minkowski spacetime, where static observers in Schwarzschild coordinates become accelerating observers.

By using the Unruh effect for accelerating observers, we were able to show that the horizon looks like a thermal region for a static Schwarzschild observer, with temperature $T = 1/8\pi M$, where M is the mass of the black hole. This leads to the statement of the laws of black hole thermodynamics, which are quite similar to the usual laws of thermodynamics. This is the first hint that there should be an entropy associated to a black hole, proportional to its horizon area.

The uniqueness of a black hole in classical field theories, meaning that the solution of the field equations only depends on its mass, and possibly charges, leads to the second hint of its entropy. If there is truly only one solution, then it would be impossible to trace it back to its origins, implying that the formation of a black hole is accompanied by loss of information. This constitutes the *information paradox*, which we also briefly discuss in chapter 2. The entropy, found by the reasoning of the previous paragraph should thus be taken as a real thermodynamic entropy, encoding the amount of microscopic disorder of a given macroscopic object.

Taking all these elements together, we arrive at the conclusion that a decent theory of quantum gravity should be able to provide for a large amount of microstates for a black hole of fixed mass and charge. This is where string theory enters the arena, as a prime candidate for a unified theory of quantum gravity.

Starting from chapter 3, we introduced the reader to an array of physical concepts and tools, necessary for arriving at the results of chapter 4. First, an overview of string theory was given, providing the basic perturbative formulation but also introducing non-perturbative objects such as D-branes. We showed that at low energy, these string theories can be approximated by supergravity theories.

Since the models, used in chapter 4, are Calabi Yau compactifications of type II superstring theory and these constructs result in the preservation of a $\mathcal{N} = 2$ supersymmetry in four dimensions, the main characteristics of this $\mathcal{N} = 2$ algebra and its representations were stated. Next, we discussed the main tools for studying supersymmetric black holes in the resulting low energy description: the attractor mechanism, split flow trees and elliptic genera.

The attractor mechanism states that the moduli fields of a supersymmetric black hole solution will have a fixed value at the horizon, undisturbed by changes in their background values at infinity (this is strictly only true when the background value does not cross a wall of marginal stability). Combined with a description of multicenter solutions, this observation naturally leads to the split flow tree picture,

giving a representation in moduli space of the variation of these moduli fields from spatial infinity up to the different centers of the solution. These split flow trees are also conjectured to be an existence criterion for BPS solutions in the full string theory. We will make use of this conjecture in chapter 4 to assert the existence of certain bound states.

The elliptic genus of BPS black holes is a formal partition sum, encoding the degeneracies of BPS solutions with fixed magnetic and variable electric charges. Because it displays particular transformation properties under the modular group, one can construct the whole partition sum from the knowledge of just a finite number of terms, called the polar terms. This is put to good use in our own research, since it enables us to verify the validity of our calculations.

Chapter 4 is completely devoted to original research, performed during my doctoral studies. After elucidating a correspondence between BPS solutions in supergravity and B branes in the topological B model, we provided the reader with some insights on how these B branes are represented as objects in the derived category of coherent sheaves. This rather mathematical description enabled us to formulate the origin of our main result: a refined description and calculation of the index of BPS states.

Then, the results of this research [18, 19] were presented. By calculating the indices of the polar states in three different compactification models, we were able to construct their elliptic genera. For one model, the decantic Calabi Yau, this resulted in a corrected elliptic genus (in the sense that it differs from an earlier calculation in [87]).

The calculation of the indices for some non-polar states then showed the correctness of our method since these results matched perfectly with the values from the modular expansion of the elliptic genus. Furthermore, in the case of the decantic Calabi Yau, the new elliptic genus was confirmed. The use of a generalized technique, able to also deal with states which correspond to single flows in the supergravity picture and developed in [19], was put to test in these calculations. The exact correspondence with the elliptic genus again provided strong evidence of the correctness of this generalized technique.

The main benefits of this work could be summarized as follows. First, it provides for a clear and well defined mathematical framework in which to study BPS solutions of type II string theory. The finiteness of the resulting indices and their correspondence with the indices of the elliptic genus is exactly what we were looking for when discussing how a theory of quantum gravity should resolve some open questions in black hole physics.

Secondly, by offering such a strict mathematical framework, these results open up paths for future research. As mentioned in section 4.3.5, their relation to wall crossing formulas would form an interesting subject of its own. Another possibility would be the study of the asymptotics of these indices for large charges, which

could result in a better understanding of various topics that arise in this regime: the entropy enigma [65] or the OSV conjecture [91] to name just two of them.

Finally, due the enormous complexity of performing calculations in string theory, our results, which provide exact numbers, should be seen as a step towards a better understanding of the theory and, more specifically, its finiteness.

Appendix A

Calabi Yau geometry

This appendix gives a short overview of the notions of complex geometry and Calabi Yau manifolds we use throughout this thesis. A nice reference for geometric and topological concepts, from a physics perspective, is [38]. Some shorter introductions, more specifically oriented towards Calabi Yau manifolds and their use as compactifying spaces of (topological) string theory, can be found in [92, 80], while [93] provides a very thorough treatment of Calabi Yau manifolds, oriented to physicists.

A.1 Complex geometry and Kähler manifolds

Many manifolds

A *real manifold* of dimension n is a topological space that locally looks like n -dimensional Euclidean space \mathbb{R}^n . This can be made precise by saying that the space has an open cover $\{U_\alpha\}$ and a set of homeomorphisms $\{\phi_\alpha\}$, such that ϕ_i maps U_i onto an open subset of \mathbb{R}^n . The U_i are called *patches*, while the set of these patches and maps is referred to as an *atlas*. By using the Euclidean coordinates of \mathbb{R}^n , the map ϕ_i defines coordinates x_i^μ , $\mu = 1, \dots, n$ on the patch U_i ¹. On an overlap between two open sets U_i and U_j , one can construct the *transition functions* $\psi_{ij} \equiv \phi_i \circ \phi_j^{-1}$, forming a continuous map between two open subsets of \mathbb{R}^n . A manifold is called *differentiable* if these transition function are

¹The subscript on the coordinates, referring to the specific patch and homeomorphism used, will often be omitted. One has to keep in mind however that these coordinates are only defined locally.

also infinitely differentiable, or equivalently $\psi_{ij} \in C^\infty(U_i \cap U_j)$. We will always assume manifolds to be differentiable.

The method of providing a differentiable structure to manifolds by putting conditions on their transition functions, can also be used to give manifolds other structures. For example, this allows us to define *complex manifolds*. On a specific patch U_i of an $2m$ -dimensional real manifold, one can always define complex coordinates $z^i, \bar{z}^i, i = 1, \dots, m$ from the real coordinates $x^i, i = 1, \dots, 2m$:

$$\begin{aligned} z^i &\equiv x^i + ix^{m+i} \\ \bar{z}^i &\equiv x^i - ix^{m+i}, \end{aligned} \tag{A.1}$$

for $i = 1, \dots, m$. However, for these complex coordinates to make sense globally, one requires the transition functions to be holomorphic functions. To see this, suppose that we have a holomorphic function on the patch U_i . Note that the complex coordinates on U_i allow to define a holomorphic function. If the transition functions ψ_{ji} are not holomorphic, then on the overlap $U_i \cap U_j$, this same function would not be holomorphic in the complex coordinates defined by ϕ_j . A *complex manifold* of dimension m is thus defined as a topological space, endowed with an atlas $\{(U_\alpha, \phi_\alpha)\}$, where the ϕ_i are now homeomorphism from U_i to an open subset of \mathbb{C}^m and with the extra condition that the transition functions are holomorphic.

Tangent spaces and metrics

For an n -dimensional real manifold M , the *tangent space* TM can be defined as the set of vector fields V , of the form

$$V \equiv \sum_{i=1}^n V^i(x) \frac{\partial}{\partial x^i}, \tag{A.2}$$

which is a linear map from the set of differentiable functions $C^\infty(M)$ to itself². The tangent space in a point p , denoted TM_p is then a n -dimensional vector space. Its elements are of the form (A.2), where the $V^i(x)$ are now evaluated at the point p .

For a complex manifold of dimension m , we use the notation with unbarred and barred indices:

$$V \equiv \sum_{i=1}^m V^i(z, \bar{z}) \frac{\partial}{\partial z^i} + V^{\bar{i}}(z, \bar{z}) \frac{\partial}{\partial \bar{z}^i}. \tag{A.3}$$

A real vector field on the manifold will then satisfy $V^{\bar{i}} = (V^i)^*$. By dropping this condition, one gets the complexified tangent space $TM^{\mathbb{C}}$. Note that in this case $TM_p^{\mathbb{C}}$ has *complex* dimension $2m$.

²More specifically, these vector fields are a \mathbb{R} -derivation on $C^\infty(M)$.

The dual space of the tangent space is called the *cotangent space* T^*M , and they contain the cotangent vectors A , denoted

$$A \equiv \sum_{i=1}^n A_i(x) dx^i, \tag{A.4}$$

such that $A(V) = \sum_i A_i V^i \in C^\infty(M)$.

A metric g on a real manifold M is a symmetric bilinear form on the tangent space TM , usually taken to be nondegenerate. This means that

$$g : TM \times TM \rightarrow C^\infty(M) : (V, W) \rightarrow g_{ij} V^i W^j, \tag{A.5}$$

where repeated indices are summed over. The metric components are given by $g_{ij}(x) = g(\frac{\partial}{\partial x^i}, \frac{\partial}{\partial x^j})(x)$. On the vector space TM_p , it maps two vectors to a real number. On a complex manifold of dimension m , the components of a real metric, which is one that maps real vector fields to real functions, should satisfy:

$$g_{ij} = (g_{\bar{i}\bar{j}})^*, \quad g_{i\bar{j}} = (g_{\bar{i}j})^*. \tag{A.6}$$

On a complex manifold M , we can also define a complex structure $J : TM \rightarrow TM$, which in a local chart maps $\frac{\partial}{\partial z^i} \rightarrow i \frac{\partial}{\partial z^i}$ and $\frac{\partial}{\partial \bar{z}^i} \rightarrow -i \frac{\partial}{\partial \bar{z}^i}$. The holomorphicity of the transition functions then guarantees that the complex structure is globally well defined. Equipped with this structure, we can now define a Hermitian metric as one that preserves the complex structure:

$$g(J(X), J(Y)) = g(X, Y), \tag{A.7}$$

where $X, Y \in TM$. A *Hermitian manifold* (M, g) is then a complex manifold M , endowed with a Hermitian metric g .

Kähler manifolds

On a Hermitian manifold, we define a *local Kähler metric* to be a Hermitian metric that on a certain patch can be written as:

$$g_{i\bar{j}} = \frac{\partial^2 K(z, \bar{z})}{\partial z^i \partial \bar{z}^j}. \tag{A.8}$$

Because a patch is homeomorphic to a m -dimensional ball in \mathbb{C}^m , the Poincaré lemma states that the existence of such a function $K(z, \bar{z})$ is equivalent to the condition:

$$\frac{\partial g_{i\bar{j}}}{\partial z^k} = \frac{\partial g_{k\bar{j}}}{\partial z^i}, \tag{A.9}$$

and a similar one for the anti-holomorphic partial derivatives. These conditions then are equivalent to saying that the two-form

$$\omega \equiv \partial\bar{\partial}K \tag{A.10}$$

is closed: $d\omega = 0$. The components of ω are $\omega_{i\bar{j}} = -\omega_{\bar{j}i} = ig_{i\bar{j}}$. This $(1,1)$ -form can be defined globally from the metric and a *Kähler manifold* will then be a Hermitian manifold where this two-form is closed. The cohomology class $[\omega] \in H^{(1,1)}(X)$ is called the *Kähler class*. This somewhat obscure definition can be shown to be equivalent to defining a Kähler manifold as a Hermitian manifold with a covariantly constant complex structure:

$$\nabla_i J = 0, \tag{A.11}$$

with ∇ the Levi-Civita connection associated with the metric g .

A.2 Calabi Yau manifolds

Definition and general properties

Armed with the definitions from section A.1, we are now ready to define and describe the manifolds we are most interested in. A *Calabi Yau manifold* M is a compact Kähler manifold with Ricci-flat metric:

$$R_{i\bar{j}} = 0, \tag{A.12}$$

where $R_{i\bar{j}} = R_{\bar{j}i}$ is the only component of the Ricci tensor that does not vanish automatically for a Kähler manifold. This definition implies that the first Chern class $c_1(M)$ vanishes. The Calabi conjecture [94], proven by Yau [95], states that for a compact Kähler manifold with vanishing first Chern class, each Kähler class contains exactly one Ricci-flat metric. Since it is very hard to find a concrete metric of a Calabi Yau, one usually just takes a Kähler manifold M , with $c_1(M) = 0$, and defines the metric indirectly by choosing a Kähler class. In this thesis, we restrict to three-dimensional manifolds with $SU(3)$ holonomy (instead of a subgroup of $SU(3)$ for general Calabi Yau manifolds). As a result, the Hodge diamond for a Calabi Yau threefold, which gives the dimensions of the Dolbeault cohomology groups, will look as in figure A.1. From this figure, one can read off the Euler characteristic of the Calabi Yau manifold as $\chi(X) = 2(h^{1,1} - h^{2,1})$.

Moduli spaces of Calabi Yau manifolds

As seen in the previous section, a Calabi Yau manifold is a Kähler manifold with a Ricci-flat metric. Starting from a real six-dimensional manifold, one can construct

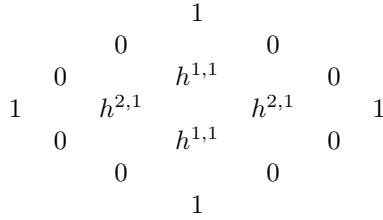


Figure A.1: Hodge diamond of a Calabi Yau with $SU(3)$ holonomy

a Calabi Yau threefold by adding a complex structure J and a metric g , satisfying the required conditions. This also means that we can deform a given Calabi Yau manifold X into another one by carefully deforming these structures, without breaking the conditions. These deformations will give rise to moduli spaces of Calabi Yau's, parameterizing different Calabi Yau spaces with the same topology. One can show that this moduli space consists of the direct product of the Kähler and complex structure moduli space.

The first of these parametrizes the different Ricci-flat Kähler metrics on the complex manifold. Since each Kähler class contains exactly one of these, the moduli space should just be the vector space of $(1, 1)$ -forms $H^{1,1}(X)$. Requiring the metric to be positive definite however reduces this space to a cone. Locally, away from the boundary of this *Kähler cone*, the allowed deformations of the metric are isomorphic to $H^{1,1}(X)$, with dimension $h^{1,1}$. This can also be stated as saying that the tangent space to the Kähler structure moduli space is isomorphic to $H^{1,1}(X)$.

As for the complex structure, from the Hodge diamond one can see that there is just a one-dimensional space of harmonic $(3, 0)$ -forms. A generator of this space can be chosen to be $\Omega = f(z)dz^1 \wedge dz^2 \wedge dz^3$, with $f(z)$ an arbitrary holomorphic function on X . It is clearly harmonic, as $\partial\Omega = \bar{\partial}\Omega = 0$, with ∂ and $\bar{\partial}$ the Dolbeault operators on X . Since this harmonic three-form will also fix the complex structure, one can study the allowed deformations of the complex structure J by analyzing the allowed deformations of Ω , which are given by $H^{2,1}(X)$, up to an irrelevant scaling factor. The tangent space of the complex structure moduli space is thus isomorphic to $H^{2,1}(X)$ and has dimension $h^{2,1}$.

As a result, the dimensions of the moduli spaces are exactly given by the two non-trivial Hodge numbers of the manifold.

Calabi Yau's in weighted projective spaces

To gain more familiarity with Calabi Yau manifolds, in this section we will construct the examples that are used in this thesis. They are all one-modulus, that is $h^{1,1} = 1$, Calabi Yau threefolds defined as hypersurfaces in weighted projective spaces. A *weighted projective space* is a generalization of standard complex projective space. A weighted projective space of dimension n is determined by the set of weights (a_0, a_1, \dots, a_n) and will be denoted $W\mathbb{C}P^n_{a_0 a_1 \dots a_n}$. One can then define the homogeneous complex coordinates $(z_0, z_1, \dots, z_n) \in \mathbb{C}^{n+1} \setminus \{(0, 0, \dots, 0)\}$ and for each $\lambda \in \mathbb{C}^*$ an equivalence relation

$$(z_0, z_1, \dots, z_n) \sim (z_0 \lambda^{a_0}, z_1 \lambda^{a_1}, \dots, z_n \lambda^{a_n}). \quad (\text{A.13})$$

As these weighted projective spaces can contain orbifold singularities, it is important that the defining equations of the smooth Calabi Yau hypersurface avoid these singular points. The appearance of these singularities can be best seen in concrete examples and will be given below.

The Chern class of a weighted projective space can easily be obtained from the splitting principle and is given by:

$$c(W\mathbb{C}P^n_{a_0 a_1 \dots a_n}) = \prod_{i=0}^n (1 + a_i H), \quad (\text{A.14})$$

where H denotes the cohomology class of the curvature two-form of the degree one line bundle. By picking a homogeneous polynomial of degree $\sum_i a_i$, one can then construct a Calabi Yau hypersurface X as the zero locus of this polynomial. Its Chern class can be calculated as follows:

$$c(X) = \frac{c(W\mathbb{C}P^n_{a_0 a_1 \dots a_n})}{1 + \sum_i a_i H} = \frac{\prod_{i=0}^n (1 + a_i H)}{1 + \sum_i a_i H}, \quad (\text{A.15})$$

which clearly has $c_1(X) = 0^3$. This formula follows from the adjunction formula, which gives the following short exact sequence:

$$0 \rightarrow TX \rightarrow TW\mathbb{C}P^4|_X \rightarrow NX \rightarrow 0, \quad (\text{A.16})$$

with TX the holomorphic tangent bundle of the Calabi Yau X , $TW\mathbb{C}P^4|_X$ the holomorphic tangent bundle of the embedding projective space, restricted to X , and NX the normal bundle of the embedding $X \hookrightarrow W\mathbb{C}P^4$.

Now we can see how this all works out for some concrete examples.

³The division of polynomials with coefficients in the even cohomology of X should be performed as a Taylor series, where products are wedge products and the series always terminates because the homology groups of dimension higher than n , being the dimension of X , are trivial.

The sextic

The *sextic* X_6 is defined to be a smooth hypersurface in $W\mathbb{C}P^4_{11112}$, determined as the zero locus of a degree six homogeneous polynomial. The Chern class of $W\mathbb{C}P^4_{11112}$ is:

$$c(W\mathbb{C}P^4_{11112}) = (1 + H)^4 \cdot (1 + 2H) = 1 + 6H + 14H^2 + 16H^3 + 9H^4, \quad (\text{A.17})$$

while the Chern class of the degree six line bundle is just $1 + 6H$, so

$$c(X_6) = 1 + 14H^2 - 68H^3. \quad (\text{A.18})$$

The Euler characteristic can be calculated as the integral over the top Chern class. Using $\int_{X_6} H^3 = \int_{W\mathbb{C}P^4} 6H^4 = 3$, this gives:

$$\int_{X_6} -68H^3 = -204. \quad (\text{A.19})$$

To find the Hodge numbers, we now look for the dimension of the complex structure moduli space, which should equal $h^{2,1}$. By deforming the defining degree six polynomial, and taking the complex structure of the Calabi Yau as the one inherited from the embedding space, we can actually obtain all possible complex structures on the manifold. These deformations are given by the set of degree six monomials in the homogeneous coordinates, which contains 130 different elements. However, redefinitions of the homogeneous coordinates, leaving the embedding space invariant, produce an overcounting, so we have to subtract these. The coordinates with weight one can be linearly transformed into each other by an element of the general linear group $GL(4)$, while the coordinate with weight two can be transformed into a linear combination of any degree two monomial. The general linear group has dimension $4^2 = 16$, and there are 11 linearly independent degree two monomials, resulting in $h^{2,1} = 130 - 16 - 11 = 103$. Since the Euler characteristic is also given by the Hodge numbers: $\chi = 2(h^{1,1} - h^{2,1})$, we find the remaining Hodge number to be $h^{1,1} = h^{2,1} + \chi(X_6)/2 = 103 - 102 = 1$.

The octic

The *octic* X_8 is the smooth hypersurface in $W\mathbb{C}P^4_{11114}$, determined as the zero locus of a degree eight homogeneous polynomial. The Chern class of $W\mathbb{C}P^4_{11114}$ is:

$$c(W\mathbb{C}P^4_{11114}) = (1 + H)^4 \cdot (1 + 4H) = 1 + 8H + 22H^2 + 28H^3 + 17H^4, \quad (\text{A.20})$$

while the Chern class of the degree eight line bundle is just $1 + 8H$, so

$$c(X_8) = 1 + 22H^2 - 148H^3. \quad (\text{A.21})$$

The Euler characteristic can be calculated as the integral over the top Chern class. Using $\int_{X_8} H^3 = \int_{W\mathbb{C}P^4} 8H^4 = 2$, this gives:

$$\int_{X_8} -148H^3 = -296. \quad (\text{A.22})$$

To find the Hodge numbers, we again look for the dimension of the complex structure moduli space, which should equal $h^{2,1}$. This time there are 201 homogeneous degree eight monomials. The redefinitions of the homogeneous coordinates consists of the general linear group $GL(4)$, with dimension 16, and the redefinition of the coordinate with weight four, determined by a linear combination of the 36 independent degree four monomials. This gives $h^{2,1} = 201 - 16 - 36 = 149$. From the Euler characteristic we find the remaining Hodge number to be $h^{1,1} = h^{2,1} + \chi(X_8)/2 = 149 - 148 = 1$.

The decantic

The *decantic* X_{10} is the smooth hypersurface in $W\mathbb{C}\mathbb{P}_{11125}^4$, determined as the zero locus of a degree ten homogeneous polynomial. The Chern class of $W\mathbb{C}\mathbb{P}_{11125}^4$ is:

$$c(W\mathbb{C}\mathbb{P}_{11125}^4) = (1+H)^3 \cdot (1+2H) \cdot (1+5H) = 1 + 10H + 34H^2 + 52H^3 + 37H^4, \quad (\text{A.23})$$

while the Chern class of the degree ten line bundle is just $1 + 10H$, so

$$c(X_{10}) = 1 + 34H^2 - 288H^3. \quad (\text{A.24})$$

The Euler characteristic can again be calculated as the integral over the top Chern class. Using $\int_{X_{10}} H^3 = \int_{W\mathbb{C}\mathbb{P}^4} 10H^4 = 1$, this gives:

$$\int_{X_{10}} -288H^3 = -288. \quad (\text{A.25})$$

To find the Hodge numbers, we again look for the dimension of the complex structure moduli space, which should equal $h^{2,1}$. This time there are 196 homogeneous degree ten monomials. The redefinitions of the homogeneous degree one coordinates consist of the general linear group $GL(3)$, with dimension 9. The redefinition of the coordinate with weight two is determined by a linear combination of the 7 independent degree two monomials, while the coordinate with weight five can be redefined using the 35 linearly independent degree five monomials. This gives $h^{2,1} = 196 - 9 - 7 - 35 = 145$. So from the Euler characteristic we at last find the remaining Hodge number: $h^{1,1} = h^{2,1} + \chi(X_{10})/2 = 145 - 144 = 1$.

Topological invariants

Here we will briefly introduce some topological invariants of Calabi Yau threefolds and outline how they are calculated in concrete examples.

Gopakumar–Vafa invariants

The Gopakumar–Vafa invariants n_β^g [96, 97] are defined indirectly from the topological string free energy:

$$F^{GV}(X) \equiv \sum_{m,g,\beta} n_\beta^g \frac{1}{m} \left(2 \sin \frac{m\lambda}{2} \right)^{2g-2} t^{m\beta}, \tag{A.26}$$

where λ parametrizes the string coupling constant. More informally, these invariants count the number of curves in a fixed homology class $\beta \in H_2(X)$ and genus g . By summing only over non-zero β , one obtains the reduced free energy $F^{GV}(X)'$ and the reduced Gopakumar–Vafa partition function:

$$Z^{GV}(X)' \equiv \exp(F^{GV}(X)'), \tag{A.27}$$

which will be used later on in relating these invariants to the Donaldson–Thomas invariants.

For the Calabi Yau manifolds we use in this thesis, the Gopakumar–Vafa invariants can be taken from [88]. For convenience, we list some of these invariants in tables A.1, A.2 and A.3, for degree β up to two.

g	$\beta = 1$	$\beta = 2$
0	7'884	6'028'452
1	0	7'884
2	0	0

Table A.1: Gopakumar–Vafa invariants for the sextic

g	$\beta = 1$	$\beta = 2$
0	29'504	128'834'912
1	0	41'312
2	0	864
3	0	6
4	0	0

Table A.2: Gopakumar–Vafa invariants for the octic

g	$\beta = 1$	$\beta = 2$
0	231'200	12'215'785'600
1	280	207'680'960
2	3	-537'976
3	0	-1'656
4	0	-12
5	0	0

Table A.3: Gopakumar–Vafa invariants for the decantic

Donaldson–Thomas invariants

For a Calabi Yau threefold X , take $I_n(X, \beta)$ to be the part of the Hilbert scheme parameterizing subschemes $Z \subset X$ satisfying:

- $[Z] = \beta \in H_2(X)$,
- $\chi_{\mathbb{C}}(\mathcal{O}_Z) = n$,

with \mathcal{O}_Z the structure sheaf of the subscheme Z and $\chi_{\mathbb{C}}$ denoting the holomorphic Euler characteristic⁴. The Donaldson–Thomas invariants [76, 77, 78] are then defined to be:

$$N_{DT}(\beta, n) \equiv \deg [I_n(X, \beta)]^{vir} \in \mathbb{Z}, \quad (\text{A.28})$$

where $[I_n(X, \beta)]^{vir}$ denotes the virtual fundamental class associated to a perfect obstruction theory. This rather mathematical definition can be phrased more colloquially by saying that $N_{DT}(\beta, n)$ ‘counts’ the number of ideal sheaves in a fixed homology class β with a fixed number of induced $\overline{\text{D0}}$ brane charge n . It should be noted that in practice, the induced $\overline{\text{D0}}$ brane charge can come directly from the Euler characteristic of the curve or from adding $\overline{\text{D0}}$ particles to a subscheme. This can be seen more directly from the expression of the D–brane charges in appendix C.

From these invariants, one can construct a formal series, containing all Donaldson–Thomas invariants, called the *Donaldson–Thomas partition function*:

$$Z^{DT}(X) \equiv \sum_{\beta, n} N_{DT}(\beta, n) q^n t^\beta. \quad (\text{A.29})$$

Defining the degree β Donaldson–Thomas partition function

$$Z_\beta^{DT}(X) \equiv \sum_n N_{DT}(\beta, n) q^n, \quad (\text{A.30})$$

⁴The holomorphic Euler characteristic as we use it here, reduces in the cases of our interest to $1 - g + N$, where g denotes the genus of the curve and N is the number of added $\overline{\text{D0}}$ branes.

one can construct the reduced Donaldson–Thomas partition function:

$$Z^{DT}(X)' = \frac{Z^{DT}(X)}{Z_0^{DT}(X)}, \quad (\text{A.31})$$

which will be related to another partition function, allowing us to calculate Donaldson–Thomas invariants indirectly. The degree zero partition function $Z_0^{DT}(X)$ is conjectured to be:

$$Z_0^{DT}(X) = M(-q)^{\chi(X)}, \quad (\text{A.32})$$

with $\chi(X)$ the Euler characteristic of X and $M(q)$ the McMahan function:

$$M(q) \equiv \prod_{i=1}^{\infty} (1 - q^i)^{-i}. \quad (\text{A.33})$$

With equation (A.32), one can calculate all degree zero Donaldson–Thomas invariants of X from the knowledge of only its Euler characteristic. To calculate the invariants for higher degree, one can use the correspondence between the reduced Donaldson–Thomas and Gopakumar–Vafa partition function [98, 99, 100]:

$$Z^{DT}(X)'(q, t) = Z^{GV}(X)'(\lambda, t), \quad (\text{A.34})$$

with $q = -e^{i\lambda}$.

Appendix B

Categories and sheaves

The framework describing branes in the topological B model, which we use to enumerate BPS brane states in the untwisted σ -model, relies heavily on mathematical structures, including categories, schemes and sheaves. The reader who is unfamiliar with (part of) these concepts, can find a short overview in this appendix. For a more complete treatment on sheaves and schemes, we refer to [84, 101], while [102] gives an in-depth analysis of categories and sheaves. A more rapid route to understanding these topics from the perspective of topological models on Calabi Yau manifolds can be pursued using [81]. The author also used the structure of [103], a classic textbook on categories, as a guiding principle in the section on abelian categories.

B.1 Categories, morphisms and functors

Categories are a mathematical abstraction, used primarily for dealing in an abstract way with mathematical structures and relations between these structures. By using for example the category of abelian groups, one can state or prove many of the properties, shared by all abelian groups, without making reference to any specific group. As an example that is more related to the subject of this thesis, branes in the topological B model are in a natural way identified with objects in a specific category.

In this subsection, the main definitions of categories and functors will be given. At each point, the category of abelian groups, denoted $\mathcal{A}b$ will be used to make these abstract definitions more concrete and provide the reader some intuition.

A *category* \mathcal{C} consists of a class¹ of objects $\text{Ob}(\mathcal{C})$ and a class of morphisms $\text{Hom}(\mathcal{C})$ obeying the following properties:

- For all objects $X, Y, Z \in \text{Ob}(\mathcal{C})$, there is a composition \circ of morphisms: $\circ : \text{Hom}(X, Y) \times \text{Hom}(Y, Z) \rightarrow \text{Hom}(X, Z)$, where $\text{Hom}(X, Y)$ denotes the class of morphisms from X to Y .
- This composition is associative.
- For each object $X \in \text{Ob}(\mathcal{C})$, there is an identity morphism $\text{Id}_X \in \text{Hom}(X, X)$, such that for each morphism $f \in \text{Hom}(X, Y)$, we have the identity: $\text{Id}_Y \circ f = f \circ \text{Id}_X$.

For $\mathcal{A}b$, the category of abelian groups, the class of objects $\text{Ob}(\mathcal{A}b)$ consists of all abelian groups while the morphisms are the homomorphisms between them. Clearly, every abelian group has an identity morphism, which is just the map that sends every element of the group to itself. In addition, the composition of two homomorphisms is again a homomorphism and this composition is trivially associative.

One can also define some special morphisms:

- An *isomorphism* $h \in \text{Hom}(X, Y)$ is a morphism with an inverse $h^{-1} \in \text{Hom}(Y, X)$, such that $h^{-1} \circ h = \text{Id}_X$ and $h \circ h^{-1} = \text{Id}_Y$.
- A *monomorphism* $m \in \text{Hom}(X, Y)$ is morphism, such that for every two morphisms $f_1, f_2 \in \text{Hom}(A, X)$ one has: $m \circ f_1 = m \circ f_2 \Rightarrow f_1 = f_2$.
- An *epimorphism* $e \in \text{Hom}(X, Y)$ is morphism, such that for every two morphisms $f_1, f_2 \in \text{Hom}(Y, A)$ one has: $f_1 \circ e = f_2 \circ e \Rightarrow f_1 = f_2$.

A *functor* can informally be thought of as a mapping between two categories. More precisely, a functor F from the category \mathcal{C} to \mathcal{D} has the following properties:

- It maps objects in $\text{Ob}(\mathcal{C})$ to objects in $\text{Ob}(\mathcal{D})$: $\forall X \in \text{Ob}(\mathcal{C}) : F(X) \in \text{Ob}(\mathcal{D})$.
- It also maps morphisms in $\text{Hom}(\mathcal{C})$ to morphisms in $\text{Hom}(\mathcal{D})$: $\forall f \in \text{Hom}(\mathcal{C}) : F(f) \in \text{Hom}(\mathcal{D})$.

On top of this, the mapping of morphisms should obey some extra properties. For a *covariant* functor, these are:

¹The use of a *class*, instead of just a set, is mainly intended to avoid some paradoxes, such as Russel's paradox. All sets are classes, but classes can also be collections of objects without being a set, such as the class of sets that do not contain themselves.

- $f \in \text{Hom}(X, Y) \Rightarrow F(f) \in \text{Hom}(F(X), F(Y))$;
- $F(\text{Id}_X) = \text{Id}_{F(X)}$;
- $F(f \circ g) = F(f) \circ F(g)$.

For a *contravariant* functor, the direction of the morphisms is reversed, such that if $f \in \text{Hom}(X, Y)$, then $F(f) \in \text{Hom}(F(Y), F(X))$. The third property listed above then also changes accordingly.

As an example of a covariant functor, let us consider the *Hom functor* on $\mathcal{A}b$. Fix an abelian group A , for which the Hom functor becomes $\text{Hom}(A, -)$. This functor maps into the category of sets as follows:

- Each object $X \in \text{Ob}(\mathcal{A}b)$ is mapped to the set $\text{Hom}(A, X)$.
- Each morphism $f : X \rightarrow Y$ is mapped to a function between sets: $\text{Hom}(A, f) : \text{Hom}(A, X) \rightarrow \text{Hom}(A, Y)$, defined by $g \in \text{Hom}(A, X) \rightarrow f \circ g \in \text{Hom}(A, Y)$.

B.2 Abelian and derived categories

Since the category of branes in the topological B model is the derived category of coherent sheaves, this section provides the reader with a short overview of what a derived category is and how it is constructed from an abelian category.

After having defined the notions of zero objects, kernels and cokernels, the concept of additive and abelian categories will be defined. Finally, the derived category will be described, using the previous concepts.

Zero objects, kernels and cokernels

A *zero object* 0 in a category \mathcal{C} is an object such that for each object $X \in \text{Ob}(\mathcal{C})$, both $\text{Hom}(0, X)$ and $\text{Hom}(X, 0)$ contain exactly one morphism. One can then show that such a zero object is unique, up to isomorphism. The uniqueness of morphisms to (or from) the zero object ensures that for every two objects X and Y , there is a unique morphism in $\text{Hom}(X, Y)$ that is the composition of the morphisms $X \rightarrow 0$ and $0 \rightarrow Y$, which is called the zero morphism (also denoted 0 if no confusion can arise). For $\mathcal{A}b$, it is easy to show that the trivial group, containing only the identity element, forms a zero object. The zero morphism between two abelian groups then maps every element of the first group to the identity element in the second.

The *kernel* of a morphism $f \in \text{Hom}(X, Y)$ is a morphism $k \in \text{Hom}(A, X)$, such that:

- $f \circ k = 0$,
- For each $h \in \text{Hom}(B, X)$ that obeys $f \circ h = 0$, there is a unique $h' \in \text{Hom}(B, A)$, such that h factorizes as $h = k \circ h'$.

We denote $k = \ker f$. This last condition can be visualized by the following diagram:

$$\begin{array}{ccccc}
 A & \xrightarrow{k} & X & \xrightarrow{f} & Y \\
 & \swarrow h' & \uparrow h & & \\
 & & B & &
 \end{array}$$

While this definition may seem strange for people used to the definition of kernels as subsets that are mapped to a zero element, one can show that the object A corresponds to this more familiar subset in the case the objects are sets. The object A is referred to as the *kernel object*.

The *cokernel* of a morphism is defined in a similar way. The cokernel of $f \in \text{Hom}(X, Y)$ is a morphism $c \in \text{Hom}(Y, A)$, denoted $c = \text{coker } f$, such that:

- $c \circ f = 0$,
- For each $h \in \text{Hom}(Y, B)$ that obeys $h \circ f = 0$, there is a unique $h' \in \text{Hom}(A, B)$, such that h factorizes as $h = h' \circ c$.

Again, we can represent this last condition as:

$$\begin{array}{ccccc}
 X & \xrightarrow{f} & Y & \xrightarrow{c} & A \\
 & & \searrow h & & \downarrow h' \\
 & & & & B
 \end{array}$$

And finally, we define the *image* of a morphism f as the kernel of the cokernel of f : $\text{im } f = \ker(\text{coker } f)$, and the *coimage* as the cokernel of the kernel: $\text{coim } g = \text{coker}(\ker f)$.

Consider as an example the abelian groups $(\mathbb{Z}, +)$ and $(\{0, 1\}, + \text{ mod } 2)$ and the morphism f between them, defined by $f(x) = x \text{ mod } 2$. The kernel of f is the morphism g from $(\mathbb{Z}, +)$ to itself, defined by multiplication by 2. It should be clear that every morphism h obeying $f \circ h = 0$ can be uniquely factorized as $h = g \circ h'$.

Additive and abelian categories

An *additive* category \mathcal{C} is a category where each $\text{Hom}(X, Y)$ is a set with an additive abelian group structure and composition of morphisms is bilinear in this group structure. Note that this implies the existence of a zero morphism between any two objects of the category. Moreover, an additive category has a *biproduct* that is defined for any two objects $X, Y \in \text{Ob}(\mathcal{C})$. This biproduct can be schematically represented as

$$\begin{array}{ccccc}
 & p_1 & & p_2 & \\
 X & \begin{array}{c} \longleftarrow \\ \longrightarrow \end{array} & X \oplus Y & \begin{array}{c} \longrightarrow \\ \longleftarrow \end{array} & Y \\
 & i_1 & & i_2 &
 \end{array}$$

where $p_1 \circ i_1 = \text{Id}_X$, $p_2 \circ i_2 = \text{Id}_Y$ and $i_1 \circ p_1 + i_2 \circ p_2 = \text{Id}_{X \oplus Y}$.

As an example, take our favorite category \mathcal{Ab} and two identical objects $(\mathbb{Z}_2, +)$, which we will call X and Y . We can easily construct the direct sum of these groups $X \oplus Y$ as the group with elements (x, y) , where $x, y \in \{0, 1\}$, and addition is defined as $(a, b) + (c, d) \equiv (a + c, b + d)$. Now define the embedding $i_1 : X \rightarrow X \oplus Y : x \rightarrow (0, x)$ and the projection $p_1 : X \oplus Y \rightarrow X : (x, y) \rightarrow y$ and similar for Y : $i_2 : Y \rightarrow X \oplus Y : x \rightarrow (x, 0)$ and $p_2 : X \oplus Y \rightarrow Y : (x, y) \rightarrow x$. With these definitions, all conditions, stated above, are satisfied and we establish that the biproduct in \mathcal{Ab} is just the usual direct sum of groups (this also explains why we use the notation \oplus for the biproduct). Also note that for \mathcal{Ab} , there is a very natural additive structure in $\text{Hom}(X, Y)$, provided by the group operation of Y .

An *abelian* category \mathcal{C} is an additive category, obeying:

- Every morphism has a kernel and a cokernel.
- Every monomorphism is a kernel and every epimorphism is a cokernel.

All these rather abstract definitions can now be given a more intuitive meaning. The conditions for a category to be abelian suffice to define exact sequences and cohomology for complexes in the category. Recall that a complex \mathcal{E}^\bullet is a series of objects \mathcal{E}^i , with morphisms $f_i \in \text{Hom}(\mathcal{E}^i, \mathcal{E}^{i+1})$, such that $f_i \circ f_{i-1} = 0$ for each i .

These complexes are usually represented as follows:

$$\cdots \xrightarrow{f_{n-2}} \mathcal{E}^{n-1} \xrightarrow{f_{n-1}} \mathcal{E}^n \xrightarrow{f_n} \mathcal{E}^{n+1} \xrightarrow{f_{n+1}} \cdots$$

If $\text{im } f_{i-1} = \ker f_i$ for each i , the complex is said to be an exact sequence. For all complexes one can find a unique morphism k_n , such that $\text{im } f_{n-1} = \ker f_n \circ k_n$. One then defines the cohomology $H^n(\mathcal{E}^\bullet)$ at position n , to be the cokernel object of k_n . The reader can verify that for objects consisting of elements, this definition reduces to the usual $H^n = \ker f_n \setminus \text{im } f_{n-1}$.

The derived category

Now we are ready to describe the construction of the *derived* category. One starts with an abelian category \mathcal{C} and defines the objects of the derived category $\mathbf{D}(\mathcal{C})$ to be complexes of objects in $\text{Ob}(\mathcal{C})$. To define the morphisms between these complexes is a bit trickier, so we will define these in steps.

A chain map between two complexes $\mathcal{E}^\bullet, \mathcal{F}^\bullet$ is a set of morphisms $h_n : \mathcal{E}^n \rightarrow \mathcal{F}^n$, such that the following diagram commutes:

$$\begin{array}{ccccccc} \cdots & \xrightarrow{e_{n-2}} & \mathcal{E}^{n-1} & \xrightarrow{e_{n-1}} & \mathcal{E}^n & \xrightarrow{e_n} & \mathcal{E}^{n+1} & \xrightarrow{e_{n+1}} & \cdots \\ & & \downarrow h_{n-1} & & \downarrow h_n & & \downarrow h_{n+1} & & \\ & & \mathcal{F}^{n-1} & \xrightarrow{f_{n-1}} & \mathcal{F}^n & \xrightarrow{f_n} & \mathcal{F}^{n+1} & \xrightarrow{f_{n+1}} & \cdots \end{array}$$

In the above case, the statement that the diagram commutes, is equivalent to $\forall n : h_n \circ e_{n-1} = f_{n-1} \circ h_{n-1}$.

Next, we define two chain maps g_\bullet, h_\bullet to be homotopy equivalent if there exists a set of maps $k_n : \mathcal{E}^n \rightarrow \mathcal{F}^{n-1}$, such that $g_i - h_i = f_{i-1} \circ k_i + k_{i+1} \circ e_i$, for all i . The first type of morphisms we will add to our derived category are then chain maps modulo this homotopy equivalence.

A last ingredient is the notion of a *quasi-isomorphism*. These are defined to be chain maps that induce an isomorphism between the cohomologies of the complexes. These quasi-isomorphisms are then treated as isomorphisms by adding their formal inverses to the class of morphisms. Note that these inverses do not always exist, which is why they are *formally* added to the derived category.

The derived category $\mathbf{D}(\mathcal{C})$ of the category \mathcal{C} can then be defined as the category whose objects are complexes of objects in $\text{Ob}(\mathcal{C})$ and whose morphisms are chain maps modulo homotopy equivalence plus the formal inverses of quasi-isomorphisms.

It is important to understand that this construction crucially depends on the fact that the original category, \mathcal{C} in our case, is abelian. This guarantees the existence of the cohomologies, used to define a quasi-isomorphism.

For the reader who is familiar with simplicial (co)homology, we mention the fact that if this construction is applied to chain complexes, each belonging to a simplicial complex, then these definitions ensure that quasi-isomorphic chain complexes have homotopy equivalent topological realizations. Much of the vocabulary of the derived category is derived from this perspective.

B.3 Sheaves

In the topological B model, branes are objects in the derived category of coherent sheaves. In section B.2, the notion of a derived category was introduced. Here, we will introduce the concept of sheaves and explain why these appear naturally as representations of branes.

Definitions

A *presheaf* \mathcal{F} on a topological space X is a function that assigns an abelian group $\mathcal{F}(U)$ to every open set $U \subset X$. On top of this, it contains a restriction map r that assigns to every pair $V \subset U$ of open sets a homomorphism

$$r_{U,V} : \mathcal{F}(U) \rightarrow \mathcal{F}(V), \quad (\text{B.1})$$

such that

$$\begin{aligned} r_{U,U} &= \text{Id}_{\mathcal{F}(U)} \\ r_{U,W} &= r_{V,W} \circ r_{U,V} \quad \forall W \subset V \subset U. \end{aligned} \quad (\text{B.2})$$

In the language of category theory, a presheaf on X is then a contravariant functor from the category of open sets of X , with the inclusion as morphisms, to the category of abelian groups. An element of the abelian group $\sigma \in \mathcal{F}(U)$ is called a *section* of \mathcal{F} over U .

A *sheaf* \mathcal{F} on X is then a presheaf subject to the following conditions:

- For every pair of open sets $U, V \subset X$ and sections $\sigma \in \mathcal{F}(U), \tau \in \mathcal{F}(V)$, one has

$$r_{U, U \cap V}(\sigma) = r_{V, U \cap V}(\tau) \Rightarrow \exists \nu \in \mathcal{F}(U \cup V) : r_{U \cup V, U}(\nu) = \sigma, r_{U \cup V, V}(\nu) = \tau.$$

This essentially means that if two sections are equal on their overlap, there must exist a section on their union that, when properly restricted, equals these sections.

- If $\sigma \in \mathcal{F}(U \cup V)$ and $r_{U \cup V, U}(\sigma) = r_{U \cup V, V}(\sigma) = 0$ then $\sigma = 0$.

The combination of these two conditions implies that a sheaf is defined by local information, which is the data of the sheaf on small open sets.

A very important example of a sheaf, which we use throughout this thesis, is the *structure sheaf* \mathcal{O}_X on a complex manifold X . It is defined by stating that $\mathcal{O}_X(U)$ is the abelian group, under addition, of holomorphic functions on U , with the natural restriction map.

To make a category of sheaves, we need to define the morphisms between sheaves. A morphism $\phi : \mathcal{F} \rightarrow \mathcal{G}$ of sheaves is defined to be a function that assigns to every open set $U \subset X$ a homomorphism $\phi(U) : \mathcal{F}(U) \rightarrow \mathcal{G}(U)$ such that the following diagram commutes

$$\begin{array}{ccc} & \phi(U) & \\ \mathcal{F}(U) & \longrightarrow & \mathcal{G}(U) \\ \downarrow r_{U,V} & & \downarrow s_{U,V} \\ \mathcal{F}(V) & \xrightarrow{\phi(V)} & \mathcal{G}(V), \end{array}$$

where r, s are the restriction maps of \mathcal{F} and \mathcal{G} respectively.

Coherent sheaves

To understand what a coherent sheaf means, one must start with locally free sheaves. These will be defined first and their relation to holomorphic vector bundles will provide a first hint of how these structures enter the description of B branes.

First note that the abelian group $\mathcal{O}_X(U)$ has a natural ring structure. This allows us to define a \mathcal{O}_X module \mathcal{F} as a sheaf for which $\mathcal{F}(U)$ is a module of $\mathcal{O}_X(U)$. Clearly, \mathcal{O}_X is itself a \mathcal{O}_X module and so are its direct sums $\mathcal{O}_X \oplus \cdots \oplus \mathcal{O}_X$, which, for n terms \mathcal{O}_X , is called the free \mathcal{O}_X module of rank n .

A *locally free sheaf* \mathcal{F} of rank n is then a sheaf, such that there exists an open covering $\{U_\alpha\}$ of X with the property

$$\mathcal{F}(U_\alpha) \cong \mathcal{O}_X(U_\alpha)^{\oplus n}. \quad (\text{B.3})$$

Such a sheaf will thus locally look like the free \mathcal{O}_X module. One can see that these locally free sheaves of rank n are in one-to-one correspondence with holomorphic vector bundles of rank n . The isomorphism $\phi_\alpha : \mathcal{F}(U_\alpha) \rightarrow \mathcal{O}_X(U_\alpha)^{\oplus n}$ allows to define holomorphic transition functions on intersections $U_\alpha \cap U_\beta$, which define a holomorphic vector bundle. In the other direction, if $\{U_\alpha\}$ trivializes the vector bundle, then $\mathcal{F}(U_\alpha)$ is the group of holomorphic sections of this vector bundle over U_α . Since spacefilling branes, which are 6-branes in the case of the topological B model, are defined by a holomorphic vector bundle over X , these locally free sheaves provide a good starting point in describing B branes.

As an example, consider the projective space $\mathbb{C}\mathbb{P}^n$ with homogeneous coordinates (x_0, x_1, \dots, x_n) . Take an open covering of this space U_i , where $U_i \subset \mathbb{C}\mathbb{P}^n$ is the subset of points with $x_i \neq 0$. On each subset U_i , we can define the inhomogeneous coordinates $(y_{i,0}, y_{i,1}, \dots, 1, \dots, y_{i,n}) \equiv (x_0/x_i, x_1/x_i, \dots, x_n/x_i)$, where we keep the trivial $y_{i,i} = x_i/x_i = 1$ for notational simplicity. We can then define a holomorphic line bundle with fiber coordinate w_i over U_i and take as transition functions:

$$w_j = \left(\frac{x_i}{x_j}\right)^m w_i = (y_{j,i})^m w_i. \quad (\text{B.4})$$

The associated sheaf will then be denoted $\mathcal{O}_{\mathbb{C}\mathbb{P}^n}(m)$. One can generalize this definition to weighted projective spaces and, by use of the restriction map, to complex subspaces thereof. The structure sheaf is then seen to be $\mathcal{O} = \mathcal{O}(0)$. A morphism between \mathcal{O} and $\mathcal{O}(m)$ is then defined by a homogeneous function f of degree m as follows: on U_i , the elements of $\mathcal{O}(U_i)$ are multiplied by f/x_i^m . One can easily check that this is consistent with the transition functions of both vector bundles.

At last we are ready to define coherent sheaves. Since the category of locally free sheaves is not abelian, we cannot construct its derived category. This is solved by adding to the category of locally free sheaves all objects in the category of \mathcal{O}_X modules that appear as (co)kernel objects of morphisms in the category of locally free sheaves. We should then also add the morphisms between these new objects. In this way, one obtains an abelian category, whose objects are now called *coherent sheaves*. This construction is often referred to as saying that the category of coherent sheaves is the minimal abelian full subcategory of \mathcal{O}_X modules containing the locally free sheaves. These coherent sheaves are necessary to be able to represent lower-dimensional branes, whose gauge bundle is only supported on a submanifold of X . Some examples of these coherent sheaves are presented in section 4.2.

B.4 Schemes

In this section, we will briefly outline the definition of a scheme and why they are important in describing branes. The notion of a blowup in algebraic geometry, which becomes important when placing two branes on top of each other, will also be discussed. We refer the reader to [104] for more details. The reader who just wants an intuitive picture of schemes can think of them as describing algebraic sets, which are the zero locus of a set of polynomial equations, with multiplicity. That is, if two pointlike branes sit at the same location, the notion of a scheme is necessary to account for their multiplicity, while the algebraic set would ‘forget’ that there are two branes at this location.

Definitions

In the remainder of this section, we will only describe affine algebraic sets and schemes. The generalization to projective varieties and schemes can be found in many textbooks, including [104]. We will also be only concerned with the field $k = \mathbb{C}$, which is of particular importance in the description of B branes.

An *algebraic set* V in the affine space k^n is defined as the zero locus of a set of polynomials, which are elements of the polynomial ring $\Gamma(k^n) \equiv k[X_1, \dots, X_n]$. Denote the set of polynomials as $\{P_i\}$. Then, we have

$$V = \{x \in k^n \mid \forall P_i \in \{P_i\}, P_i(x) = 0\}. \quad (\text{B.5})$$

Clearly, every polynomial in the ideal generated by these polynomials will also vanish on V . Also, every polynomial Q , for which Q^N is an element of this ideal for $N \in \mathbb{N}$, will vanish on V . This leads to the following correspondence:

The algebraic sets in k^n are in one-to-one correspondence
with the radical ideals of $\Gamma(k^n)$,

where a radical ideal I is an ideal that also contains the elements Q for which $Q^N \in I$. We denote by $V(I)$ the vanishing set of the ideal I and by $I(V)$ the ideal defined as the set of polynomials that vanish on V . Note that $I(V)$ is always a radical ideal.

One also defines algebraic varieties in k^n as the zero locus of a prime ideal of $\Gamma(k^n)$, where a prime ideal J is an ideal such that if $P_1 \cdot P_2 \in J$ implies $P_1 \in J$ or $P_2 \in J$.

The algebraic structure² on the algebraic set V is inherited by the polynomial ring of its embedding space as follows:

$$\Gamma(V) = \Gamma(k^n)/I(V), \quad (\text{B.6})$$

which, since $I(V)$ is radical, is a reduced ring (i.e. a ring without non-zero nilpotent elements). This ring is also called the *coordinate ring* of V . From this ring of functions on V , one can define the spectrum of V :

$$\text{spec}(\Gamma(V)) \equiv \{J \subset \Gamma(V) | J \text{ is a prime ideal of } V\}. \quad (\text{B.7})$$

The spectrum contains the ‘points’ of V , which are identified with the maximal ideals of $\Gamma(V)$ ³. It also contains every irreducible algebraic subset of V , called the algebraic varieties in V .

If one uses this construction on non-reduced rings, one immediately arrives at schemes. A *scheme* is the spectrum of a commutative ring, equipped with the Zariski topology and a sheaf of regular functions, where a regular function is just an element of the commutative ring.

Examples

Let us consider an example. Consider the affine space $k = \mathbb{C}$ with polynomial ring $\Gamma(k) = \mathbb{C}[X]$. The origin, as an algebraic variety, is then $V((X))$, where (X) is the ideal generated by the polynomial X . The coordinate ring is then $\mathbb{C}[X]/(X) = \mathbb{C} = k$, which makes sense, since the regular functions on a point should be constant functions. Now consider what happens if we would try to describe this origin with multiplicity two. We can start with the union of two separate points, one at the origin and one at location $X = \epsilon$. This algebraic set is defined by the radical ideal $(X \cdot (X - \epsilon))$ and has a coordinate ring $\mathbb{C}[X]/(X \cdot (X - \epsilon)) = \mathbb{C}^2 = k^2$, corresponding to the two values of a regular function when evaluated at the two distinct points. As we take $\epsilon \rightarrow 0$, corresponding to moving the second point to the origin, the ideal becomes (X^2) , which is no longer radical, meaning we should describe this as a scheme. The set of regular functions on this scheme becomes $\mathbb{C}[X]/(X^2) = \mathbb{C} \oplus \mathbb{C}X$, with $X^2 = 0$. This is a non-reduced ring, since X squares to zero. The scheme $\text{spec}(\mathbb{C}[X]/(X^2))$ contains the ‘points’ (0) and (X) , accounting for the multiplicity of the point.

As a second example, which illustrates the origin of blowups when particles or branes sit at the same location, take the two pointlike varieties in \mathbb{C}^3 , defined by the ideals $I_1 = (X, Y, Z)$ and $I_2 = (X, Y, Z - \epsilon)$. Their union is defined by the

²An algebraic structure on a set will in this text always be linked to a set of polynomial functions on the set.

³A maximal ideal is an ideal which is maximal with respect to inclusion among the proper ideals, i.e. not equal to the whole ring. Such an ideal is automatically prime.

intersection of their ideals, which is $I \equiv I_1 \cap I_2 = (X, Y, Z \cdot (Z - \epsilon))$. When taking the limit $\epsilon \rightarrow 0$, this becomes $I = (X, Y, Z^2)$, which is not radical. The set of regular functions is the non-reduced ring $\mathbb{C} \oplus \mathbb{C}Z$, with $Z^2 = 0$. Its spectrum consists of the ‘points’ (0) and (Z) . In the case at hand, we have taken the second point to approach the origin from the Z -direction. We could also have chosen any other direction, which generally results in the spectrum containing the zero ideal and the ideal (f_1) , with f_1 being a homogeneous degree one function in X, Y, Z : $f_1 = aX + bY + cZ$. Clearly, an overall multiplication by a non-zero constant would result in the same ideal, so the moduli space of directions is actually the projective space $\mathbb{C}P^2$. The total moduli space of the two colliding points is then the product of the moduli space of one point (which in this case is just the space itself, or \mathbb{C}^3), times this $\mathbb{C}P^2$. This procedure is called a blowup of the point and it can be generalized to higher-dimensional examples. In general, the blowup of a point on a codimension n space will result in a $\mathbb{C}P^{n-1}$ factor in the moduli space.

Appendix C

D–brane charges

The classification of D–brane charges, which are the sources for the Ramond–Ramond fluxes in type II string theory, is a complex issue. In [105], it was first suggested that these are classified by K–theory. This was later seen as a classification of stable D–branes [106], representing conserved charges. In this appendix, we give a short overview of this classification, presenting mainly the results that are of importance in the context of this thesis. The index calculation techniques, worked out in previous chapters, are concerned with BPS states, which simplifies the classification as we will see. For more details, the reader is referred to the review article [107].

C.1 K–theory charge

Since most of the calculations in this thesis are concerned with D–branes in a six–dimensional Calabi Yau manifold, in the remainder of this appendix, it will be assumed that the total spacetime is of this form. This does not however pose any serious restrictions to the following discussion.

Since D–branes wrap submanifolds of the whole spacetime, it is natural to think of a classification of stable D–branes in terms of homology. The reason why homotopy classes, as opposed to homology classes, do not represent stable D–branes, is shown in figure C.1. This figure shows that a brane in a certain homotopy class can decay or be deformed to a brane in a different homotopy class. For these reasons, one should not expect that conserved D–brane charges are classified by homotopy. By looking at figure C.1, one sees that this issue in the homotopy classification can be cured by a classification based on homology: the branes in the figure are wrapped around submanifolds with dimension n that are boundaries

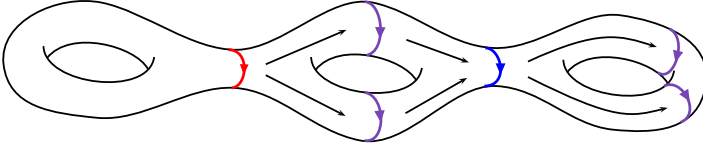


Figure C.1: Unstable D-brane on non-trivial homotopy class. The D-brane on the left, represented by the red curve, can be moved continuously to the right, where it splits into two separate D-branes, represented by the two middle purple curves. Moving these further, they can merge into the blue D-brane, which is in a different homotopy class than the original red one. By performing this operation one more time, one sees that these brane states are not even stable, because the purple D-branes on the right can annihilate each other, since they have opposite orientation.

of a submanifold with dimension $n+1$. For example, the red minus the blue brane¹ forms a boundary of two-dimensional submanifold, meaning that these correspond to the same conserved charge. In the case at hand, this charge is zero, because each one of these submanifolds, red or blue, is also a boundary.

However, in [108], it was shown that certain D-branes wrapped on non-trivial homology classes are actually unstable and may thus decay. Furthermore, some branes wrapping non-trivial homology classes can be anomalous and can thus not be identified with physical branes (see [106] for examples). When these two cases are taken into account, the stable D-brane charges are classified not by homology, but by K-theory. Without going into the details of the K-theoretical classification of D-brane charges, the elements of the K-theory group of a manifold M , denoted $K^0(M)$, are represented by a pair of vector bundles (E, F) , with the following equivalence relation:

$$(E, F) \sim (E \oplus G, F \oplus G). \quad (\text{C.1})$$

These are also sometimes written as $E - F$, where the subtraction provides the inverse of the direct sum, thereby resulting in a group structure. One can also define an inner product in K-theory, which for two vector bundles E and F , is defined as:

$$\langle E, F \rangle \equiv \int_M \text{ch}(E) \wedge \text{ch}(F) \wedge \hat{A}(TM), \quad (\text{C.2})$$

where $\text{ch}(E)$ is the Chern character of E , \hat{A} is the A-roof genus and TM is the tangent bundle of M . There is also a natural inner product on cohomology classes

¹The minus means that one reverses its orientation.

of M^2 , defined as the integral of the wedge product of the classes, where only top classes are integrated:

$$\langle \omega_1, \omega_2 \rangle \equiv \int_M \omega_1 \wedge \omega_2. \quad (\text{C.3})$$

Relating these two inner products, the charge associated to a brane, represented by the vector bundle E , becomes:

$$Q(E) \equiv \text{ch}(E) \wedge \sqrt{\hat{A}(TM)}. \quad (\text{C.4})$$

This formula can easily be extended to charges of sheaf complexes, which represent branes in the B model. For a B brane on a Calabi Yau threefold X , represented by the complex \mathcal{E}^\bullet , one has:

$$Q(\mathcal{E}^\bullet) \equiv \text{ch}(\mathcal{E}^\bullet) \wedge \sqrt{\text{td}(X)}, \quad (\text{C.5})$$

where $\text{td}(X)$ denotes the Todd class of X , which for a Calabi Yau manifold equals its A-roof genus and the Chern character of a sheaf complex is defined as the alternating sum of the Chern characters of its constituent sheaves.

C.2 Some useful examples

We conclude this appendix by giving convenient expressions of equation (C.5) for some specific cases.

The Todd classes of a manifold can be expressed in terms of its Chern classes. The first three Todd classes for a manifold X are given by:

$$\text{td}(X) = 1 + \frac{1}{2}c_1(X) + \frac{1}{12}(c_1(X)^2 + c_2(X)) + \frac{1}{24}c_1(X)c_2(X) + \dots \quad (\text{C.6})$$

Note that for a Calabi Yau threefold the first Chern class vanishes, giving:

$$\text{td}(X) = 1 + \frac{1}{12}c_2(X), \quad (\text{C.7})$$

where every higher Todd class vanishes because the degree of the corresponding differential form would be higher than the dimension of the manifold, which is six.

For a D6 brane with flux $F_1 \in H^2(X)$, a $\overline{\text{D2}}$ on a curve C of degree $\beta_1 \in H^4(X)$ and Euler characteristic χ_C and N_1 added $\overline{\text{D0}}$ branes, equation(C.5) gives for the

²From here on, the cohomology of charges is used, instead of the homology. Note that Poincaré duality relates the two.

total charge:

$$\begin{aligned}
 \Gamma_{\text{D6}} &= e^{F_1} (1 - \beta_1 - (\frac{\chi_C}{2} + N_1)\omega) (1 + \frac{c_2(X)}{24}) \\
 &= (1, F_1, \frac{c_2(X)}{24} - \beta_1 + \frac{F_1^2}{2}, -\frac{\chi_C}{2} - N_1 + \frac{F_1 c_2(X)}{24} - F_1 \beta_1 + \frac{F_1^3}{6}),
 \end{aligned} \tag{C.8}$$

with ω the volume form on X and products between differential forms are understood to be wedge products. For its charge conjugate, which is a $\overline{\text{D6}}$ with flux F_2 , a D2 on a curve C of degree β_2 and N_2 added $\overline{\text{D0}}$ branes, we similarly get:

$$\begin{aligned}
 \Gamma_{\overline{\text{D6}}} &= -e^{F_2} (1 - \beta_2 + (\frac{\chi_C}{2} + N_2)\omega) (1 + \frac{c_2(X)}{24}) \\
 &= (-1, -F_2, -\frac{c_2(X)}{24} + \beta_2 - \frac{F_2^2}{2}, -\frac{\chi_C}{2} - N_2 - \frac{F_2 c_2(X)}{24} + F_2 \beta_2 - \frac{F_2^3}{6}).
 \end{aligned} \tag{C.9}$$

Finally, for a D4 brane on a divisor Σ of class $P \in H^2(X)$, with flux³ $F = P/2$, a degree β curve with Euler characteristic χ_C and n added $\overline{\text{D0}}$ branes, we have:

$$\begin{aligned}
 \Gamma_{\text{D4}} &= e^{P/2+\beta} (1 - n\omega) (1 + \frac{c_2(P)}{24}) \\
 &= (0, 1, P/2 + \beta, \frac{\chi(\Sigma)}{24} + \frac{P^2}{8} - \frac{\chi_C}{2} - n),
 \end{aligned} \tag{C.10}$$

³This half-integer flux is needed to cancel the Freed–Witten anomaly [67].

Bijlage D

Nederlandse Samenvatting

Ondanks de overvloed aan successen van Kwantum Veldentheorie en Algemene Relativiteit, twee grote verwezenlijkingen van twintigste-eeuwse theoretische fysica, blijven een aantal vragen onbeantwoord. Aangezien deze theorieën op fundamenteel verschillende wijzen geformuleerd zijn, de ene als een kwantum theorie van relativistische velden, de andere als een klassieke veldentheorie, roept dit de vraag op hoe beide met elkaar kunnen verzoend worden. Deze vraag wordt des te acuter wanneer men poogt fysische systemen te beschrijven die beide theorieën vereisen.

In de inleiding toonden we dat verschillende fysische beschrijvingen kunnen worden toegepast en dit al naargelang de waarde van een aantal parameters in het betreffende fysische systeem. Meer precies wil dit zeggen dat we in sommige limieten onze toevlucht kunnen nemen tot eenvoudigere modellen en theorieën. Wanneer de snelheid van de deeltjes in een systeem bijvoorbeeld klein is ten opzichte van de lichtsnelheid, en kwantummechanische effecten ook verwaarloosd kunnen worden, voldoet klassieke mechanica om dit systeem met grote precisie te beschrijven. Dit suggereert dat er één overkoepelende theorie is, waarvan de andere slechts limieten vormen.

Zoals reeds vermeld is zulk een ‘theorie van alles’ noodzakelijk wanneer men fysische fenomenen probeert te beschrijven die zowel een kwantummechanische als een algemeen relativistische behandeling vereisen. Dit is het geval voor fenomenen op de Planck schaal, die als lengte- en als energie-eenheid kan worden uitgedrukt. De twee meest in het oog springende voorbeelden zijn de Oerknal, in het beginstadium van ons heelal, en zwarte gaten.

Het eerste hoofdstuk was toegewijd aan de kenmerkende eigenschappen van zwarte gaten. Deze objecten onderscheiden zich in de Algemene Relativiteitstheorie (en

veralgemeningen daarvan, die ijktheorieën bevatten) door de aanwezigheid van een horizon, die de grens vormt van een gebied in ruimtetijd waarbinnen licht, en dus alle materie, gevangen zit. Door het gebruik van Penrose diagrammen toonden we de causale structuur van deze objecten en bevestigden we het feit dat de horizon een globaal concept is, dat dus niet lokaal kan worden waargenomen. Dit impliceert dat een waarnemer die in een zwart gat valt, in principe niets speciaals zou merken bij het overschrijden van de horizon. In het geval van zeer massieve zwarte gaten worden de getijdenkrachten verwaarloosbaar klein zodat we het gebied vlakbij de horizon kunnen beschrijven door de Rindler benadering. In dit coördinatensysteem is de ruimtetijd Minkowski en statische waarnemers in Schwarzschild coördinaten worden hier voorgesteld als versnelde waarnemers. Deze overeenkomst ligt tevens aan de basis van Einsteins equivalentie principe, dat zegt dat een versnellend systeem lokaal niet te onderscheiden is van één dat onderhevig is aan zwaartekracht.

Vervolgens pasten we het Unruh effect toe op deze versnelde waarnemers, met als resultaat dat de statische Schwarzschild waarnemers de horizon als een thermische zone zien, met karakteristieke temperatuur $1/8\pi M$, met M de massa van het zwarte gat. Dit leidt tot de vaststelling van de thermodynamische wetten van zwarte gaten, die een opmerkelijke overeenkomst vertonen met de klassieke wetten van de thermodynamica. Dit vormt de eerste aanwijzing dat zwarte gaten een intrinsieke entropie bezitten, die evenredig is met de oppervlakte van hun horizon.

Aangezien zwarte gaten unieke oplossingen zijn in een klassieke veldentheorie, enkel bepaald door hun massa en eventuele ladingen, kan hun oorsprong dus ook niet worden afgeleid uit hun toestand. Dit is echter in tegenspraak met een fundamentele eigenschap van zowel klassieke als kwantumtheorieën: het behoud van informatie. Deze informatieparadox, en vooral de uitweg hieruit, vormt een tweede aanwijzing naar zijn entropie en wijst er tevens op dat deze dient te worden beschouwd als een reële thermodynamische grootheid, die de microscopische wanorde van een macroscopische toestand beschrijft.

Als we al deze elementen samenvoegen, komen we tot de conclusie dat een succesvolle theorie van kwantumgravitatie in staat zou moeten zijn om deze entropie te verklaren door te voorzien in een groot aantal microtoestanden voor een zwart gat. Op dit punt verschijnt de snaartheorie in deze thesis.

In hoofdstuk 3 bieden we de lezer een inleiding in een aantal concepten en technieken die een belangrijke rol spelen in het onderzoek dat in deze thesis wordt beschreven. We beginnen bij een korte inleiding tot de snaartheorie, waarbij we eerst de perturbatieve formulering geven en vervolgens tevens niet-perturbatieve objecten, D-branen, behandelen. Deze introductie eindigt met de bespreking van hoe snaartheorie bij lage energie kan worden beschreven door een supergravitatie theorie.

De modellen die in hoofdstuk 4 worden gebruikt, zijn compactificaties van

snaartheorie door een Calabi Yau variëteit, met reële dimensie zes. Dit resulteert in een effectieve supergravitatie in vier dimensies met zogenaamde $\mathcal{N} = 2$ supersymmetrie. Een kort overzicht van de $\mathcal{N} = 2$ algebra en diens representaties wordt dan ook gegeven in deel 3.2. Vervolgens bespreken we een aantal concepten die een belangrijke rol spelen in de studie van supersymmetrische zwarte gaten: het attractor mechanisme, split flow trees en elliptische genera.

Het attractor mechanisme is verantwoordelijk voor het feit dat de moduli velden in een supersymmetrische oplossing een vaste waarde aannemen op de horizon, ongeacht veranderingen van hun waarde op oneindig (strikt genomen is dit enkel zo wanneer de waarde op oneindig geen muur van marginale stabiliteit overschrijdt). De combinatie van dit mechanisme met een beschrijving van zwarte gaten met meerdere centra geeft aanleiding tot het beeld van split flows. Deze geven een vereenvoudigd beeld van hoe de moduli velden variëren van oneindig tot de horizon. Deze split flows worden ook geacht een criterium te zijn voor het bestaan van BPS oplossingen in de volledige snaartheorie. Hiervan maken we gebruik in hoofdstuk 4 om het bestaan vast te stellen van sommige gebonden toestanden van D-branen.

Als laatste hulpmiddel in de beschrijving van supersymmetrische oplossingen in $\mathcal{N} = 2$ supergravitatie in vier dimensies worden elliptische genera besproken. Dit zijn formele partitiesommen die de ontaarding weergeven van BPS oplossingen met vaste magnetische en variabele elektrische ladingen. Deze genera blijken bijzondere transformatie-eigenschappen te bezitten onder de modulaire groep $SL(2, \mathbb{Z})$, waardoor ze volledig kunnen worden gereconstrueerd uit de kennis van slechts een eindig aantal termen. Deze eindige verzameling termen komt overeen met BPS toestanden die we polair noemen. Deze eigenschap van de elliptische genera zorgt ervoor dat we de berekeningen in hoofdstuk 4 konden verifiëren, wat we dan ook deden.

In het volgende hoofdstuk werden de resultaten van mijn eigen onderzoekswerk besproken, meer bepaald de artikels [18, 19]. Eerst werd de overeenkomst tussen BPS oplossingen in supergravitatie en B branen in een topologisch model behandeld. Door deze B braan oplossingen meer in detail te bekijken en te laten zien hoe deze kunnen worden voorgesteld in de afgeleide categorie, kwamen we tot de vaststelling van een fundamenteel inzicht dat de basis vormt van mijn onderzoek: een verfijnde beschrijving van BPS toestanden en een berekeningsmethode voor hun indices.

De resultaten zelf kwamen vervolgens aan bod. In dit gedeelte werden de indices berekend voor drie verschillende modellen, waardoor we hun elliptische genera konden bepalen. Voor één specifiek model, de decantic Calabi Yau, mondde dit uit in een nieuw elliptisch genus (in vergelijking met een eerdere berekening in [87]).

De berekening van de indices voor enkele niet polaire toestanden maakte een verificatie van onze methode mogelijk. Doordat de resultaten in perfecte

overeenstemming waren met deze van een modulaire expansie van het elliptische genus, bevestigden ze de juistheid van de methode. Ook het nieuwe elliptische genus van de decantie Calabi Yau werd bevestigd. Daar bovenop kon een uitbreiding van de methode, die werd ontwikkeld in [19], getest worden. Deze uitbreiding maakt het mogelijk om ook de index van een toestand te berekenen, die overeenkomt met één enkel centrum in de supergravitatie benadering. De techniek doorstond de test met glans: opnieuw was de uitkomst perfect in overeenstemming met de modulaire voorspelling.

Het belang van dit onderzoek kan kort worden samengevat in de volgende drie punten. Vooreerst biedt het een duidelijk en goed gedefinieerd wiskundig raamwerk voor de studie van BPS oplossingen in type II snaartheorie. De eindigheid van de resultaten en hun overeenkomst met modulaire verwachtingen geeft een gedeeltelijk antwoord op de vragen, die aan het begin van deze samenvatting werden geformuleerd. Ze tonen namelijk aan dat zulke oplossingen een zekere ontanding bevatten, die in snaartheorie exact kan worden berekend (tenminste voor de specifieke modellen die hier werden behandeld).

Ten tweede openen de resultaten deuren voor nieuwe onderzoekspistes, door een robuust en goed gedefinieerd wiskundig kader te scheppen. Zoals vermeld in deel 4.3.5, zou het interessant zijn om de relatie van onze resultaten met wall crossing formules te onderzoeken. Een andere mogelijkheid zou kunnen bestaan in de studie van het asymptotische gedrag van de index voor grote ladingen. Dit laatste zou meer licht kunnen werpen op de OSV conjectuur [91] of het entropie enigma [65].

Tenslotte kunnen de resultaten gezien worden als een stap naar een beter begrip van de snaartheorie. Door de enorme complexiteit van deze theorie zijn exacte resultaten steeds bijzonder welkom. Meer bepaald biedt ons onderzoek meer licht op de eindigheid van de theorie.

Bibliography

- [1] J.-L. Basdevant and J. Dalibard, *Quantum Mechanics*. Springer-Verlag, 2005.
- [2] J. D. Bekenstein, *Black holes and entropy*, *Phys. Rev.* **D7** (1973) 2333–2346.
- [3] S. W. Hawking, *Particle Creation by Black Holes*, *Commun. Math. Phys.* **43** (1975) 199–220.
- [4] L. Susskind, *Some speculations about black hole entropy in string theory*, [hep-th/9309145](#).
- [5] A. Strominger and C. Vafa, *Microscopic Origin of the Bekenstein-Hawking Entropy*, *Phys. Lett.* **B379** (1996) 99–104, [[hep-th/9601029](#)].
- [6] J. M. Maldacena, A. Strominger, and E. Witten, *Black hole entropy in M-theory*, *JHEP* **12** (1997) 002, [[hep-th/9711053](#)].
- [7] S. D. Mathur, *The fuzzball proposal for black holes: An elementary review*, *Fortsch. Phys.* **53** (2005) 793–827, [[hep-th/0502050](#)].
- [8] I. Bena and N. P. Warner, *Black holes, black rings and their microstates*, *Lect. Notes Phys.* **755** (2008) 1–92, [[hep-th/0701216](#)].
- [9] V. Balasubramanian, E. G. Gimon, and T. S. Levi, *Four Dimensional Black Hole Microstates: From D-branes to Spacetime Foam*, *JHEP* **01** (2008) 056, [[hep-th/0606118](#)].
- [10] K. Skenderis and M. Taylor, *The fuzzball proposal for black holes*, *Phys. Rept.* **467** (2008) 117–171, [[arXiv:0804.0552](#)].
- [11] J. Adam, B. Janssen, W. Troost, and W. Van Herck, *Some thoughts about matrix coordinate transformations*, *Phys. Lett.* **B662** (2008) 220–226, [[arXiv:0712.0918](#)].

- [12] J. Raeymaekers, W. Van Herck, B. Vercnocke, and T. Wyder, *5D fuzzball geometries and 4D polar states*, *JHEP* **10** (2008) 039, [[arXiv:0805.3506](#)].
- [13] T. S. Levi, J. Raeymaekers, D. Van den Bleeken, W. Van Herck, and B. Vercnocke, *Godel space from wrapped M2-branes*, *JHEP* **01** (2010) 082, [[arXiv:0909.4081](#)].
- [14] A. Simons, A. Strominger, D. M. Thompson, and X. Yin, *Supersymmetric branes in AdS(2) x S**2 x CY(3)*, *Phys. Rev.* **D71** (2005) 066008, [[hep-th/0406121](#)].
- [15] D. Gaiotto, A. Strominger, and X. Yin, *Superconformal black hole quantum mechanics*, *JHEP* **11** (2005) 017, [[hep-th/0412322](#)].
- [16] D. Gaiotto *et. al.*, *D4-D0 Branes on the Quintic*, *JHEP* **03** (2006) 019, [[hep-th/0509168](#)].
- [17] S. R. Das *et. al.*, *Branes wrapping black holes*, *Nucl. Phys.* **B733** (2006) 297–333, [[hep-th/0507080](#)].
- [18] W. Van Herck and T. Wyder, *Black Hole Meiosis*, *JHEP* **04** (2010) 047, [[arXiv:0909.0508](#)].
- [19] W. Van Herck, *Exact indices for D-particles, flow trees and the derived category*, [arXiv:1010.0686](#).
- [20] M. Ludvigsen, *General Relativity: A Geometric Approach*. Cambridge University Press, 1999.
- [21] R. d’Inverno, *Introducing Einstein’s Relativity*. Oxford University Press, 1992.
- [22] R. M. Wald, *General Relativity*. University Of Chicago Press, 1984.
- [23] S. Weinberg, *Gravitation and Cosmology: Principles and Applications of the General Theory of Relativity*. John Wiley & Sons, 1972.
- [24] R. M. Wald, *Quantum Field Theory in Curved Spacetime and Black Hole Thermodynamics*. Chicago Lectures in Physics. University Of Chicago Press, 1994.
- [25] L. Susskind and J. Lindesay, *An introduction to black holes, information, and the string theory revolution*. World Scientific, 2005.
- [26] W. G. Unruh, *Notes on black hole evaporation*, *Phys. Rev.* **D14** (1976) 870.
- [27] W. Troost and H. Van Dam, *Thermal Effects for an Accelerating Observer*, *Phys. Lett.* **B71** (1977) 149.

- [28] W. Troost and H. van Dam, *Thermal Propagators and Accelerated Frames of Reference*, *Nucl. Phys.* **B152** (1979) 442.
- [29] J. M. Bardeen, B. Carter, and S. W. Hawking, *The Four laws of black hole mechanics*, *Commun. Math. Phys.* **31** (1973) 161–170.
- [30] M. B. Green, J. H. Schwarz, and E. Witten, *Superstring Theory: Volume 1, Introduction*. Cambridge Monographs on Mathematical Physics. Cambridge University Press, 1987.
- [31] M. B. Green, J. H. Schwarz, and E. Witten, *Superstring Theory: Volume 2, Loop Amplitudes, Anomalies and Phenomenology*. Cambridge Monographs on Mathematical Physics. Cambridge University Press, 1988.
- [32] J. Polchinski, *String Theory: Volume 1, An Introduction to the Bosonic String*. Cambridge Monographs on Mathematical Physics. Cambridge University Press, 2005.
- [33] J. Polchinski, *String Theory: Volume 2, Superstring Theory and Beyond*. Cambridge Monographs on Mathematical Physics. Cambridge University Press, 2005.
- [34] C. V. Johnson, *D-Branes*. Cambridge Monographs on Mathematical Physics. Cambridge University Press, 2002.
- [35] K. Becker, M. Becker, and J. H. Schwarz, *String Theory and M-Theory. A Modern Introduction*. Cambridge University Press, 2007.
- [36] J. Polchinski, *Lectures on D-branes*, [hep-th/9611050](#).
- [37] C. P. Bachas, *Lectures on D-branes*, [hep-th/9806199](#).
- [38] M. Nakahara, *Geometry, Topology and Physics*. Graduate Student Series in Physics. Taylor & Francis, 2003.
- [39] J. Polchinski, *Dirichlet-Branes and Ramond-Ramond Charges*, *Phys. Rev. Lett.* **75** (1995) 4724–4727, [[hep-th/9510017](#)].
- [40] W. Nahm, *Supersymmetries and their representations*, *Nucl. Phys.* **B135** (1978) 149.
- [41] E. Cremmer, B. Julia, and J. Scherk, *Supergravity theory in 11 dimensions*, *Phys. Lett.* **B76** (1978) 409–412.
- [42] M. B. Green and J. H. Schwarz, *Extended Supergravity in Ten-Dimensions*, *Phys. Lett.* **B122** (1983) 143.
- [43] P. S. Howe and P. C. West, *The Complete $N=2$, $D=10$ Supergravity*, *Nucl. Phys.* **B238** (1984) 181.

- [44] J. H. Schwarz and P. C. West, *Symmetries and Transformations of Chiral $N=2$ $D=10$ Supergravity*, *Phys. Lett.* **B126** (1983) 301.
- [45] J. H. Schwarz, *Covariant Field Equations of Chiral $N=2$ $D=10$ Supergravity*, *Nucl. Phys.* **B226** (1983) 269.
- [46] J. Wess and J. Bagger, *Supersymmetry and Supergravity*. Princeton University Press, second ed., 1992.
- [47] E. B. Bogomolny, *Stability of Classical Solutions*, *Sov. J. Nucl. Phys.* **24** (1976) 449.
- [48] M. K. Prasad and C. M. Sommerfield, *An Exact Classical Solution for the 't Hooft Monopole and the Julia-Zee Dyon*, *Phys. Rev. Lett.* **35** (1975) 760–762.
- [49] S. Ferrara, R. Kallosh, and A. Strominger, *$N=2$ extremal black holes*, *Phys. Rev.* **D52** (1995) 5412–5416, [hep-th/9508072].
- [50] A. Strominger, *Macroscopic Entropy of $N = 2$ Extremal Black Holes*, *Phys. Lett.* **B383** (1996) 39–43, [hep-th/9602111].
- [51] G. W. Moore, *Arithmetic and attractors*, hep-th/9807087.
- [52] G. W. Moore, *Attractors and arithmetic*, hep-th/9807056.
- [53] G. W. Moore, *Les Houches lectures on strings and arithmetic*, hep-th/0401049.
- [54] P. Candelas, G. T. Horowitz, A. Strominger, and E. Witten, *Vacuum Configurations for Superstrings*, *Nucl. Phys.* **B258** (1985) 46–74.
- [55] A. Strominger and E. Witten, *New Manifolds for Superstring Compactification*, *Commun. Math. Phys.* **101** (1985) 341.
- [56] S. Cecotti, S. Ferrara, and L. Girardello, *Geometry of Type II Superstrings and the Moduli of Superconformal Field Theories*, *Int. J. Mod. Phys.* **A4** (1989) 2475.
- [57] F. Denef, *Supergravity flows and D-brane stability*, *JHEP* **08** (2000) 050, [hep-th/0005049].
- [58] F. Denef, B. R. Greene, and M. Raugas, *Split attractor flows and the spectrum of BPS D-branes on the quintic*, *JHEP* **05** (2001) 012, [hep-th/0101135].
- [59] F. Denef, *Quantum quivers and Hall/hole halos*, *JHEP* **10** (2002) 023, [hep-th/0206072].

- [60] B. Bates and F. Denef, *Exact solutions for supersymmetric stationary black hole composites*, [hep-th/0304094](#).
- [61] N. Seiberg and E. Witten, *Electric-magnetic Duality, Monopole Condensation, And Confinement In $N=2$ Supersymmetric Yang-Mills Theory*, *Nucl. Phys.* **B426** (1994) 19–52, [[hep-th/9407087](#)].
- [62] A. Strominger, *Massless black holes and conifolds in string theory*, *Nucl. Phys.* **B451** (1995) 96–108, [[hep-th/9504090](#)].
- [63] F. Denef, *On the correspondence between D-branes and stationary supergravity solutions of type II Calabi-Yau compactifications*, [hep-th/0010222](#).
- [64] K. p. Tod, *All Metrics Admitting Supercovariantly Constant Spinors*, *Phys. Lett.* **B121** (1983) 241–244.
- [65] F. Denef and G. W. Moore, *Split states, entropy enigmas, holes and halos*, [hep-th/0702146](#).
- [66] A. Dabholkar, F. Denef, G. W. Moore, and B. Pioline, *Precision counting of small black holes*, *JHEP* **10** (2005) 096, [[hep-th/0507014](#)].
- [67] D. S. Freed and E. Witten, *Anomalies in string theory with D-branes*, [hep-th/9907189](#).
- [68] I. V. Melnikov, M. R. Plesser, and S. Rinke, *Supersymmetric boundary conditions for the $N = 2$ sigma model*, [hep-th/0309223](#).
- [69] R. Dijkgraaf, J. M. Maldacena, G. W. Moore, and E. P. Verlinde, *A black hole farey tail*, [hep-th/0005003](#).
- [70] J. de Boer, M. C. N. Cheng, R. Dijkgraaf, J. Manschot, and E. Verlinde, *A farey tail for attractor black holes*, *JHEP* **11** (2006) 024, [[hep-th/0608059](#)].
- [71] J. Manschot and G. W. Moore, *A Modern Fareytail*, *Commun. Num. Theor. Phys.* **4** (2010) 103–159, [[arXiv:0712.0573](#)].
- [72] J. M. Maldacena, *The large N limit of superconformal field theories and supergravity*, *Adv. Theor. Math. Phys.* **2** (1998) 231–252, [[hep-th/9711200](#)].
- [73] E. Witten, *Anti-de Sitter space and holography*, *Adv. Theor. Math. Phys.* **2** (1998) 253–291, [[hep-th/9802150](#)].
- [74] S. S. Gubser, I. R. Klebanov, and A. M. Polyakov, *Gauge theory correlators from non-critical string theory*, *Phys. Lett.* **B428** (1998) 105–114, [[hep-th/9802109](#)].

- [75] O. Aharony, S. S. Gubser, J. M. Maldacena, H. Ooguri, and Y. Oz, *Large N field theories, string theory and gravity*, *Phys. Rept.* **323** (2000) 183–386, [[hep-th/9905111](#)].
- [76] S. K. Donaldson and R. P. Thomas, *Gauge theory in higher dimensions*, . Prepared for Conference on Geometric Issues in Foundations of Science in honor of Sir Roger Penrose’s 65th Birthday, Oxford, England, 25–29 Jun 1996.
- [77] R. P. Thomas, *Gauge theory on Calabi-Yau manifolds*. PhD thesis, University of Oxford, 1997.
- [78] R. P. Thomas, *A holomorphic Casson invariant for Calabi-Yau 3-folds, and bundles on $K3$ fibrations*, [math/9806111](#).
- [79] T. Damour and G. Veneziano, *Self-gravitating fundamental strings and black holes*, *Nucl. Phys.* **B568** (2000) 93–119, [[hep-th/9907030](#)].
- [80] M. Vonk, *A mini-course on topological strings*, [hep-th/0504147](#).
- [81] P. S. Aspinwall, *D-branes on Calabi-Yau manifolds*, [hep-th/0403166](#).
- [82] E. Witten, *Mirror manifolds and topological field theory*, [hep-th/9112056](#).
- [83] M. Kontsevich, *Homological Algebra of Mirror Symmetry*, in *eprint arXiv:alg-geom/9411018*, pp. 11018–+, nov, 1994.
- [84] R. Hartshorne, *Algebraic Geometry*, vol. 52 of *Graduate Texts in Mathematics*. Springer-Verlag, 1977.
- [85] D. Gaiotto, A. Strominger, and X. Yin, *The $M5$ -brane elliptic genus: Modularity and BPS states*, *JHEP* **08** (2007) 070, [[hep-th/0607010](#)].
- [86] A. Collinucci and T. Wyder, *The elliptic genus from split flows and Donaldson-Thomas invariants*, [arXiv:0810.4301](#).
- [87] D. Gaiotto and X. Yin, *Examples of $M5$ -brane elliptic genera*, *JHEP* **11** (2007) 004, [[hep-th/0702012](#)].
- [88] M.-x. Huang, A. Klemm, and S. Quackenbush, *Topological String Theory on Compact Calabi-Yau: Modularity and Boundary Conditions*, *Lect. Notes Phys.* **757** (2009) 45–102, [[hep-th/0612125](#)].
- [89] M. Kontsevich and Y. Soibelman, *Stability structures, motivic Donaldson-Thomas invariants and cluster transformations*, *ArXiv e-prints* (nov, 2008) [[arXiv:0811.2435](#)].
- [90] M. Kontsevich and Y. Soibelman, *Motivic Donaldson-Thomas invariants: summary of results*, [arXiv:0910.4315](#).

- [91] H. Ooguri, A. Strominger, and C. Vafa, *Black hole attractors and the topological string*, *Phys. Rev.* **D70** (2004) 106007, [[hep-th/0405146](#)].
- [92] B. R. Greene, *String theory on Calabi-Yau manifolds*, [hep-th/9702155](#).
- [93] T. Hübsch, *Calabi-Yau manifolds. A bestiary for physicists*. World Scientific Publishing Co., 1992.
- [94] E. Calabi, *On Kähler manifolds with vanishing canonical class*, *Algebraic geometry and topology. A symposium in honor of S. Lefschetz* (1957) 78–89.
- [95] S.-T. Yau, *On the Ricci curvature of a compact Kähler manifold and the complex Monge-Ampère equation. I*, *Comm. Pure Appl. Math.* **31** (1978) 339–411.
- [96] R. Gopakumar and C. Vafa, *M-theory and topological strings. I*, [hep-th/9809187](#).
- [97] R. Gopakumar and C. Vafa, *M-theory and topological strings. II*, [hep-th/9812127](#).
- [98] A. O. D. Maulik, N. Nekrasov and R. Pandharipande, *Gromov-witten theory and donaldson-thomas theory*, [math-AG/0312059](#).
- [99] A. O. D. Maulik, N. Nekrasov and R. Pandharipande, *Gromov-witten theory and donaldson-thomas theory*, [math-AG/0406092](#).
- [100] A. Klemm, M. Kreuzer, E. Riegler, and E. Scheidegger, *Topological string amplitudes, complete intersection Calabi-Yau spaces and threshold corrections*, *JHEP* **05** (2005) 023, [[hep-th/0410018](#)].
- [101] G. E. Bredon, *Sheaf theory*, vol. 170 of *Graduate texts in mathematics*. Springer-Verlag, 1997.
- [102] M. Kashiwara and P. Schapira, *Categories and Sheaves*, vol. 332 of *Grundlehren der mathematischen Wissenschaften*. Springer-Verlag, 2006.
- [103] S. Mac Lane, *Categories for the Working Mathematician*, vol. 5 of *Graduate Texts in Mathematics*. Springer-Verlag, 2 ed., 1998.
- [104] D. Eisenbud and J. Harris, *The geometry of schemes*, vol. 197 of *Graduate texts in mathematics*. Springer-Verlag, 2000.
- [105] R. Minasian and G. W. Moore, *K-theory and Ramond-Ramond charge*, *JHEP* **11** (1997) 002, [[hep-th/9710230](#)].
- [106] J. M. Maldacena, G. W. Moore, and N. Seiberg, *D-brane instantons and K-theory charges*, *JHEP* **11** (2001) 062, [[hep-th/0108100](#)].
- [107] J. Evslin, *What does(n't) K-theory classify?*, [hep-th/0610328](#).

- [108] D.-E. Diaconescu, G. W. Moore, and E. Witten, *$E(8)$ gauge theory, and a derivation of K -theory from M -theory*, *Adv. Theor. Math. Phys.* **6** (2003) 1031–1134, [[hep-th/0005090](#)].

Arenberg Doctoral School of Science, Engineering & Technology

Faculty of Science

Department of Physics and Astronomy

High Energy Physics Research Group

Celestijnenlaan 200D, B-3001 Leuven

KATHOLIEKE UNIVERSITEIT
LEUVEN

K.U.-LEUVEN
ASSOCIATE